

ENCLOSURE 4 to NG-16-0052

NEXTERA ENERGY DUANE ARNOLD, LLC
DUANE ARNOLD ENERGY CENTER

**License Amendment Request (TSCR-159) to Revise Technical Specification
Fuel Storage Requirements**

**NON-PROPRIETARY VERSION OF SPENT FUEL POOL CRITICALITY SAFETY
ANALYSIS REPORT**

89 pages follow

Criticality Safety Evaluation of the PaR Racks in the Duane Arnold Spent Fuel Pool

March 2016

Non-Proprietary Information



Table of Contents

1	Introduction	1
2	Acceptance Criteria and Regulatory Guidance	2
3	Storage Rack Description	9
4	Fuel Designs Description	12
5	Method of Analysis.....	15
5.1	Computer Codes.....	16
5.2	Isotopic Content Validation	18
5.3	Criticality Analysis Validation.....	18
5.4	Assumptions and Simplifications.....	20
6	Criticality Safety Analysis	22
6.1	Depletion Analysis.....	22
6.2	Rack Model.....	25
6.3	Correlation of SCCG kinf to Rack keff.....	26
6.4	Limiting Fuel Assembly Lattice.....	34
6.5	Uncertainties Calculations	35
6.6	Orientation and Eccentricity.....	36
6.7	Additional Biases.....	37
6.8	Interface Analysis.....	38
6.9	Summary of Normal Conditions.....	41
6.10	Accident Analysis	41
6.11	Final Calculation of k95/95	42
7	Summary and Conclusions.....	44
7.1	Limits of the Analysis	44
7.2	SCCG kinf Limit Calculations.....	44
8	References	45
Appendix A: Criticality Analysis Validation.....		A-1
A.1	Fresh Fuel Critical Experiments	A-1
A.2	HTC Critical Experiments	A-13
A.3	Summary.....	A-17
A.4	References	A-18
Appendix B: Results.....		B-1

List of Tables

Table 2.1: DSS-ISG-2010-01 Guidance Implementation.....	4
Table 3.1: PaR Racks Dimensions	10
Table 4.1: Fuel Designs Overview	14
Table 4.2: Tolerance Values for GNF2 Fuel.....	14
Table 5.1: Cross Section Libraries	17
Table 6.1: Control Blade Model	22
Table 6.2: Core Thermal Power Cycles 1-25	23
Table 6.3: Depletion Analyses Sensitivity Calculation Matrix.....	23
Table 6.4: Depletion Analyses Sensitivity Study Results.....	24
Table 6.5: DAEC Cycle 1-25 Maximum SCCG k_{inf}	25
Table 6.6: Lattices Added With Higher SCCG k_{inf}	28
Table 6.7: SCCG k_{inf} to Rack k_{eff} Relation Comparison.....	30
Table 6.8: Rack k_{eff} for the Limiting SCCG k_{inf} for Various Correlations	34
Table 6.9: Reactivity Uncertainty Due to Manufacturing Tolerances	35
Table 6.10: Orientation and Eccentricity Results	36
Table 6.11: Determination of the Final $k_{95/95}$	43
Table A.1: Criticality Benchmarks Selection Review	A-2
Table A.2: Fresh Fuel Critical Experiment Results.....	A-4
Table A.3: Area of Applicability.....	A-12
Table A.4: HTC Phase 1 Results.....	A-14
Table A.5: HTC Phase 2a, Gadolinium Solutions, Results	A-14
Table A.6: HTC Phase 3 Results – Water Reflected Assemblies.....	A-15
Table A.7: Biases and Uncertainties.....	A-17

List of Figures

Figure 3.1: PaR Racks Illustration.....	9
Figure 3.2: DAEC Spent Fuel Pool Showing Placement of PaR Racks	11
Figure 4.1: GE 8x8 Fuel Designs.....	12
Figure 4.2: GE 10x10 Fuel Designs.....	13
Figure 6.1: PaR Rack Model Schematic	26
Figure 6.2: MCNP6 PaR Rack Model.....	26
Figure 6.3: SCCG k_{inf} to Rack k_{eff} Relation For 10x10 Fuel	27
Figure 6.4: Lattice Designs for Higher SCCG k_{inf}	29
Figure 6.5: SCCG k_{inf} to Rack k_{eff} Relation with Limiting Correlation	30
Figure 6.6: SCCG k_{inf} to Rack k_{eff} Relation for GNF2 Data	31
Figure 6.7: SCCG k_{inf} to Rack k_{eff} Relation for GNF2 No Vanished Rod Lattices	32
Figure 6.8: SCCG k_{inf} to Rack k_{eff} Relation for GNF2 6 Vanished Rod Lattices	33
Figure 6.9: Limiting Lattice Design.....	35
Figure 6.10: Eccentric Model with Limiting Orientation.....	37
Figure 6.11: PaR-PaR Rack Interface Model.....	38
Figure 6.12: PaR-Holtec Rack Interface Model.....	40
Figure A.1: Fresh Fuel Critical Experiments Histogram.....	A-7
Figure A.2: Fresh Fuel Experiments as a Function of EALF	A-10
Figure A.3: Fresh Fuel Experiments as a Function of Enrichment.....	A-11
Figure A.4: HTC Critical Experiments Histogram	A-15
Figure A.5: HTC Experiments as a Function of EALF.....	A-16

1 Introduction

This report presents the results of a criticality safety analysis performed for storage of BWR fuel assemblies in the Duane Arnold Energy Center (DAEC) Programmed and Remote (PaR) Systems Corporation spent fuel pool racks. The DAEC spent fuel pool contains two types of spent fuel storage racks: twelve PaR racks, and nine Holtec racks. The PaR racks were approved for installation in 1978 and have Boral panels, used as the neutron absorber for criticality safety.

This criticality safety analysis is performed with a reduced Boral areal density in the PaR spent fuel pool racks, compared to the current licensing basis criticality safety analysis. The reduction is to accommodate for the results of the first in-situ neutron absorber test [1], which indicated some of the panels had Boral areal densities below what was credited in the criticality analysis. The analysis addresses all fuel assemblies used and currently stored in the spent fuel pool at DAEC, including legacy 7x7 and 8x8 fuel designs as well as various 10x10 fuel designs. The analysis is performed consistent with existing applicable regulatory requirements and guidance, using methodologies that have been reviewed and approved by the NRC in previous applications.

Criticality control in the PaR spent fuel pool racks, as credited in this criticality safety analysis, relies on the following:

- Boral fixed neutron absorbers on the PaR spent fuel pool racks cell walls
- Gadolinia integrated neutron absorbers (lattice peak reactivity composition)

The analysis demonstrates that the effective neutron multiplication factor (k_{eff}) in the PaR spent fuel pool racks fully loaded with fuel of the highest reactivity is less than 0.95 with a 95% probability and 95% confidence level. Reactivity effects of normal and accident conditions are also evaluated to assure that under all credible normal and accident conditions, the reactivity will not exceed the regulatory limit.

2 Acceptance Criteria and Regulatory Guidance

The Code of Federal Regulations Title 10 Part 50 Section 68 (10CFR50.68) [2] section (b).4 states:

“(4) If no credit for soluble boron is taken, the k -effective of the spent fuel storage racks loaded with fuel of the maximum fuel assembly reactivity must not exceed 0.95, at a 95 percent probability, 95 percent confidence level, if flooded with unborated water.”

This analysis shows if the fuel loaded in the spent fuel pool meets the Technical Specification maximum k -infinity in the standard core configuration at cold conditions and the racks maintain the Technical Specification on spacing and minimum Boron areal density, the k_{eff} will be less than 0.95 at a 95% probability and 95% confidence level as specified in 10CFR50.68.

Meeting 10CFR50.68 also satisfies 10CFR50, Appendix A, General Design Criteria 62 [3] which states:

“Criticality in the fuel storage and handling system shall be prevented by physical systems or processes, preferably by use of geometrically safe configurations.”

Guidance for the regulatory review is found in the Standard Review Plan, NUREG-0800 Section 9.1.1, “Criticality Safety of Fresh and Spent Fuel Storage and Handling” [4]. Below are the eleven specific areas of review from this guidance, followed by the section where the information is found in this report (note that there are actually 13 areas of review but the last two do not apply to License Amendment Requests.)

1. *Fuel assembly design to verify that appropriate fuel assembly data were used.*
Fuel assembly design data is found in Section 4.
2. *Fuel storage rack design to verify that appropriate fuel storage rack data were used.*
Storage rack design data is found in Section 3.
3. *Evaluation of performance effectiveness of the neutron absorbing materials in the fresh and spent fuel racks.*
The effectiveness of the neutron absorbing materials is discussed in Section 5.
4. *Computational methods and related data to verify that acceptable computational methods and data were used.*
Computational methods are described in Sections 5 and 6.
5. *Computational method validation to verify that the validation study is thorough and uses benchmark critical experiments that are similar to the normal-conditions and abnormal conditions models and to verify that the neutron distribution coefficient ($K(\text{eff})$) bias and bias uncertainty values are conservatively determined.*
Validation is summarized in Section 5 and the details are provided in Appendix A.
6. *Identification of normal conditions to verify that the scope of specified normal conditions is comprehensive.*
Range of normal conditions is identified in Section 6.

7. *Normal-conditions models to verify that normal conditions are modeled conservatively and that all modeling approximations and assumptions are appropriate.*

Normal conditions models are described in Section 6.2 and the tolerances and uncertainties in these models are described in Section 6.5.

8. *Identification of abnormal conditions to verify that the scope of considered abnormal conditions is comprehensive.*

Abnormal conditions are described in Section 6.

9. *Abnormal-conditions models to verify that abnormal conditions are modeled conservatively and that all modeling approximations and assumptions are appropriate.*

Abnormal condition models are described in Section 6.

10. *Analysis of normal and credible abnormal conditions to verify that the analysis is complete and logically sound and that assumptions, limits, and controls are clearly stated.*

The analysis of normal and credible abnormal conditions is presented in Section 6. The limitations of the analysis are listed in Section 7.1.

11. *Analysis conclusions to verify the applicant's conclusions regarding maintaining subcriticality for all normal and credible abnormal conditions.*

The final conclusion of the analysis is in Section 7.

Guidance for spent fuel pool criticality analysis is given in NRC Interim Staff Guidance DSS-ISG-2010-01 [5]. Table 2.1 notes where each of the items technical guidance section of DSS-ISG-2010-01 are addressed in this report.

Table 2.1: DSS-ISG-2010-01 Guidance Implementation

Guidance from DSS-ISG-2010-01	Implementation	Report Section
1. Fuel Assembly Selection Demonstrate analysis bounds all designs, including variations within a design	All existing and additional 10x10 lattices are analyzed to determine the most limiting lattice. Legacy 7x7 and 8x8 fuel designs are also addressed.	Section 6.4
2. Depletion Analysis a. Depletion uncertainty i. Only used for isotopic concentration	Critical experiments cover the major actinides, and a 5% depletion uncertainty is used. A bias of 1.5% of the fission products and minor actinides worth is used to cover their bias and uncertainty in reactivity worth.	Section 6.5
2. Depletion Analysis a. Depletion uncertainty ii. Reactivity decrement	Reactivity decrement was calculated as the k_{eff} of a fresh unburned assembly with no integral burnable absorbers minus the k_{eff} of the fuel assembly at the burnup of interest with residual integral burnable absorbers.	Section 6.5
2. Depletion Analysis b. Reactor Parameters i. Bounding values should be used	The range of depletion conditions is used for all fuel designs and the isotopic concentrations from the highest lattice peak reactivity are used.	Section 6.1
2. Depletion Analysis b. Reactor Parameters ii. Use the more limiting bounding parameter when a conflict occurs	Limiting values were used for all parameters. The only exception is that 100% void conditions were not used for the rodde depletions.	Section 6.1
2. Depletion Analysis b. Reactor Parameters iii. Use of non-bounding values	Bounding values were used for all parameters.	Section 6.1
2. Depletion Analysis c. Burnable Absorbers i. All removable burnable absorbers must be considered	Removable burnable absorbers are not used.	N/A

Guidance from DSS-ISG-2010-01	Implementation	Report Section
2. Depletion Analysis c. Burnable Absorbers ii. Limiting integral burnable absorbers should be used	A full range of Gadolinia content is used in the depletion analysis.	Section 6
2. Depletion Analysis c. Burnable Absorbers iii. Model the burnable absorbers appropriately	The burnable absorbers are modeled correctly; the analysis assumes most limiting lattice.	Section 5
2. Depletion Analysis c. Burnable Absorbers iv. Consider competing effects	All types of lattices with different number of burnable absorbers and placement are evaluated, thus addressing potential competing effects. Sensitivity study was performed to determine most reactive of all potential competing effects.	Section 6
2. Depletion Analysis d. Rodded Operation i. Spectrum hardening from rodDED operation should be considered	The depletion analysis uses the most limiting of rodDED and non-rodDED operation.	Section 6.1
2. Depletion Analysis d. Rodded Operation ii. Effect of control rods on the axial burnup profile should be considered	The analysis assumes the most limiting lattice for the full axial length, ignoring blankets.	Section 6.1
3. Criticality Analysis a. Axial Burnup Profile	The analysis assumes the most limiting lattice for the full axial length, ignoring blankets.	Section 5
3. Criticality Analysis b. Rack Model i. Model inputs should be traceable	The rack dimensions and materials are taken from the manufacturer's drawings.	Section 3

Guidance from DSS-ISG-2010-01	Implementation	Report Section
3. Criticality Analysis b. Rack Model ii. Efficiency of the neutron absorber should be established	The Boral panels are modeled using a value lower than the minimum areal density for the PaR racks. The Monte Carlo analysis correctly accounts for self-shielding and streaming through the absorber panels as seen by use of the validation cases.	Section 5
3. Criticality Analysis b. Rack Model iii. Degradation should be modeled conservatively	The Boral is modeled using a value lower than the minimum measured areal density for the PaR racks. A bias was added to account for potential blisters on the neutron absorber panels.	Section 6.7
3. Criticality Analysis c. Interfaces	All interfaces (PaR rack to PaR rack, PaR rack to Holtec rack) were analyzed.	Section 6.8
3. Criticality Analysis d. Normal Conditions	All normal conditions are considered and addressed.	Section 6.9
3. Criticality Analysis e. Accident Conditions	All credible accidents are considered and addressed.	Section 6.10
4. Criticality Code Validation NUREG/CR-6698	NUREG/CR-6698 was followed for the validation.	Appendix A
4. Criticality Code Validation a. Area of Applicability i. Validation appropriately considers actinides and fission products	The HTC critical experiments are included in the validation analysis.	Appendix A
4. Criticality Code Validation a. Area of Applicability ii. Experiments should be appropriate to the system being analyzed	Appropriate critical experiments are used.	Appendix A

Guidance from DSS-ISG-2010-01	Implementation	Report Section
4. Criticality Code Validation a. Area of Applicability iii. Sufficient criticals for analysis and appropriate grouping	A large sample of critical experiments is used providing adequate statistics for all the conclusions made.	Appendix A
4. Criticality Code Validation a. Area of Applicability iv. Experiments are not all highly correlated	Due to the large number of experiments from multiple facilities, the critical experiments are not highly correlated.	Appendix A
4. Criticality Code Validation b. Trend Analysis	The trend analysis is performed on the major parameters. The trend analysis finds the best linear fit. No trends are rejected. The most limiting bias and uncertainty for the area of applicability is applied.	Appendix A
4. Criticality Code Validation c. Statistical Treatment i. Use the variance of the population about the mean	The statistical approach recommended in NUREG/CR-6698 is used. Thus the variance of the population about the mean rather than the variance of the mean is used.	Appendix A
4. Criticality Code Validation c. Statistical Treatment ii. Use correct confidence factors	The statistical approach recommended in NUREG/CR-6698 is used. The correct confidence factors were used.	Appendix A
4. Criticality Code Validation c. Statistical Treatment iii. Non-normal distributions	Normality testing was performed and the appropriate statistical treatment was applied.	Appendix A
4. Criticality Code Validation d. Lumped Fission Products	The depletion analysis uses lumped fission products to assure proper spectrum hardening but the criticality analysis conservatively ignores the lumped fission products.	Section 5
4. Criticality Code Validation e. Code-to-Code Comparisons	No code-to-code comparisons were used for validation.	N/A

Guidance from DSS-ISG-2010-01	Implementation	Report Section
5. Miscellaneous a. Precedence	Precedence is not quoted as a licensing basis.	N/A
5. Miscellaneous b. References	References used were carefully chosen to be applicable to the criticality analysis.	Section 8
5. Miscellaneous c. Assumptions	Assumptions are identified and justified.	Section 5.4

3 Storage Rack Description

The PaR spent fuel racks are a bolted anodized aluminum construction having a neutron absorber medium of natural B_4C in an aluminum matrix core clad with 1100 series aluminum. The neutron absorber, marketed under the trade name of Boral, is sealed within two concentric square aluminum tubes forming the poison can. The PaR spent fuel pool racks contain formed and resultant cells, as illustrated in Figure 3.1 (the curved corners are simplified for the drawing). The formed cells are made of the two concentric aluminum boxes with four Boral panels placed between the boxes. The boxes have curved corners, which allow the outer diameter of the outer box to line up with the inner diameter of the inner box of the formed cells. The width of the inner and outer aluminum boxes are the same. The net effect is that the formed and the resultant cells have the same cell ID and the same separation from the Boral panels. Table 3.1 provides the dimensions of the PaR spent fuel pool racks.

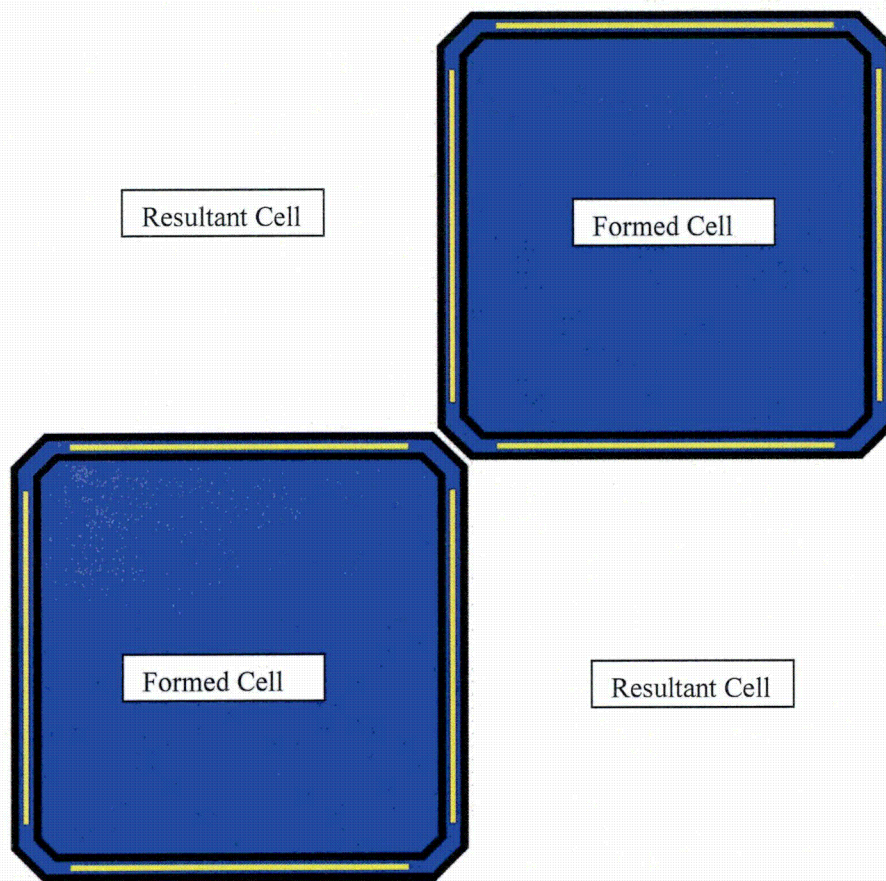


Figure 3.1: PaR Racks Illustration

Table 3.1: PaR Racks Dimensions

Parameter	Nominal	Tolerance
Cell Pitch (inches)	6.625	+/- 0.05
Inner Box Inner Width (inches)	6.156	+/- 0.05
Inner Box Thickness (inches)	0.125	+/- 0.007
Outer Box Inner Width (inches)	6.843	+/- 0.05
Outer Box Thickness (inches)	0.125	+/- 0.007
Boral Panel Thickness (inches)	0.115	+/- 0.010
Boral Panel Width (inches)	5.25	+0.062 / -0.031
Boral Panel Axial Length (inches)	152.0	+/- 0.156
Rack Separation, PaR to Holtec (inches)	3.1	N/A
Boral Areal Density Used in Analysis (gm B-10/cm ²)*	0.0150	N/A

* The nominal Boral areal density is 0.0250 gm B-10/cm², with a minimum of 0.0232 gm B-10/cm²

There are twelve PaR spent fuel pool rack modules in the Duane Arnold Energy Center (DAEC) spent fuel pool. The modules are identified as E10 through E21 in Figure 3.2. To the right side of the PaR spent fuel pool racks are nine Holtec spent fuel pool racks. There is a 3.1 inch separation between the PaR and Holtec spent fuel pool racks, same as among PaR spent fuel pool racks.

Since it is required to show that the Holtec spent fuel pool racks do not increase the reactivity of the PaR spent fuel pool racks at the interface, some description of the Holtec spent fuel pool racks is required. The Holtec spent fuel pool racks include Boral panels on the side of every cell at the rack interface. The Holtec spent fuel pool rack Boral panels have a minimum Boral areal density of 0.015 gm B-10/cm², same as used for the PaR spent fuel pool racks in this analysis. The Holtec spent fuel pool racks contain formed and resultant cells, same as for the PaR spent fuel pool racks. The formed cells are created by a stainless steel box with an inside diameter of 5.90 inches and a wall thickness of 0.060 inches. On the outside of the box are Boral panels that are 0.070 inches thick and 5.00 inches wide. A stainless steel sheathing 0.0235 inch thick covers the Boral panels. The resultant cell has an inner diameter that is also 5.90 inches. The cell pitch for the Holtec spent fuel pool racks is 6.06 inches.

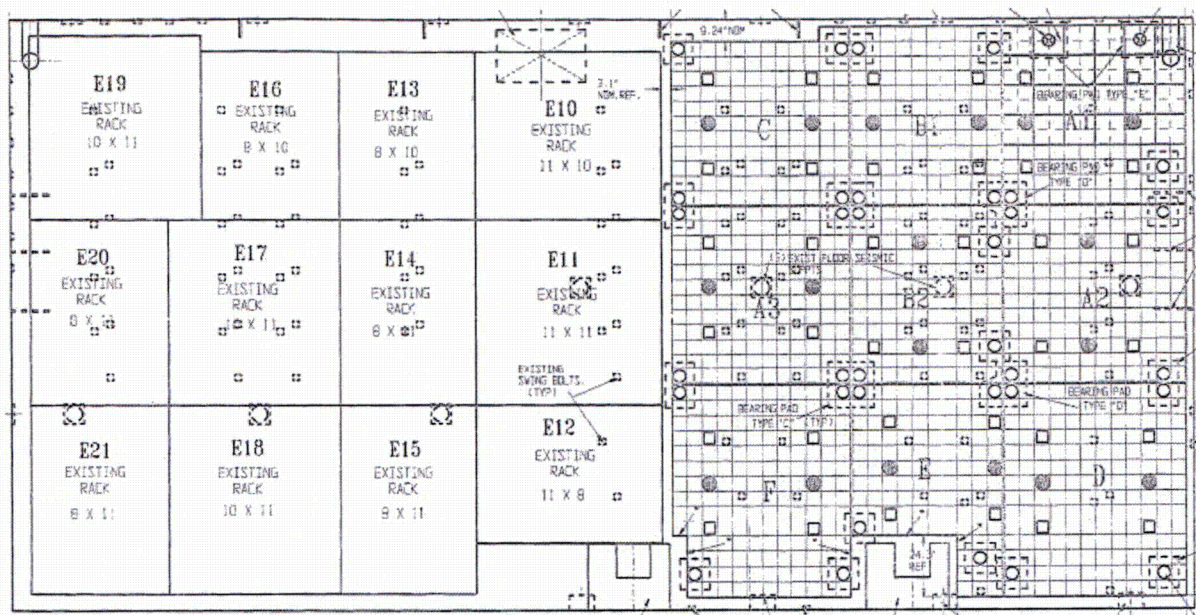


Figure 3.2: DAEC Spent Fuel Pool Showing Placement of PaR Racks

4 Fuel Designs Description

Nine different fuel designs have been used in the Duane Arnold reactor core from its initial cycle in 1974 through Cycle 25. Figures 4.1 and 4.2 provide illustrations of the various 8x8 and 10x10 fuel designs, noting placement of water holes and part-length rods, as applicable. Table 4.1 provides key parameters of the nine fuel designs. Table 4.2 provides tolerances for the GNF2 fuel design. Note that in Cycle 8 lead test assemblies were used, which were similar to the design used in Cycles 11 through 16.

[[

]]

Figure 4.1: GE 8x8 Fuel Designs

[[

]]

Figure 4.2: GE 10x10 Fuel Designs

Table 4.1: Fuel Designs Overview
(Dimensions in cm)

Name	Cycles Used	Array	Pitch	Pellet Radius	Clad Inner Radius	Clad Outer Radius	Channel Inner Width	Channel Thickness	Water Rod IR	Water Rod OR	# of Water Rods	# of Part-length Rods
GE7x7	1	7x7	[[0	Some part length Gd Rods
GE8x8	2-4	8x8									1	0
GE5	5-7	8x8									2	0
GE6B	8	8x8									2	0
GE8B	9-10	8x8									4	0
GE10	11-16	8x8									1	0
GE12	17	10x10									2	14
GE14	18-23	10x10									2	14
GNF2	24-25	10x10]]	2	6S, 8L

Table 4.2: Tolerance Values for GNF2 Fuel
(Values in cm)

Parameter	Dimension	Tolerance
Pin Pitch	[[
Pellet Diameter		
Clad Thickness		
Channel Thickness		
Water Rod Thickness]]

The fuel density has ranged from [[]] for non-Gadolinia fuel pins (except blanket pellets, which have been as high as [[]]). Gadolinia fuel pins have been as low as [[]].

5 Method of Analysis

The general methodology for BWR spent fuel pool criticality analyses is to perform in-core depletion calculations for the various assembly designs in use, then to restart the calculations with the assemblies in the standard cold core geometry (SCCG), and then in the storage rack geometry. The SCCG is defined as an infinite array of fuel assemblies in a 6-inch lattice spacing at 20°C, without any control rods or voids. The limiting k_{inf} in the SCCG is determined and then the k_{eff} in the storage rack geometry is calculated at this burnup. A reactivity allowance for applicable biases and uncertainties is added to the calculated k_{eff} in the rack geometry and the resulting k_{eff} is compared to the regulatory limit of 0.95.

The calculations are performed in a manner that accounts for the radial and axial pin locations. The radial effects are addressed by modeling and extracting isotopic compositions for each individual pin. The peak reactivity method inherently bounds all axial effects by modeling the peak axial reactivity across all exposures at all axial nodes.

The criticality safety analysis follows these steps to demonstrate that fuel assembly storage in the DAEC PaR spent fuel pool racks meets the criticality safety requirements:

1. Identify all fuel designs used at DAEC. For all fuel assemblies of each fuel design, identify the axial lattices (combination of fuel, burnable absorbers, water rods and vanished rods).
2. Perform sensitivity study to determine bounding reactor parameters at all conditions (all exposure statepoints, rodged and unrodged, and 0, 40, 70 and 100% void).
3. Generate two-dimensional models for each lattice and deplete with bounding reactor parameters with unrodged conditions at 0, 40, 70 and 100% void, and also with rodged conditions at 0, 40 and 70% void. These calculations establish the SCCG k_{inf} for each lattice.
4. Additional lattices with higher enrichments and less burnable absorbers, resulting in higher SCCG k_{inf} values are developed and evaluated. These results are included with the data generated for the historical DAEC lattices.
5. Evaluate storage of all of the lattices in the PaR spent fuel pool racks. These calculations are used to establish a relationship between the SCCG k_{inf} and the in-rack k_{eff} . This correlation is used to determine the limiting SCCG k_{inf} that can be safely stored in the PaR spent fuel pool racks, and bounds all fuel assemblies used at DAEC. The correlation is also used to establish the base k_{eff} .
6. Using a lattice design near the limiting SCCG k_{inf} , PaR spent fuel pool rack calculations are performed to determine the impact of the fuel tolerances. Those tolerances include pellet stack density, pellet outside diameter, clad thickness, pin pitch, water rod thickness and channel thickness.
7. Using a lattice design near the limiting SCCG k_{inf} , PaR spent fuel pool rack calculations are performed to determine the impact of the rack tolerances. Those tolerances include rack pitch, cell wall thickness, Boral panel width, and Boral panel thickness.
8. Using a lattice design near the limiting SCCG k_{inf} , PaR spent fuel pool rack calculations are performed to determine the depletion uncertainty.
9. Using a lattice design near the limiting SCCG k_{inf} , PaR spent fuel pool rack calculations are performed to determine the impact of orientation and eccentricity effects.
10. Using a lattice design near the limiting SCCG k_{inf} , PaR spent fuel pool rack calculations are performed to determine the impact of the fission product worth.
11. Using a lattice design near the limiting SCCG k_{inf} , PaR spent fuel pool racks calculations are performed to determine the impact of different zirconium alloys.
12. Using a lattice design near the limiting SCCG k_{inf} , PaR spent fuel pool rack calculations are performed to determine the impact of potential Boral panel blisters.

13. Using a lattice design near the limiting SCCG k_{inf} , PaR spent fuel pool rack calculations are performed to determine the impact of the interface effects.
14. Using a lattice design near the limiting SCCG k_{inf} , PaR spent fuel pool rack calculations are performed to determine the impact of accidents. The accidents evaluated include a dropped fuel assembly, missing absorber panel, misplaced fuel assembly, and maximum water temperature.
15. All normal conditions are reviewed and analyses performed to demonstrate that each is in compliance with criticality safety requirements.
16. Validate computer codes and cross section libraries. The validation process is composed of selecting critical experiments, modeling the critical experiments, and then performing data analysis with the results. The data analysis includes determination of the bias and bias uncertainty, identification of trends in data, and testing for normal distribution. The process also includes documenting the area of applicability for the validation.
17. Determine maximum in-rack k_{eff} by adding biases and uncertainties to calculated base k_{eff} for limiting SCCG lattice, ensuring that it is below the regulatory limit of 0.95 with sufficient margin.

All delta k calculations are performed using equation $k_1 - k_2 + 2 \cdot \sqrt{\sigma_1^2 + \sigma_2^2}$.

5.1 Computer Codes

The analysis is performed using CASMO-4 [6] for the depletion analysis for the determination of SCCG infinite multiplication factor (k_{inf}) and MCNP6 [7] for the rack analysis and calculation of the in-rack effective multiplication factor (k_{eff}).

5.1.1 CASMO-4

CASMO-4 is a two-dimensional multi-group transport theory code for burnup calculations of BWR and PWR fuel assemblies developed by Studsvik. The code handles a geometry consisting of cylindrical fuel rods of varying composition in a square pitch array including fuel rods loaded with Gadolinia. The code handles the BWR channels as well as water gaps and cruciform control rods in the regions separating fuel assemblies. The analysis presented here used version 2.05.17.

The CASMO-4 neutron data library is based on data from ENDF/B-IV although some data comes from other sources. It contains cross sections for 108 materials, most of which are individual nuclides. Nuclear data are collected in a library containing microscopic cross sections in 70 energy groups. The code models multiple individual fission products, and uses two lumped fission products for those that are not specifically modeled.

For this application, CASMO-4 is used to predict isotopic content where the standard 5% of the delta k of burnup given in DSS-ISG-2010-01 is applied for the uncertainty [5]. CASMO-4 is also used for calculation of the SCCG k_{inf} . However, this SCCG k_{inf} is only used via a conservative correlation to the validated code for the calculation of the rack k_{eff} . A validation of CASMO-4 to develop a bias and bias uncertainty is not necessary because the use of the code is only to generate isotopic compositions, which are addressed by the depletion uncertainty.

5.1.2 MCNP6

MCNP6 is a general-purpose Monte Carlo N-Particle code that can be used for neutron, photon, electron, or coupled neutron/photon/electron transport. The calculations use continuous energy cross section data base on ENDF/B-VII.1. MCNP6 was selected because it has a history of successful use in fuel storage criticality analyses and has most of the necessary features for the analyses performed. The code treats an arbitrary three-dimensional configuration of materials in geometric cells bounded by first- and second-degree surfaces and fourth-degree elliptical tori. Pointwise cross-section data is used. All reactions given in a particular cross-section evaluation (such as ENDF/B-VII.1) are accounted for. Thermal neutrons are described by both the free gas and S(alpha, beta) models.

For this application, MCNP6 Version 1.0 is used. It is the latest fully released version of MCNP at the time of this analysis. The cross sections used are ENDF/B-VII.1, which is also the latest cross section set available at the time of this work. MCNP6's elemental cross sections generally come from an earlier cross section evaluation. Table 5.1 shows the isotopes used in this analysis noting the cross section library version.

Table 5.1: Cross Section Libraries

Identifier	Isotope	Library
1001.80c	H-1	ENDF/B-VII.1
8016.80c	O-16	ENDF/B-VII.1
lwtr.20t	H in H ₂ O	ENDF/B-VII
5010.80c	B-10	ENDF/B-VII.1
5011.80c	B-11	ENDF/B-VII.1
6000.80c	C	ENDF/B-VII.1
13027.80c	Al-27	ENDF/B-VII.1
14000.60c	Si	ENDF/B-VI
15031.80c	P-31	ENDF/B-VII.1
16000.62c	S	ENDF/B-VI.8
24000.50c	Cr	ENDF/B-V.0
25055.80c	Mn-55	ENDF/B-VII.1
26000.55c	Fe	LANL/T
28000.50c	Ni	ENDF/B-V.0
40000.66c	Zr	ENDF/B-VI.1
50000.42c	Sn	LLNL:X
45103.80c	Rh-103	ENDF/B-VII.1
47109.80c	Ag-109	ENDF/B-VII.1
54131.80c	Xe-131	ENDF/B-VII.1
55133.80c	Cs-133	ENDF/B-VII.1
55134.80c	Cs-134	ENDF/B-VII.1
55135.80c	Cs-135	ENDF/B-VII.1
60143.80c	Nd-143	ENDF/B-VII.1
60145.80c	Nd-145	ENDF/B-VII.1
61147.80c	Pm-147	ENDF/B-VII.1
61148.80c	Pm-148	ENDF/B-VII.1
61548.80c	Pm-148m	ENDF/B-VII.1
62147.80c	Sm-147	ENDF/B-VII.1
62149.80c	Sm-149	ENDF/B-VII.1
62150.80c	Sm-150	ENDF/B-VII.1
62151.80c	Sm-151	ENDF/B-VII.1
62152.80c	Sm-152	ENDF/B-VII.1
63153.80c	Eu-153	ENDF/B-VII.1
63154.80c	Eu-154	ENDF/B-VII.1
63155.80c	Eu-155	ENDF/B-VII.1
64152.80c	Gd-152	ENDF/B-VII.1
64154.80c	Gd-154	ENDF/B-VII.1
64155.80c	Gd-155	ENDF/B-VII.1
64156.80c	Gd-156	ENDF/B-VII.1
64157.80c	Gd-157	ENDF/B-VII.1
64158.80c	Gd-158	ENDF/B-VII.1
64160.80c	Gd-160	ENDF/B-VII.1
92234.80c	U-234	ENDF/B-VII.1
92235.80c	U-235	ENDF/B-VII.1
92236.80c	U-236	ENDF/B-VII.1

Identifier	Isotope	Library
92238.80c	U-238	ENDF/B-VII.1
92239.80c	U-239	ENDF/B-VII.1
93237.80c	Np-237	ENDF/B-VII.1
94238.80c	Pu-238	ENDF/B-VII.1
94239.80c	Pu-239	ENDF/B-VII.1
94240.80c	Pu-240	ENDF/B-VII.1
94241.80c	Pu-241	ENDF/B-VII.1
94242.80c	Pu-242	ENDF/B-VII.1
95241.80c	Am-241	ENDF/B-VII.1
95242.80c	Am-242m	ENDF/B-VII.1
95243.80c	Am-243	ENDF/B-VII.1
96242.80c	Cm-242	ENDF/B-VII.1
96243.80c	Cm-243	ENDF/B-VII.1
96244.80c	Cm-244	ENDF/B-VII.1
96245.80c	Cm-245	ENDF/B-VII.1
96246.80c	Cm-246	ENDF/B-VII.1

The convergence of a Monte Carlo criticality case is sensitive to the number of histories (neutrons) per generation, the total number of generations, the number of generations skipped before averaging, and the initial source distribution. All the computer runs in this analysis use a sampling of at least 800 generations and 5000 neutrons per generation. A minimum of 200 cycles are skipped. Note that these are minimum values for all cases combined, so some cases used a much higher number of neutrons per generation, while other cases used a much higher total number of generations. Sufficient neutrons and generations were used to ensure the Monte Carlo uncertainty was in the range of 0.0001 to 0.0003. The initial source is placed in the highest reactive area of the model. All cases were verified to have source convergence.

5.2 Isotopic Content Validation

The isotopic content as a function of depletion is calculated using CASMO-4. There is insufficient data to validate the isotopic content for all of the individual isotopes. Therefore, this criticality evaluation uses 5% of the depletion reactivity as the depletion isotopic uncertainty as noted in DSS-ISG-2010-01 [5].

Since DSS-ISG-2010-01 was issued, there have been many developments that confirm the use of a 5% depletion uncertainty for this application. ORNL performed studies using MCNP to determine an appropriate reactivity to cover the isotopic uncertainty [8]. CASMO-4 has been shown to yield similar results to MCNP in international studies on BWR burnup credit [9]. This ORNL study suggests that the 5% depletion uncertainty is approximately correct. Further, EPRI sponsored efforts to determine the uncertainty in the delta k of depletion using power reactor data [10, 11]. The EPRI effort used CASMO-4 (and CASMO-5) in their evaluation. The EPRI work suggests that the 5% depletion uncertainty is conservative.

5.3 Criticality Analysis Validation

MCNP6 version 1.0 and the ENDF/B-VII.1 continuous energy cross sections are used for the criticality analysis calculations. Its validation is done in two steps. The first step is to use laboratory critical experiments to validate the major actinides and structural materials in a variety of geometries which produce a range of neutron spectrum. The second step is to validate the minor actinides and fission products.

5.3.1 Major Actinides and Structural Materials

The criticality validation follows NUREG/CR-6698 [12]. One hundred thirty one (131) fresh UO_2 critical experiments from the OECD/NEA handbook [13] and fifty-three (53) HTC critical experiments [14-16] were selected that match the conditions of the DAEC PaR spent fuel pool racks. These experiments were analyzed with MCNP6 version 1.0 using the continuous energy ENDF/B-VII.1 cross-section library. The results were then tested for trends on key parameters. Using these trends, the most limiting bias and uncertainty in the area of applicability was determined. Although some of the trends may not be statistically significant, it is conservative to use all of the trends in determining the limiting bias and uncertainty and that was the approach used. Appendix A documents the area of applicability for the validation. The DAEC spent fuel pool is covered by the area of applicability of the validation. Specifically,

- Enrichment: The benchmarks selected range from 2.35 to 4.31 wt% U-235. The fuel in the spent fuel pool ranges from 1.1 to 5.0 wt% U-235.
- Spectrum: The benchmarks cover a wide range of spectrum by varying the pin pitch. The Energy of the Average Lethargy causing Fission (EALF) of the benchmarks ranges from 0.068 to 0.6 eV. The calculated EALF in the criticality safety analysis ranges from 0.14 to 0.33 eV.
- Fuel Pin Pitch: The fuel pin pitch of the benchmarks ranges from 1.3 to 2.54 cm. The DAEC fuel pin pitch is [[]] for the 7x7 fuel designs, [[]] for the 8x8 fuel designs, and [[]] for the 10x10 fuel designs.
- Boron Areal Density: The benchmarks range from 0 to 0.067 gm B-10/cm². The spent fuel pool credits absorber panels with an areal density of 0.015 gm B-10/cm².

The most limiting bias from the validation was from the non-parametric analysis of the UO_2 critical experiments and it is 0.0031. The most limiting uncertainty comes from the EALF trend from the HTC experiments and it is 0.0079.

5.3.2 Minor Actinides and Fission Products

Since there are few to no critical experiments that contain some of the isotopes used in this criticality evaluation, validation is done by estimating the maximum error in the multiplication factor due to cross section measurement uncertainty. The cross section measurement uncertainty is provided with the ENDF/B cross sections and this uncertainty is propagated to the final criticality application by use of the TSUNAMI sequence in SCALE [17]. This technique of propagation of cross section error to criticality application is a recent development and although other computer codes are being developed to perform this function, SCALE is one of the few codes that can perform this calculation. Rather than specify software the NRC, in the transport division, has allowed applications to use a bias of 1.5% of the worth of the minor actinides and fission products to account for both the bias and uncertainty due to the minor actinides and fission products [18]. This bias came from NUREG-7109 [19] which concentrates on a limited set of isotopes but on the last sentence of page 106 it states, "An upper value of 1.5% of the worth is also applicable for SNF isotopic compositions consisting of all nuclides in the SFP configuration, as well as the cask configuration as depicted in Table 7.11 and Table 7.12." NUREG-7109 limits the applicability to certain cross section sets but ENDF/B-VII is one of those sets.

The minor actinides are defined as actinides not contained in the criticality validation benchmarks. For this analysis that is isotopes U-236, U-239, Np-237, Am-242m, Am-243, Cm-242, Cm-243, Cm-244, Cm-245, and Cm-246.

Nineteen fission products are used in this analysis and they are Rh-103, Ag-109, Xe-131, Cs-133, Cs-134, Cs-135, Nd-143, Nd-145, Pm-147, Pm-148, Pm-148m, Sm-147, Sm-149, Sm-150, Sm-151, Sm-152, Eu-153, Eu-154, and Eu-155.

One of these fission products is a gas, Xe-131. A review of fission gas releases was done for the Indian Point Unit 2 spent fuel pool and it was concluded that the Xe-131 should be reduced 32% [20]. For this analysis no reduction of the Xe-131 is taken. This is acceptable since no credit is taken for the lumped fission products. To show that this is still conservative the worth of the lumped fission products and Xe-131 are compared at peak reactivity in SCCG conditions using CASMO-4. The Xe-131 worth is 0.0025 delta k and the lumped fission product worth was calculated to be about 0.0065 delta k. These values will change for various fuel designs, depletion conditions, and rack conditions but the lumped fission product worth will always be higher than the worth of released Xe-131.

There has also been a concern raised about movement of cesium isotopes in the fuel. Cs-137 has been used as a burnup indicator in chemical assays and burnup measurement devices. If cesium isotopes moved significantly these measurements would not work but when compared to other methods (e.g., Nd-148 content for chemical assays or neutron flux for the Fork detector) the cesium isotopes approach accuracy is similar [21, 22]. Therefore, no reduction in cesium isotopes is taken.

5.4 Assumptions and Simplifications

The analysis relies on the assumptions listed below.

1. Dishing and chamfering of the fuel pellets is neglected. This is acceptable since the amount of fuel is maintained, and the water to fuel ratio and the principal location of the fuel remains unchanged.
2. Each lattice in each fuel assembly in the storage rack is assumed to be at its lifetime maximum reactivity level. There is no assumption of a specific burnup profile for the discharged assemblies. In other words, this is a peak reactivity analysis that does not take credit for lower reactivity conditions associated with burnup past the maximum reactivity.
3. All fuel compositions are at zero hours cooling time. The composition of Xe-135 is set to zero.
4. Fuel assemblies are assumed to contain the high reactivity limiting lattice for the entire length of the assembly (i.e., natural uranium blankets are not modeled).
5. The fuel array is modeled as being radially infinite.
6. All fuel and rack structures above and below the active region of the fuel are neglected and replaced with a 12 inch water reflector.
7. Criticality calculations are performed at normal ambient temperature (about 300K, which is the standard temperature for MCNP6 and its libraries). A water density of 1.0 gm/cm³ is used for all cases, which is the maximum value of water density at all temperatures. This bounding density corresponds to a water temperature of 4 °C.
8. Fuel rod growth and creep are not included in the models. There should not be much fuel rod growth and creep at the low burnup levels at which the peak reactivity occurs. Therefore, the impact on reactivity should be negligible.
9. Fuel assembly spacer grids are ignored in the criticality calculations. It is observed that increasing the clad outside diameter reduces k_{eff} . The spacer grids displace water just as increasing the clad outside diameter displaces water. Also, a large tolerance on the fuel assembly channel was used that approximates the modeling of the spacer grids. Furthermore, the sensitivity study notes that the SCCG k_{inf} decreases when including the spacers in the depletion analysis.
10. The criticality analysis takes no credit for the CASMO-4 lumped fission products.
11. The Boral neutron absorber in the PaR racks is 152 inches long, which is longer than the fuel active length of [[]]. In the calculations, the Boral neutron absorber is modeled to

cover the active fuel length exactly, with no additional neutron absorber above or below the active fuel.

12. In a water environment, neutron scattering ensures that neutrons approach the Boral panel from a full range of incident angles. This minimizes the potential for neutron streaming and reduces the significance of self-shielding. Therefore, no adjustment for the Boral efficiency is made.
13. A bias has been included to account for significant blistering of the Boral panels. At this time, there is no evidence of blistering within the DAEC PaR or Holtec spent fuel pool racks.

6 Criticality Safety Analysis

This section describes all of the calculations performed to demonstrate that the PaR spent fuel pool racks k_{eff} is below the regulatory limit of 0.95 with a 95/95 confidence.

6.1 Depletion Analysis

The objective of the depletion analysis is to find the most limiting composition at any time of life for any fuel assembly under any operating condition. Since BWRs generally use Gadolinia bearing rods in all the assemblies, the most limiting composition is when the reactivity peaks at around 12-18 GWd/MTU. The depletion analysis is done using CASMO-4, as discussed in Section 5.

In order to find the most limiting composition, all of the lattices from all the fuel assemblies that have been used at DAEC were analyzed with CASMO-4. For each case, the depletion analysis was performed by depleting without the control rod at voids of 0%, 40%, 70%, and 100%, and also with the control rod inserted at voids of 0%, 40%, and 70%. Using the depleted atom densities from each burnup step and each depletion condition, a k_{inf} calculation was performed where the channeled fuel assembly is centered in a 6 inch cell of water at 20° C. This condition is called the Standard Cold Core Geometry (SCCG). For each lattice, the highest k_{inf} is determined and this is the maximum SCCG k_{inf} for that lattice.

The depletion model uses the fuel dimensions found on Table 4.1. Table 6.1 provides the control blade dimensions. For the analysis of the peak SCCG k_{inf} , the rated thermal power for the cycle in which the fuel assembly was in the core was used. Table 6.2 provides the rated thermal power for each cycle.

Prior to performing the depletion analysis, a sensitivity analysis was performed on all lattices of the most reactive GNF2 fuel assembly. The matrix of the sensitivity calculations performed is shown in Table 6.3. Table 6.4 shows the results of the sensitivity study. The parameters from the cases with positive k_{inf} delta to nominal (k_{inf} case – k_{inf} nominal) were selected to calculate maximum k_{inf} values for all fuel lattices in Cycles 1-25. Note that some of the selected parameters don't necessarily represent real conditions when used together (for example, high fuel temperature is not typically occurring in lattices with the lowest power density and low moderator temperature). However, the purpose of the selected parameters was to conservatively bound the lattice reactivity in the wide range of operating conditions, rather than provide a realistic result. Based on these results, the most limiting conditions for the depletion analyses were defined. These conditions were used to deplete all the lattices in this calculation.

Table 6.1: Control Blade Model

Half Thickness of Control Rod	[[
Length of Central Steel Region	
Length of Absorbing Section	
Radius of Absorbing Cylinders	
Pitch of Absorbing Cylinders	
Absorbing Material	
Density of B ₄ C	
Blade Steel Volume Fraction Outside of B ₄ C in the Absorber Section]]

Table 6.2: Core Thermal Power Cycles 1-25

Cycle	Power (MWth)
1a	1593
1b	1593
2	1593
3	1593
4a	1593
4b	1593
5	1593
6	1593
7	1593
8	1658
9	1658
10	1658
11	1658
12	1658
13	1658
14	1658
15	1658
16	1658
17	1658
18	1790
19	1790
20	1880
21	1880
22	1912
23	1912
24	1912
25	1912

Table 6.3: Depletion Analyses Sensitivity Calculation Matrix

	Spacer	Control Blade Pitch	Control blade internal media	Control blade worth	Moderator temperature	Fuel temperature	Power density	Channel corner-wall model
Nominal Conditions	Spacer out	CB pitch [[]]	CB H ₂ O filled	CB nominal worth	TMO 561.5 degK	TFU 800 degK	Nominal PDE	Nominal
Variations	Spacer in	CB pitch [[]]	CB H ₂ O to Air	CB worth -10%	TMO 536.5 degK	TFU 1000 degK	0.5 x PDE	Adjusted
				CB worth +10%	TMO 586.5 degK	TFU 700 degK	1.5 x PDE	

Table 6.4: Depletion Analyses Sensitivity Study Results

#	k_{inf}	k_{inf} delta to Nominal	Description	Nominal Conditions							
				SPA out	CB pitch [[]]	CB H ₂ O filled	CB worth nom	TMO 561.5	TFU 800	PDE Nom	Chan corn Nom
0	1.27549		Nominal	x	x	x	x	x	x	x	x
1	1.27073	-0.00476	Spacer in		x	x	x	x	x	x	x
2	1.27549	0.00000	CB pitch [[]]	x		x	x	x	x	x	x
3	1.27579	0.00030	CB H ₂ O to Air	x	x		x	x	x	x	x
4	1.27541	-0.00008	CB worth -10%	x	x	x		x	x	x	x
5	1.27557	0.00008	CB worth +10%	x	x	x		x	x	x	x
6	1.27602	0.00053	TMO 536.5 degK	x	x	x	x		x	x	x
7	1.27469	-0.00080	TMO 586.5 degK	x	x	x	x		x	x	x
8	1.27597	0.00048	TFU 1000 degK	x	x	x	x	x		x	x
9	1.27524	-0.00025	TFU 700 degK	x	x	x	x	x		x	x
10	1.27755	0.00206	0.5 x PDE	x	x	x	x	x	x		x
11	1.27415	-0.00134	1.5 x PDE	x	x	x	x	x	x		x
12	1.27534	-0.00015	Channel corner adjusted	x	x	x	x	x	x	x	

Based on the results of the sensitivity analyses, the following depletion analysis cases were performed for all fuel assembly lattices at DAEC:

1. Base uncontrolled lattice depletion to 50.0 GWD/MTU
 - No spacer
 - No control blade (withdrawn)
 - 536.5 K moderator temperature
 - 1000 K fuel temperature
 - Power density = one half of the nominal, calculated based on core power
 - Nominal fuel and reactor geometry
 - 0, 40, 70, and 100% void fractions
2. Base controlled lattice depletion to 50.0 GWD/MTU
 - No spacer
 - Control blade pitch [[]]
 - Control blade filled with air
 - Control blade worth (B_4C density) increased by 10% from nominal
 - 536.5 K moderator temperature
 - 1000 K fuel temperature
 - Power density = one half of the nominal, calculated based on core power
 - Nominal fuel and reactor geometry
 - 0, 40, 70% void fractions
3. For each of the statepoints in 1 and 2 above, branch to cold uncontrolled core conditions to calculate the SCCG k_{inf}
 - 293.0 K fuel temperature
 - 293.0 K moderator temperature
 - 0% void fraction
 - No control blade (withdrawn)

The depletions and branches described above reasonably cover all possible operating conditions of DAEC Cycle 1-25 assemblies. All of the DAEC fuel assembly lattices were analyzed using CASMO-4 and the approach described above. The maximum SCCG k_{inf} for each of the fuel designs used at DAEC is shown on Table 6.5.

Table 6.5: DAEC Cycle 1-25 Maximum SCCG k_{inf}

Fuel Type	Cycle Loaded	Max k_{inf}
GNF2	25	1.265
GNF2	24	1.267
GE14	23	1.227
GE14	22	1.226
GE14	21	1.217
GE14	20	1.267
GE14	19	1.267
GE14	18	1.236
GE12	17	1.225
GE10	11-16	1.230
GE8B	9-10	1.229
GE6B, 8x8 LTA	8	1.223
GE5	5-7	1.246
GE 8x8	2-4	1.227
GE 7x7	1	1.190

6.2 Rack Model

The PaR rack is modeled in MCNP6. Since the cell walls on both sides of the Boral plate are the same thickness, the PaR rack is modeled as a single assembly in the cell with periodic boundary conditions. Figure 6.1 is a schematic of the rack model and Figure 6.2 is the actual MCNP6 model with a fuel assembly in the cell.

The single assembly PaR rack model misses a small amount of aluminum in the corner which is related to the rounded corners that allows the packing of the formed cells (See Figure 3.1). The reactivity impact of this small loss of aluminum (addition of water) can be estimated using the cell wall tolerance reactivity. Using the tolerance reactivity, ignoring the corner aluminum is worth a few hundredths of a percent in k_{eff} and therefore is ignored.

The Boral panel is assumed to consist of a main Boral section with pure aluminum cladding on all sides. The B_4C and aluminum atom densities in the main section are calculated such that the areal density is preserved and the density is 2.53 gm/cm^3 . Since aluminum and carbon have very small absorption cross sections, so long as the Boral areal density is preserved, use of typical values is acceptable.

Axially, the same lattice at peak reactivity is assumed to be the full length of the active fuel. The rack including the Boral panels are assumed to cover only the $[[\quad]]$ of active fuel. The Boral panels are actually 152 inches long. Above and below the fuel/rack 12 inches of water is assumed followed by a zero flux boundary condition.

The larger models necessary for the analysis of interfaces, accidents, and eccentricity will be discussed in the sections where the analyses of these conditions are described.

For the fuel assemblies, each fuel pin has its unique atom density set transferred from the CASMO-4 depletion analysis.

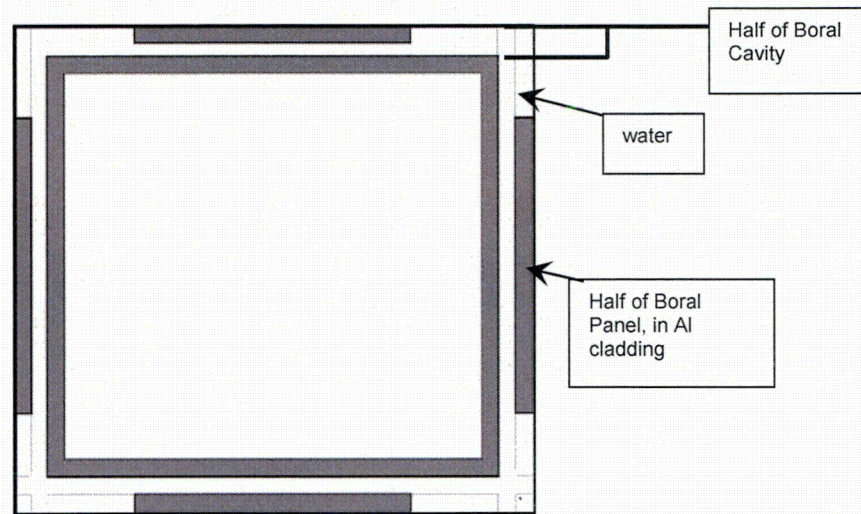


Figure 6.1: PaR Rack Model Schematic

[[

]]

Figure 6.2: MCNP6 PaR Rack Model

6.3 Correlation of SCCG k_{inf} to Rack k_{eff}

In order to find the correlation between SCCG k_{inf} and the rack k_{eff} , MCNP6 rack analyses were performed for all the peak SCCG k_{inf} calculated for all the 10x10 lattices used at DAEC.

Figure 6.3 shows the results of this analysis along with trend lines for each lattice type. Several observations can be made based on Figure 6.3. First, it is clear that changing the location of water rods in the lattice changes the correlation between SCCG k_{inf} and the rack k_{eff} . It would be inappropriate to lump different lattices together for a single statistical trend. Second, the most limiting lattices are GE 12/14 with 14 rods vanished (which is where the rods are gone, i.e., replaced with water), GNF2 with 6 vanished rods, and GNF2 with no vanished rods. Third, for a given SCCG k_{inf} there can be a large

variation in rack k_{eff} . The analysis of the two cases from GNF2 6 vanished rods and an SCCG k_{inf} of 1.195 was reviewed to determine the cause of the large variation. It was noticed that the cases for the most limiting SCCG k_{inf} came from the 40% void rather than the 0% void, which caused the shift to higher rack k_{eff} . Finally, it should be observed that there is no data with SCCG k_{inf} values greater than 1.267 and it is desired to determine the rack k_{eff} for higher values of SCCG k_{inf} .

Based on the observations from Figure 6.3, additional analyses were performed to find a conservative correlation between the SCCG k_{inf} and the rack k_{eff} . For the limiting lattices: GE12/14 all vanished, GNF2 no vanished, and GNF2 6 rods vanished, MCNP6 rack analyses were performed at all of the 7 depletion conditions (Unrodded 0, 40, 70 and 100% void, Rodded 0, 40 and 70% void). To create higher SCCG k_{inf} values, additional lattices were created and analyzed. The description for these additional lattices is found in Table 6.6 and supported by Figure 6.4. For these additional cases, only 4 depletion conditions were used since all the previous limiting cases came from these four depletion conditions (Unrodded 0% void, Rodded 0% void, 40% void and 70% void).

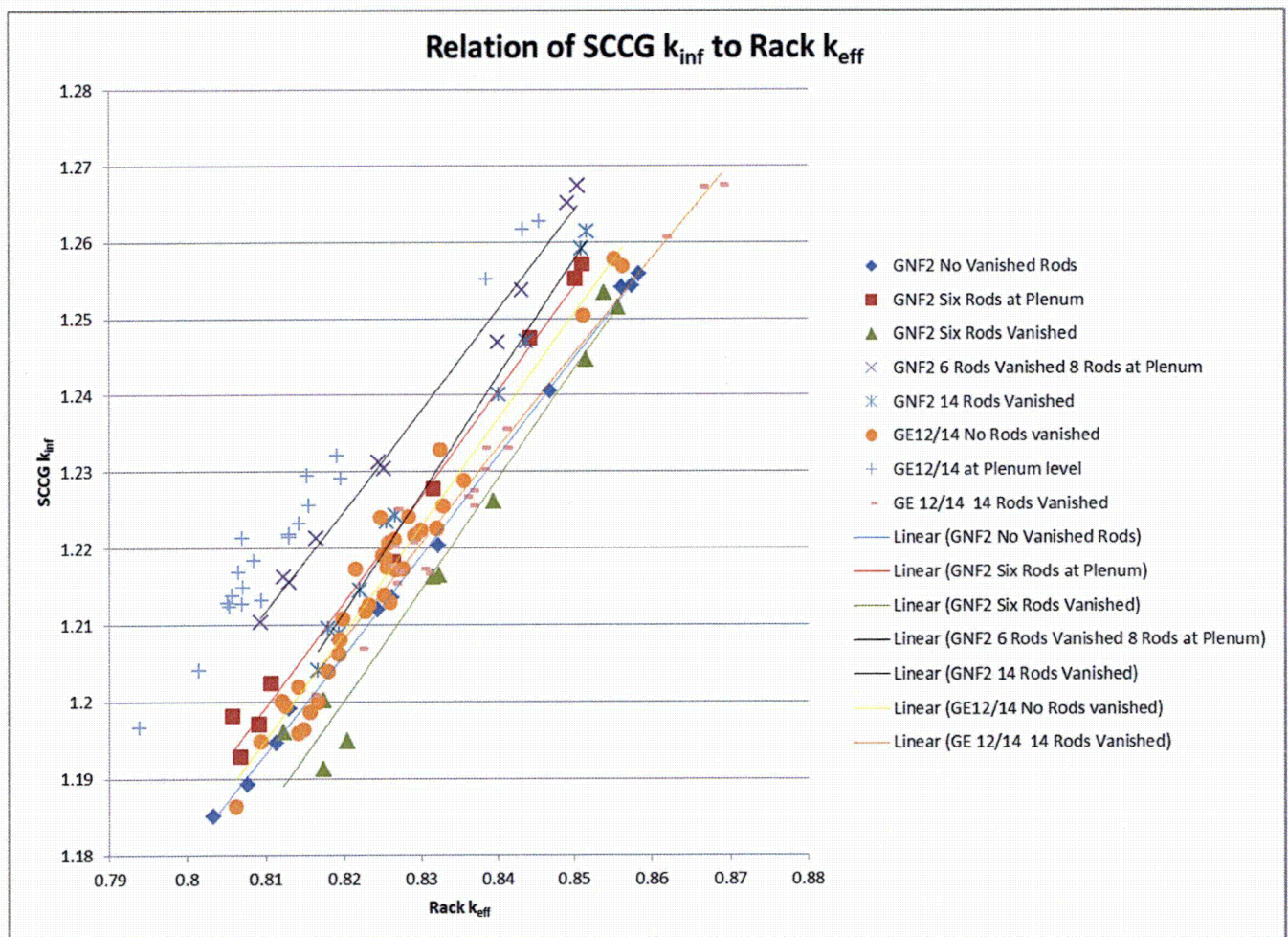


Figure 6.3: SCCG k_{inf} to Rack k_{eff} Relation For 10x10 Fuel

Table 6.6: Lattices Added With Higher SCCG k_{inf}

Design Number	Design Identification	Vanished Rods	Number of Gd Rods	Gd Rods in GNF2 C Designs	Gd wt%	U-235 Enrichment in Fuel Rods
1	GNF2 A	0	10	-	4	5
2	GNF2 B	0	10	-	4	5
3	GNF2 A	6	10	-	4	5
4	GNF2 B	6	10	-	4	5
5	GNF2 C	6	10	G1 – G6	4	5
6	GNF2 A	6	10	-	6	5
7	GNF2 B	6	10	-	6	5
8	GNF2 C	6	10	G1 – G6	6	5
9	GNF2 C	6	5	G1 – G3	8	5
10	GNF2 C	6	6	G1, G3, G4	10	5
11	GNF2 C	6	8	G1 – G5	4	5
12	GNF2 C	6	8	G1 – G5	6	5
13	GNF2 C	6	12	G1 – G7	4	5
14	GNF2 C	6	12	G1 – G7	6	5
15	GNF2 C	6	20	G1 – G8	2	5
16	GNF2 C	6	20	G1 – G8	3	5
17	GNF2 C	6	8	G1 – G5	4	4.4
18	GNF2 C	6	12	G1 – G7	4	4.4
19	GNF2 C	6	20	G1 – G8	2	4.4
20	GNF2 C	6	20	G1 – G8	3	4.4
21	GNF2 C	6	10	G1 – G6	4	4.4

The rack k_{eff} calculated by MCNP6 is plotted against the CASMO-4 SCCG k_{inf} for the GE 12/14 all vanished, GNF2 no vanished, and the GNF2 6 vanished lattices in Figure 6.5. Also in Figure 6.5 is a limiting correlation line between the SCCG k_{inf} and the rack k_{eff} , $rack\ k_{eff} = 0.69 * SCCG\ k_{inf}$.

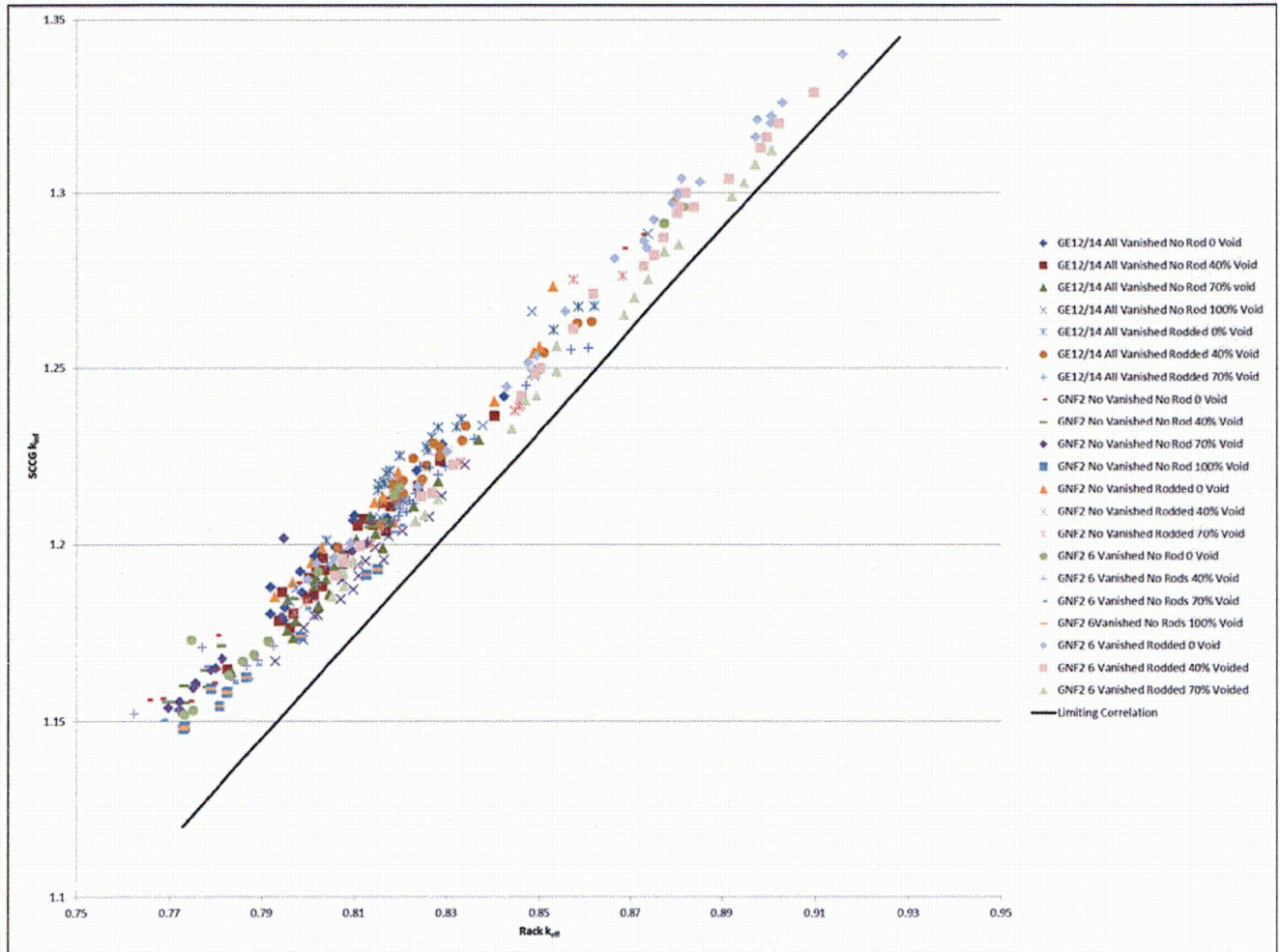
Figure 6.5 provides information on how the depletion parameters affect the SCCG k_{inf} to rack k_{eff} correlation. First, if a higher void level is used in the depletion a higher rack k_{eff} is produced for a given SCCG k_{inf} . However, it should also be observed that the higher void fraction often produces a lower maximum SCCG k_{inf} . Second, the variation of rack k_{eff} for the same SCCG k_{inf} can be greater than 1% in rack k_{eff} even with the same depletion parameters.

The additional cases shown in Table 6.6 provide information on the effect of Gadolinia rod placement. Designs 1-2, 3-5, and 6-8 move the Gadolinia rods from the control rod corner to the opposite (detector) corner. Table 6.7 shows the ratio of the rack k_{eff} to the SCCG k_{inf} for the 8 designs and shows that moving the Gadolinia rods away from the control rod corner increases the rack k_{eff} for a given SCCG k_{inf} for the rodded depletion (the limiting SCCG k_{inf}) and has a small effect on the non-rodded depletion.

[[

]]

Figure 6.4: Lattice Designs for Higher SCCG k_{inf}

Figure 6.5: SCCG k_{inf} to Rack k_{eff} Relation with Limiting CorrelationTable 6.7: SCCG k_{inf} to Rack k_{eff} Relation Comparison

			Depletion Condition	No Rod, 0 Void	Rodded, 0 Void	Rodded, 40% Void	Rodded, 70% Void
Design Number	Vanished Rods	Gd wt%	Design Identification	Rack k_{eff} / SCCG k_{inf}			
1	0	4	GNF2 A	0.678	0.670	0.670	0.673
2	0	4	GNF2 B	0.676	0.678	0.679	0.680
3	6	4	GNF2 A	0.680	0.676	0.678	0.680
4	6	4	GNF2 B	0.680	0.679	0.682	0.684
5	6	4	GNF2 C	0.680	0.681	0.684	0.687
6	6	6	GNF2 A	0.676	0.672	0.675	0.672
7	6	6	GNF2 B	0.674	0.676	0.680	0.684
8	6	6	GNF2 C	0.658	0.679	0.683	0.686

Figure 6.5 shows all the MCNP6 rack analysis results including the additional higher SCCG k_{inf} cases where the Gadolinia rods are located away from the control rod corner. The limiting line in Figure 6.5 is an engineering approximation to bound all the data. However, a more traditional approach would be to do a statistical analysis of the data and create a 95/95 line for the data. This traditional approach is not appropriate since the data points are not random but correlated to the various design features. It has already been shown in Figure 6.3 that the water locations in the lattice creates independent sets of data. Table 6.7 demonstrates that the location of the Gadolinia rods also creates independent sets of data. Although a statistical treatment of the data is not suggested by the data, it is performed to show that the correlation selected (0.69 of the SCCG k_{inf}) covers the traditional approach. Figure 6.6 shows a plot of all the GNF2 no vanished and 6 vanished rods and all depletion conditions SCCG k_{inf} versus rack k_{eff} . The 95/95 limiting line (using the same statistical approach used for the criticality validation) based on this data is shown in the figure.

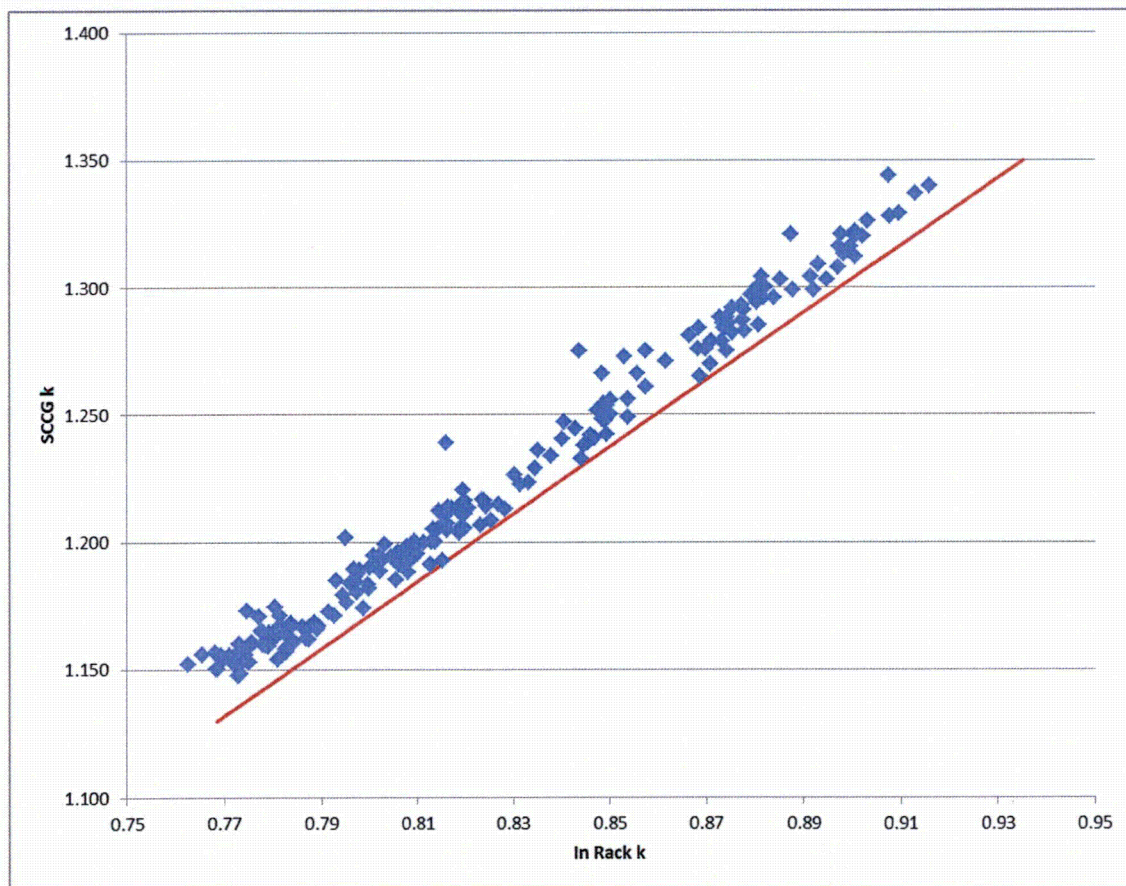


Figure 6.6: SCCG k_{inf} to Rack k_{eff} Relation for GNF2 Data

Rather than using all depletion conditions, it is traditional to use just the cases that match the highest SCCG k_{inf} of all the depletion conditions. Figures 6.7 and 6.8 show the SCCG k_{inf} from the most limiting depletion conditions for the no vanished rods and the 6 vanished rods sets along with the statistically determined limiting line, respectively.

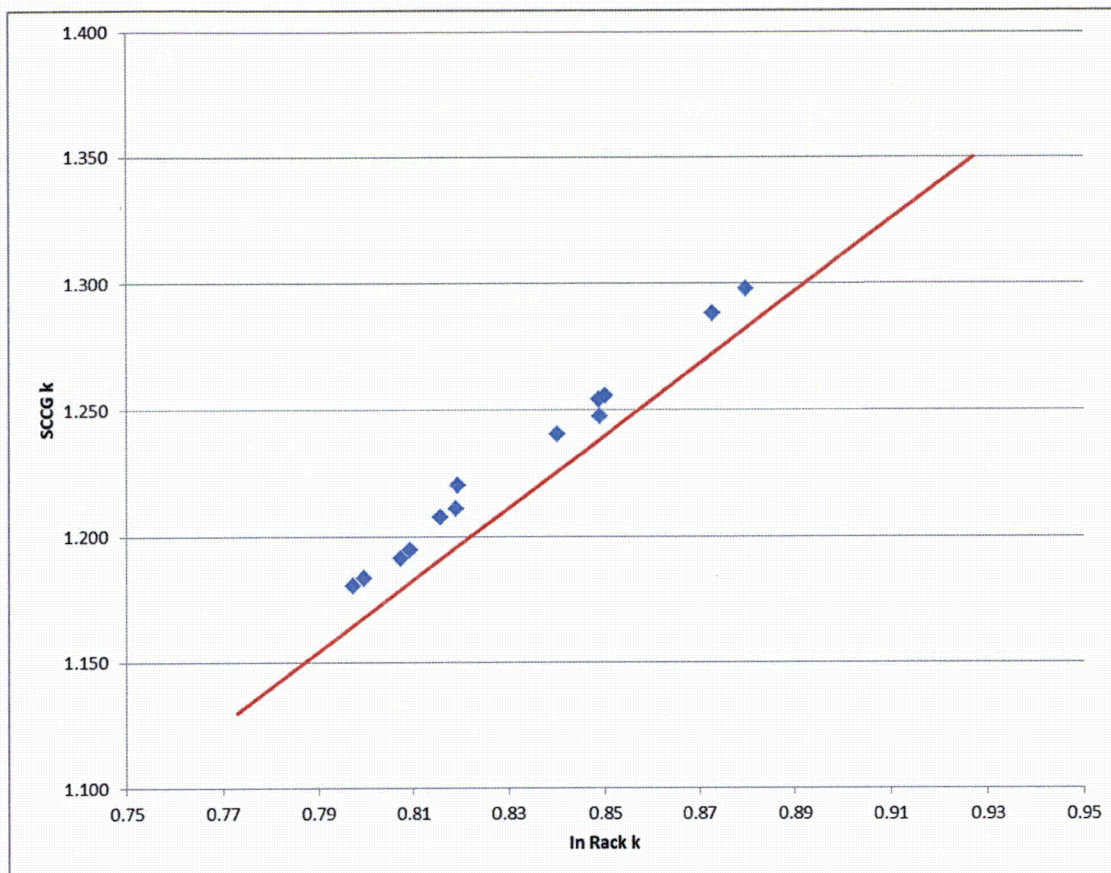


Figure 6.7: SCCG k_{inf} to Rack k_{eff} Relation for GNF2 No Vanished Rod Lattices

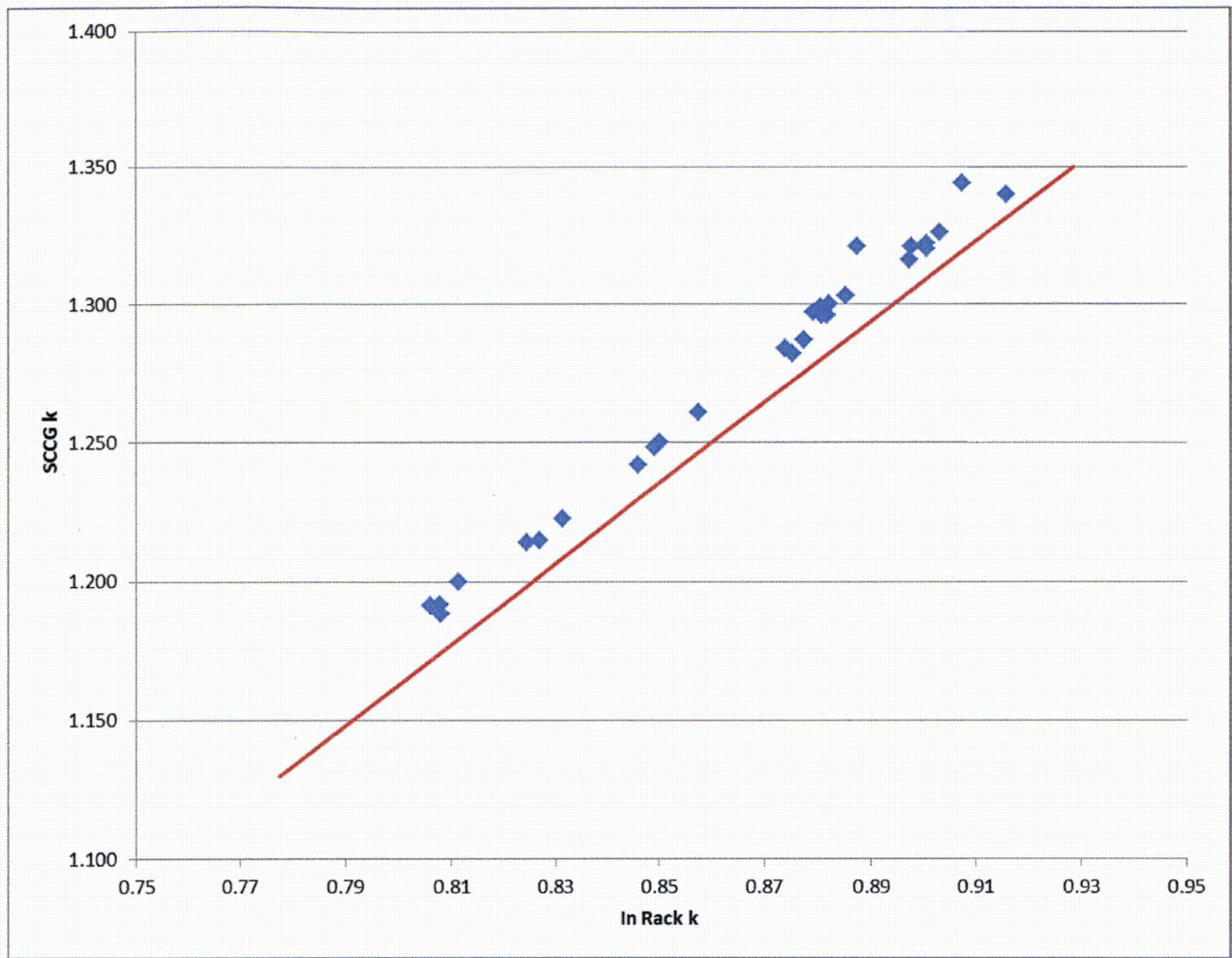


Figure 6.8: SCCG k_{inf} to Rack k_{eff} Relation for GNF2 6 Vanished Rod Lattices

The SCCG k_{inf} to rack k_{eff} correlations can be used to determine what the in-rack k_{eff} would be for the limiting SCCG k_{inf} , selected to be 1.29. Table 6.8 shows the rack k_{eff} that corresponds to the limiting SCCG k_{inf} using the statistical fits and the engineering selected ratio of 0.69. As can be seen from Table 6.8, the engineering selected limiting correlation bounds all of the statistically produced correlations. The base k_{eff} for an SCCG k_{inf} of 1.29 is established at 0.8901.

Table 6.8: Rack k_{eff} for the Limiting SCCG k_{inf} for Various Correlations

Correlation	Rack k_{eff} for an SCCG k_{inf} of 1.29
Statistical Analysis of All GNF2 No Vanished and 6 Rod Vanished Lattices Using All Depletion Conditions (Figure 6.6)	0.8898
Statistical Analysis of GNF2 No Vanished Rod Lattices Using Limiting Depletion Conditions (Figure 6.7)	0.8851
Statistical Analysis of GNF2 6 Vanished Rod Lattices Using Limiting Depletion Conditions (Figure 6.8)	0.8874
Using Engineering Approximation of 0.69×1.29	0.8901

6.4 Limiting Fuel Assembly Lattice

DAEC has used 7x7, 8x8, and 10x10 fuel designs. All the fuel assemblies have been supplied by General Electric (GE), now Global Nuclear Fuel (GNF). Table 6.5 showed the maximum SCCG k_{inf} for each of the fuel designs used at DAEC.

The maximum SCCG k_{inf} for both the GE14 and GNF2 fuel designs is the same, 1.267. Since the maximum SCCG k_{inf} of these fuel designs is more than 2% lower than the selected SCCG k_{inf} limit of 1.29, a new GNF2 lattice was created that matches the SCCG k_{inf} of 1.29. Figure 6.9 illustrates the limiting lattice design. The peak reactivity is 1.28995 which occurred when depleted unrodded at 0% void. The pin isotopics at peak reactivity were imported into the PaR rack model. This lattice was used for the tolerance and uncertainty calculations as well as the eccentricity, interface, and accident calculations.

The maximum SCCG k_{inf} for the 7x7 fuel is 1.190, whereas for the 8x8 fuel it is 1.246. Since there is a large margin to the selected SCCG k_{inf} limit of 1.29, no additional calculations are performed for those designs. Nevertheless, to assure that the margin is maintained, the calculations included here are only applicable to the 7x7 and 8x8 legacy fuel assemblies used at DAEC during Cycles 1 through 16.

[[

]]

Figure 6.9: Limiting Lattice Design

6.5 Uncertainties Calculations

Using the manufacturing tolerances found in Sections 3 and 4, rack calculations are performed with MCNP6 to determine the fuel and rack tolerances. The uncertainty in k_{eff} due to these tolerances was calculated using the MCNP6 model with the limiting fuel from Section 6.4. Table 6.9 shows the delta k_{eff} of each tolerance, using the equation $k_1 - k_2 + 2 \cdot \sqrt{\sigma_1^2 + \sigma_2^2}$.

Table 6.9: Reactivity Uncertainty Due to Manufacturing Tolerances

Case	k	Delta k
Base Case	0.8624	-
Fuel Tolerances		
Increase pellet stack density	0.8631	0.0011
Increase pellet OD	0.8631	0.0011
Decrease clad thickness	0.8659	0.0039
Increase pin pitch	0.8635	0.0015
Decrease water rod thickness	0.8628	0.0008
Increase channel thickness	0.8686	0.0066
PaR Rack Tolerances		
Decrease rack pitch	0.8659	0.0039
Increase cell wall thickness	0.8635	0.0015
Decrease Boral panel width	0.8635	0.0015
Increase Boral cladding thickness	0.8628	0.0008

The channel thickness uncertainty does not use a manufacturing tolerance but rather assumes a channel thicker than the thickest channel. That channel was from an 8x8 fuel design which is non-limiting fuel and no new 8x8 fuel will be used in the future. Due to the small size of this conservative assumption no further effort was made to refine the channel thickness tolerance.

Along with the uncertainty due to manufacturing tolerances, there is an uncertainty in isotopic concentration (depletion uncertainty) as discussed in Section 5. For the depletion uncertainty, the isotopic content was taken from the 25 GWd/MTU step of the limiting fuel depletion. The high burnup was used to maximize the effect on k_{eff} to cover any fuel meeting the SCCG k_{inf} limit. The fresh assembly k_{eff} was calculated to be 0.9714, whereas at 25 GWd/MTU the k_{eff} reduces to 0.7985, for a delta of 0.1733. Using 5% of that delta, the depletion uncertainty is conservatively approximated as 0.0087.

The final uncertainty used in the analysis is from the validation of MCNP6 and the cross sections for the major actinides and structural material. This uncertainty comes from Appendix A. Since the largest uncertainty (depletion uncertainty) is 0.0087 and the uncertainties are statistically combined, uncertainties of less than 0.0009 will have no effect on the combined uncertainty. This observation can be used in determining negligible components of the uncertainty.

6.6 Orientation and Eccentricity

Fuel assemblies used at DAEC are non-symmetric, meaning that one corner of the assembly may be more reactive than another corner. The base model assumes the same orientation of fuel assemblies in the cells. To test the orientation effect, a 30x30 rack model was constructed. In the center of the model, four assemblies were oriented such that the same corner was co-located. All other assemblies were oriented to position the same corner toward the center. The fuel assemblies are symmetric along the diagonal that would start at the control rod corner so there are three unique corners of the assembly. Two lattice designs were analyzed; the limiting fuel design given in Figure 6.9 and design number 20 from Table 6.6. Three orientation runs were made for each lattice design analyzed. The results of the analysis are shown in Table 6.10. As can be seen from Table 6.10 the reactivity effect of the various orientation cases is small.

Along with orientation it is possible to place the assemblies in the corner of the cell rather than the center of the cell as in the base models. In order to find an eccentricity bias the most limiting orientation is analyzed with the assemblies placed as close as possible in the cells (Eccentric in). Table 6.10 shows that the reactivity due to eccentric positioning is negative. Finally in order to get the fuel as close or as far apart as possible the fuel assemblies are dechanneled. Dechanneling is also a large negative reactivity.

Figure 6.10 shows the center section of the 30x30 model where the orientation and eccentricity are tested.

Table 6.10: Orientation and Eccentricity Results

Case	k	Sigma	Delta k
Base: Limiting Fuel Design	0.8625	0.0001	
Corner 1 together	0.8626	0.0001	0.0004
Corner 2 together	0.8623	0.0001	0.0001
Corner 3 together	0.8626	0.0001	0.0004
Corner 1 together and Eccentric in	0.8568	0.0001	-0.0054
Corner 1 together and Eccentric in and Dechanneled	0.8454	0.0001	-0.0168
Base: Design 20 (20 3% Gd rods in corner)	0.8794	0.0001	
Corner 1 together	0.8797	0.0001	0.0006
Corner 2 together	0.8794	0.0001	0.0003
Corner 3 together	0.8795	0.0001	0.0004
Corner 1 together and Eccentric in	0.8753	0.0001	-0.0038
Corner 1 together and Eccentric in and Dechanneled	0.8655	0.0001	-0.0136

[[

]]

Figure 6.10: Eccentric Model with Limiting Orientation

6.7 Additional Biases

MCNP6 runs were performed that removed fission products and minor actinides to determine their worth. Thus, the only isotopes modeled are U-234, U-235, U-238, Pu-238, Pu-239, Pu-240, Pu-241, Pu-242 and Am-241. The k_{eff} of the run was 0.9141, and a delta k_{eff} of is 0.0521. Applying 1.5% of the delta for the worth results in a 0.0008 bias.

Using pure zirconium instead of Zircaloy-4 is conservative for any zirconium alloy. A bias was applied so that any Zirconium alloy can be used in the future for both the channel and the fuel cladding. The k_{eff} of the run was 0.8632, with a delta of 0.0012.

It has been proposed that a large blister of the Boral clad can displace water yielding a positive reactivity. To cover this, it is assumed that all the water between the cell walls adjacent to the Boral panels is removed by the blisters (blister is modeled as a void). This conservative assumption is made to determine a blister bias. The k_{eff} of the Boral blister is 0.8643, with a delta of 0.0023.

6.8 Interface Analysis

PaR-PaR Interface

There is a Boral panel between each fuel cell in all PaR modules but the PaR rack modules have been placed in the pool such that at some module interfaces there are double Boral panels between cells and no Boral panels between other cells. Fortunately, the exterior walls of the PaR rack modules are thick and corners do not allow close placement of the modules. To analyze this situation, a 20x20 cell model of the PaR rack was created with each cell containing the limiting assembly described given in Figure 6.9. The k_{eff} of this model was 0.8571. This is slightly less than the base model k_{eff} of 0.8624 because of the leakage at the edge. The model was then split into two 20x10 cell blocks with a gap in between the two blocks. The top and bottom of each module contains an aluminum cast that extends 1.375 inches beyond the cell pitch. If two modules are touching, there would be a gap of 2.75 inches between the modules. Most of the gap contains aluminum with the rest being water. There is a minimum 0.4 inches of water between the outside of the Boral sheathing and the outer wall of the module. There would be a minimum of 0.8 inches of water between two modules and 1.95 inches of aluminum.

At the interface, the Boral was replaced with water to simulate the missing absorber panels and a double absorber panel was modeled where the formed cells lined up. Figure 6.11 shows the interface model used. The k_{eff} of the interface model was 0.8518 which is less than the k_{eff} of the 20x20 model (0.8571). This shows that there is sufficient distance between the two modules such that the reactivity of the system does not increase even though there is a missing absorber panel between some racks along the interface.

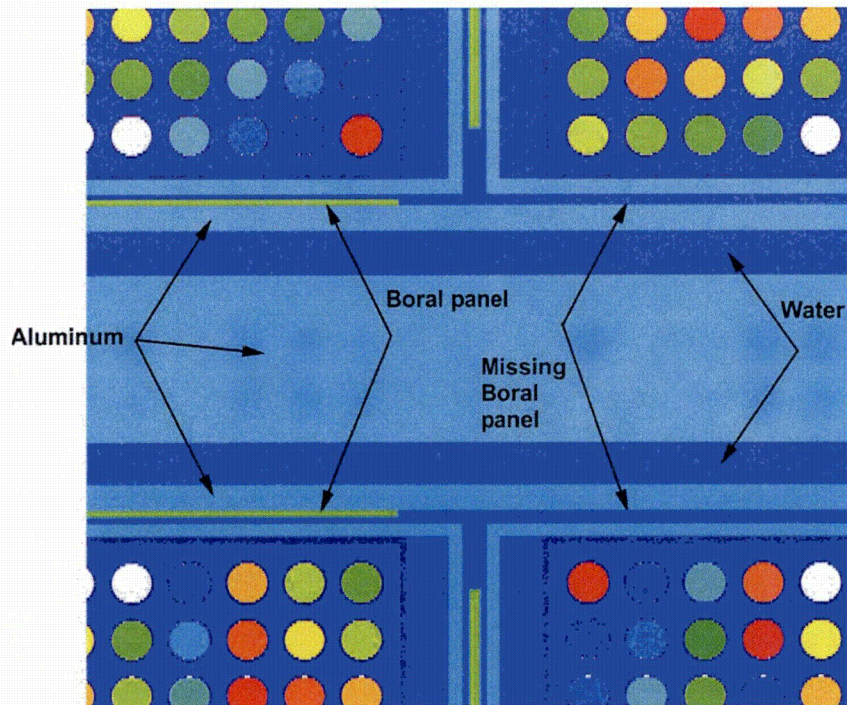


Figure 6.11: PaR-PaR Rack Interface Model

PaR-Holtec Interface

The Holtec racks have Boral panels along the interface with the PaR racks such that all cells on the Holtec rack side, including resultant cells, have Boral panels. The credited Boral areal density of the Boral panels is the same for the Holtec and PaR racks and the maximum allowable SCCG k_{inf} for both racks has been established to be the same (1.29). Looking at the interface from the Holtec rack side, neutrons that leave the Holtec rack see the same absorber panels as the Holtec rack but less fuel since the cell spacing is larger in the PaR racks. Further, the neutrons crossing to a PaR formed cell see an additional Boral panel. Thus, without modeling it is clear that the addition of the PaR racks do not increase k_{eff} in the Holtec racks. Now looking at the interface from the PaR rack side, neutrons go through the same amount of Boral when leaving the PaR rack from a resultant cell and see two Boral panels when leaving a formed cell. The reactivity of the fuel is the same in the PaR and Holtec racks but the cell separation is smaller in the Holtec racks. The PaR and Holtec racks are separated by 3.1 inches. The separation and the additional absorber panel make it clear that the PaR rack k_{eff} will not go up due to the higher density of fuel in Holtec racks. However, a conservative interface model was created to prove the lack of an interface effect on reactivity.

A 40x20 PaR rack model was positioned next to a 40x20 Holtec rack model (see Figure 6.12). The density of the fuel pellet in the Holtec rack was reduced by 23% so that the infinite k_{eff} of both racks was approximately the same (0.8592 for the PaR model and 0.8591 for the Holtec model). The two racks were modeled as touching, ignoring the 3.1 inch separation. As pointed out in the PaR-PaR rack model, the casting on the outside of the modules provides space between the rack modules. The resulting k_{eff} was 0.8573. The starting source for the interface model was in the fuel nearest the interface. Since the interface k_{eff} is less than the two sides, it can be concluded that the source had not yet converged but it is also concluded that the k_{eff} in the area where the source was started is lower than the individual racks. Therefore, it can be concluded there is no increase in k_{eff} due to the interface.

[[

]]

Figure 6.12: PaR-Holtec Rack Interface Model

6.9 Summary of Normal Conditions

During normal operating conditions:

1. Fuel is stored, or moved in and out of rack cells.

Since the most limiting lattice is assumed to be uniform over the entire axial length of the fuel assembly, there is no unanalyzed event when going in and out of cells. A single fuel assembly in the pool is covered by the analysis given in consideration of condition 4 below. Only one assembly can be moved at a time. The fuel assemblies during movement are above the racks such that there is no reactivity effect until being lowered into the desired cell.

2. The fuel can be in any location or orientation in the rack cells.

This is addressed in Section 6.6.

3. Fuel assemblies can be de-channeled.

This is addressed in Section 6.6.

4. Reconstitution is allowed in the fuel handling/inspection/reconstitution platform that is sufficiently separated from the racks to be neutronically isolated (greater than 20 cm of water from other fuel).

A 10x10 fuel assembly was created with unburned 5.0 wt% fuel in each pin, no Gadolinia rods. When isolated by at least 20 cm of water, the k_{eff} for this assembly is 0.6739. Removing 4 pins increased k_{eff} to 0.6762. Removing 4 more pins increased k_{eff} to 0.6815. Removing 2 more pins decreased k_{eff} to 0.6782. Further removal of pins continues to decrease k_{eff} . Having 14 pins removed gives about the same k_{eff} as having no pins removed (0.6741). The most reactive is to remove 8 pins which has a k_{eff} of 0.6815. The isolated assembly with removed pins is not a problem. So long as the removed pins are replaced by stainless steel rods or natural uranium rods, the reconstituted assemblies can be placed in the PaR racks since the reactivity of these replacement pins is less than the reactivity of the pins that were removed. A reconstituted assembly with missing pins would not be acceptable.

All normal operating conditions are covered by the analysis in this report.

6.10 Accident Analysis

This section includes rack analysis for credible accidents. Those are a dropped fuel assembly into a rack location, a missing absorber panel, rack movement into the worst alignment, a misplaced fuel assembly outside yet adjacent to the racks, and loss of spent fuel pool cooling resulting in an over-temperature accident.

6.10.1 Dropped Fuel Assembly

A postulated accident is that a fuel assembly is dropped into a cell, the grids fail, and all pins are separated to an optimum pitch. This accident was modeled by starting with the 20x20 model used as the base case for the interface analysis (Section 6.8).

In the center of the model, a fuel assembly is modeled that has the maximum possible pitch between fuel pins (the assembly is the limiting assembly from Section 6.4). This results in the highest reactivity ($k_{eff} = 0.8584$). The delta-k from the 20x20 base model ($k_{eff} = 0.8571$) is 0.0017.

6.10.2 Missing Boral Panel

It is postulated that there is one missing Boral panel in the rack. The 20x20 base model was modified to replace one panel with water and then to position the two fuel assemblies close together at the cell wall having the missing panel to maximize the reactivity. The k_{eff} was 0.8597 compared to the 20x20 base k_{eff} of 0.8571. The delta k is 0.0030. This is the worst case accident.

6.10.3 Rack Movement and Rack Cell Distortion

The PaR-PaR and PaR-Holtec interface models assume that the racks are touching so there is no rack movement that will increase k_{eff} . No distortion of cell geometry can exceed the impact of removing a Boral panel as done in Section 6.10.2.

6.10.4 Misplaced Assembly

There is a corner between modules E15 and E12 (Figure 3.2) where, if an assembly were to be misplaced, that assembly would not be exposed to any face-adjacent Boral panels. The limiting assembly was modeled in this corner next to three other eccentric-in assemblies with no Boral panel between assemblies. The k_{eff} for this case was 0.8659, with a delta k of 0.0011.

6.10.5 Over-temperature Effects

It is assumed that the most reactive condition in the pool is full density water. To test this assumption, the base case was run with water at a lowered density of 0.98 gm/cm³. The k_{eff} decreased to 0.8611, with a delta of -0.0009. As expected, increasing temperature in the pool reduces k_{eff} .

6.11 Final Calculation of $k_{95/95}$

The k_{eff} of the PaR rack must be below 0.95 at a 95% probability with a 95% confidence level. Using the correlation from Section 6.3, an assembly that has a SCCG k_{inf} of 1.29 has a maximum k_{eff} in the rack of 0.8901. The biases and uncertainties discussed throughout Section 6 are added to determine the 95/95 in-rack k_{eff} . Table 6.11 shows the rack up of the base k_{eff} plus the biases and uncertainties. The final rack up shows that the PaR rack has a maximum k_{eff} with a 95% probability and a 95% confidence level of 0.9160. This is 3.4% less than the allowable limit thus assuring criticality safety.

Table 6.11: Determination of the Final $k_{95/95}$

Base k_{eff}		0.8901
Uncertainties (statistically combined)		0.0149
Fuel Tolerances		
Increase pellet stack density	0.0011	
Increase pellet outside diameter	0.0011	
Decrease clad thickness	0.0039	
Increase pin pitch	0.0015	
Decrease water rod thickness	0.0008	
Increase channel thickness	0.0066	
Rack Tolerances		
Decrease rack pitch	0.0039	
Increase cell wall thickness	0.0015	
Decrease Boral panel width	0.0015	
Increase Boral cladding thickness	0.0008	
Depletion Uncertainty	0.0087	
Validation Uncertainty	0.0079	
Biases		
Orientation		0.0006
Eccentricity		0.0000
De-channeled Assembly		0.0000
Fission Product Worth		0.0008
Zirconium Alloy		0.0012
Boral Blisters		0.0023
Interface Effect		0.0000
Accidents		0.0030
Dropped fuel assembly	0.0017	
Missing absorber panel	0.0030	
Rack Movement	0.0000	
Misplaced fuel assembly	0.0011	
Maximum temperature	0.0000	
Validation		0.0031
Final $k_{95/95}$		0.9160
Margin to 0.95 limit		0.0340

7 Summary and Conclusions

A new criticality safety analysis for the PaR spent fuel pool racks at DAEC is documented in this report. This analysis uses a Boral areal density of $0.015 \text{ gm B-10/cm}^2$ which provides a large margin to the as-built Boral areal density for the PaR spent fuel pool racks and matches the Boral areal density of the Holtec spent fuel pool racks. The previous criticality analysis of record for the PaR spent fuel pool racks allowed fuel assemblies with an SCCG k_{inf} of 1.39. This analysis reduces that limit to 1.29, same as for the Holtec spent fuel pool racks. This new criticality analysis has a calculated $k_{95/95}$ of 0.9160, which provides considerable margin to the regulatory limit of 0.95.

7.1 Limits of the Analysis

The following are the limits to this criticality safety analysis of the PaR spent fuel pool racks:

1. Fuel assemblies must have a SCCG k_{inf} of 1.29 or less.
2. Only 7x7 and 8x8 fuel assemblies allowed for storage are legacy fuel assemblies from Cycles 1 through 16.
3. Future 10x10 fuel assemblies must be bounded by the fuel pellet diameter, clad outer diameter, pin pitch and pellet stack density of the GNF2 fuel lattices analyzed.
4. Fuel cladding material must be a zirconium alloy.
5. Integral burnable poison must be Gadolinia (Gd_2O_3).
6. Reconstituted fuel must contain a stainless steel or natural uranium fuel rod in any location where fuel was removed. (The reconstitution process is safe if done in an isolated area.)
7. The Boral areal density in the panels is greater than or equal to $0.015 \text{ gm B-10/cm}^2$.
8. Rack center to center distance greater or equal to 6.625 inches.
9. Spent Fuel Pool water temperature greater or equal to 4°C .

7.2 SCCG k_{inf} Limit Calculations

Each future fuel assembly must be analyzed to determine its SCCG k_{inf} and demonstrate compliance with this criticality safety analysis. Those future calculations must be performed with the same process used in this analysis to ensure its validity. The analyst is expected to utilize the same CASMO-4 input decks used for this analysis and only change the fuel rod enrichments, the number and position of the Gadolinia rods, and job titles. A brief summary of the process is provided below.

First, the SCCG k_{inf} must be calculated using CASMO-4. Use of any other computer code or cross section library may introduce a bias not included in this analysis. Second, the analysis must include depletion with bounding reactor parameters with unrodded conditions at 0, 40, 70 and 100% void, and also with rodded conditions at 0, 40 and 70% void. The bounding reactor parameters are documented in Section 6.1 of this report. Third, the SCCG k_{inf} is at 20 C and unrodded. The maximum value from all depletions evaluated for each fuel assembly must meet the limit established by this analysis.

8 References

- [1] Letter from Richard Anderson (NextEra Energy Duane Arnold) to U.S. Nuclear Regulatory Commission, "Licensee Event Report #2013-003," NG-13-0411, November 11, 2013.
- [2] Code of Federal Regulations, Title 10, Part 50, Section 68, "Criticality Accident Requirements."
- [3] Code of Federal Regulations, Title 10, Part 50, Appendix A, "General Design Criteria for Nuclear Power Plants," Criteria 62, "Prevention of Criticality in Fuel Storage and Handling."
- [4] NUREG-0800, "Standard Review Plan for the Review of Safety Analysis Reports for Nuclear Power Plants, Section 9.1.1 Revision 3 (Criticality Safety of Fresh and Spent Fuel Storage and Handling)," U.S. Nuclear Regulatory Commission, March 2007.
- [5] K. Wood, Final Division of Safety Systems Interim Staff Guidance, DSS-ISG-2010-01 Revision 0, "Staff Guidance Regarding the Nuclear Criticality Safety Analysis for Spent Fuel Pools," Nuclear Regulatory Commission, October 2011.
- [6] J. Rhodes and K. Smith, "CASMO-4 A Fuel Assembly Burnup Program User's Manual," SSP-01/400 Rev 5, Studsvik Scandpower, Inc. (proprietary).
- [7] J. T. Goorley, et al., *Initial MCNP6 Release Overview – MCNP6 version 1.0*, LA-UR-13-22934, Los Alamos National Laboratory (2013).
- [8] G. Radulescu, I. C. Gauld, G. Ilas, and J. C. Wagner, "An Approach for Validating Actinide and Fission Product Burnup Credit Criticality Safety Analyses – Isotopic Composition Predictions," NUREG/CR-7108, Office of Nuclear Regulatory Research, U.S. Nuclear Regulatory Commission, Washington, DC, USA, April 2012.
- [9] H. Okuno, Y. Naito, and K. Suyama, "OECD/NEA Burnup Credit Criticality Benchmarks Phase IIIB: Burnup Calculations of BWR Fuel Assemblies for Storage and Transport," NEA/NSC/DOC(2002)2, Organization for Economic Cooperation and Development, Nuclear Energy Agency, 2002.
- [10] K. S. Smith, et al., "Benchmarks for Quantifying Fuel Reactivity Depletion Uncertainty," EPRI Technical Report Number 1022909, 2011.
- [11] D. B. Lancaster, "Utilization of the EPRI Depletion Benchmarks for Burnup Credit Validation," EPRI Technical Report Number 1025203, 2012.
- [12] J.C. Dean and R.W. Tayloe, Jr., "Guide for Validation of Nuclear Criticality Safety Computational Methodology," NUREG/CR-6698, Nuclear Regulatory Commission, January 2001.
- [13] International Handbook of Evaluated Criticality Safety Benchmark Experiments, NEA/NSC/DOC(95)3, Volume IV, Nuclear Energy Agency, OECD, September, 2014.
- [14] F. Fernex, "Programme HTC – Phase 1: Réseaux de crayons dans l'eau pure (Water-moderated and reflected simple arrays) Réévaluation des expériences," DSU/SEC/T/2005-33/D.R., Institut de Radioprotection et de Sécurité Nucléaire, 2008.
- [15] F. Fernex, Programme HTC – Phase 2: Réseaux simples en eau empoisonnée (bore et gadolinium) (Reflected simple arrays moderated by poisoned water with gadolinium or boron) Réévaluation des expériences, DSU/SEC/T/2005-38/D.R., Institut de Radioprotection et de Sécurité Nucléaire, 2008.
- [16] F. Fernex, Programme HTC – Phase 3: Configurations "stockage en piscine" (Pool storage) Réévaluation des expériences, DSU/SEC/T/2005-37/D.R., Institut de Radioprotection et de Sécurité Nucléaire, 2008.

- [17] B. T. Rearden, D. E. Mueller, S. M. Bowman, R. D. Busch, and S. J. Emerson, "TSUNAMI Primer: A Primer for Sensitivity/Uncertainty Calculations with SCALE," ORNL/TM-2009/027, Oak Ridge National Laboratory, January 2009.
- [18] U.S. Nuclear Regulatory Commission, Spent Fuel Project Office Interim Staff Guidance – 8, Rev. 3 – Burnup Credit in the Criticality Safety Analyses of PWR Spent Fuel in Transportation and Storage Casks, Nuclear Regulatory Commission, 2012.
- [19] J. M. Scaglione, D. E. Mueller, J.C. Wagner and W. J. Marshall, "An Approach for Validating Actinide and Fission Product Burnup Credit Criticality Safety Analyses—Criticality (k_{eff}) Predictions," NUREG/CR-7109, Oak Ridge National Laboratory, 2012.
- [20] Response to Request for Additional Information NETCO Report NET-300067-01, Revision 1, (Non- proprietary), Attachment 1, Question 21, NL-15-089, Entergy Nuclear Operations. Inc., The Indian Point Nuclear Generating Unit No. 2, Spent Fuel Pool Criticality Analysis, Docket No. 50-247, (2015). (NRC Adams Accession Number ML15261A528)
- [21] SFCOMPO – Spent Fuel Isotopic Composition Database, Organization for Economic Cooperation and Development, Nuclear Energy Agency, <https://www.oecd-neo.org/sfcompo/>.
- [22] A. S. Chesterman, A. Simpson, and Martin Clapham, "Burnup Credit Measurements for Cask Loading Compliance – A Review of Techniques and Calibration Philosophies," WM2011 Conference, February 27 – March 3, 2011, Phoenix, AZ.

Appendix A: Criticality Analysis Validation

This appendix determines the computer code and cross-section library bias and uncertainty in the effective multiplication factors (k_{eff}) calculated for the DAEC spent fuel pool when using MCNP6 Version 1.0 [1]. The bias and uncertainties determined in this Appendix cover the major actinides and structural materials.

All the analyses are performed using the ENDF/B-VII.1 library except for elemental cross sections that come from an earlier library. All the computer runs use a large Monte Carlo sampling of at least 800 generations and 5000 neutrons per generation. Note that these are minimum values for all cases combined, so some cases used a much higher number of neutrons per generation, while other cases used a much higher total number of generations. A minimum of 100 cycles are skipped. All cases were verified to have source convergence.

This Appendix is divided into two sections: fresh fuel critical experiments, and HTC critical experiments.

A.1 Fresh Fuel Critical Experiments

A.1.1 Introduction

The validation consists of modeling 131 fresh fuel (UO_2) critical experiments and the determination of the bias and the uncertainty in the calculation of k_{eff} . This validation follows the direction of NUREG/CR-6698, "Guide for Validation of Nuclear Criticality Safety Calculational Methodology" [2].

A.1.2 Parameter Range Definition

The validation guidance document [2] states:

"Prior to the initiation of the validation activity, the operating conditions and parameters for which the validation is to apply must be identified. The fissile isotope, enrichment of fissile isotope, fuel density, fuel chemical form, types of neutron moderators and reflectors, range of moderator to fissile isotope, neutron absorbers, and physical configurations are among the parameters to specify. These parameters will come to define the area of applicability for the validation effort."

The racks are assumed to be flooded with water at near room temperature and below 100° C. The fuel is low enriched uranium dioxide (less than or equal to 5.0 wt% U-235). The fuel is in pellets with a density of greater than [[]] of the theoretical density. The only significant neutron moderators are water and the oxygen in the fuel pellet. The neutron absorbers credited are boron (as plates) and gadolinium (in rods). The reflectors are water, steel, or concrete. The fuel is in assemblies. The assembly arrangement can vary by design from totally isolated assemblies to a close packed array of assemblies. The fuel rods are in a square lattice.

A.1.3 Critical Benchmark Experiments Selection

The fresh fuel benchmarks that were selected met the following criteria:

- Low enriched (5 wt% U-235 or less) UO_2 to cover the principle isotopes of concern
- Fuel in rods
- Square lattices
- Presence of boron
- No emphasis on a feature or material not of importance to the rack analysis

The OECD/NEA *International Handbook of Evaluated Criticality Safety Benchmarks Experiments* [3] is considered as the appropriate reference for criticality safety benchmarks. This handbook has reviewed the available benchmarks and evaluated the uncertainties in the experiments. The appropriate modeling is presented. All of the experiments used in this validation were taken from this handbook. Volume IV of the handbook is for low enriched uranium systems. The section of Volume IV of interest to this validation is the "Thermal Compound Systems." All of the experiments selected are numbered LEU-COMP-THERM-0XX. This validation will refer to the experiments LEU-COMP-THERM-0XX as just XX where any leading zero is not included.

There are more critical experiments in the handbook that meet the requirements for this validation than would be necessary to use. Twelve (12) different evaluations (set of experiments) were used for this validation. The selected experiments cover the needed range and have sample MCNP decks as part of the handbook. Table A.1 provides a summary of all the 12 evaluations used.

Table A.1: Criticality Benchmarks Selection Review
(All Experiments Start With LEU-COMP-THERM-)

Benchmark Number	Description	Laboratory	Experiments Selected
1	WATER-MODERATED $\text{U}(2.35)\text{O}_2$ FUEL RODS IN 2.032-CM SQUARE-PITCHED ARRAYS	PNL	All 8
2	WATER-MODERATED $\text{U}(4.31)\text{O}_2$ FUEL RODS IN 2.54-CM SQUARE-PITCHED ARRAYS	PNL	All 5
6	CRITICAL ARRAYS OF LOW-ENRICHED UO_2 FUEL RODS WITH WATER-TO-FUEL VOLUME RATIOS RANGING FROM 1.5 TO 3.0	JAERI	Cases 1-12, 14-16
8	CRITICAL LATTICES OF UO_2 FUEL RODS AND PERTURBING RODS IN BORATED WATER	B&W	Cases 1-3, 16 and 17
9	WATER-MODERATED RECTANGULAR CLUSTERS OF $\text{U}(4.31)\text{O}_2$ FUEL RODS (2.54-CM PITCH) SEPARATED BY STEEL, BORAL, COPPER, CADMIUM, ALUMINUM, OR ZIRCALOY-4 PLATES	PNL	Cases 1-9 and 24-27
10	WATER-MODERATED $\text{U}(4.31)\text{O}_2$ FUEL RODS REFLECTED BY TWO LEAD, URANIUM, OR STEEL WALLS	PNL	Cases 5-19 and 24-30

Benchmark Number	Description	Laboratory	Experiments Selected
13	WATER-MODERATED RECTANGULAR CLUSTERS OF U(4.31)O ₂ FUEL RODS (1.892-CM PITCH) SEPARATED BY STEEL, BORAL, BOROFLEX, CADMIUM, OR COPPER PLATES, WITH STEEL REFLECTING WALLS	PNL	Cases 1-4
16	WATER-MODERATED RECTANGULAR CLUSTERS OF U(2.35)O ₂ FUEL RODS (2.032-CM PITCH) SEPARATED BY STEEL, BORAL, COPPER, CADMIUM, ALUMINUM, OR ZIRCALOY-4 PLATES	PNL	Cases 1-5,8,10,12,14, and 28-32
42	WATER-MODERATED RECTANGULAR CLUSTERS OF U(2.35)O ₂ FUEL RODS (1.684-CM PITCH) SEPARATED BY STEEL, BORAL, BOROFLEX, CADMIUM, OR COPPER PLATES, WITH STEEL REFLECTING WALLS	PNL	Cases 1-4
51	CRITICAL EXPERIMENTS SUPPORTING CLOSE PROXIMITY WATER STORAGE OF POWER REACTOR FUEL (PART II - ISOLATING PLATES)	B&W	Cases 10, 11a-g, 12
62	2.6%-ENRICHED UO ₂ RODS IN LIGHT-WATER MODERATOR WITH BORATED STAINLESS STEEL PLATE: SINGLE ARRAYS	JAERI	Cases 1-15
65	CRITICAL CONFIGURATIONS OF 2.6%-ENRICHED UO ₂ ROD ARRAYS IN LIGHT-WATER MODERATOR WITH BORATED STAINLESS STEEL PLATE: COUPLED ARRAYS	JAERI	Cases 1-17

A.1.4 Critical Benchmark Experiments Evaluation

MCNP input decks exist in the OECD/NEA handbook [3] disc for many of the critical experiments. In general, these input decks were used with minor modifications. All the decks were modified to at least 5000 neutrons per generation and at least 600 active cycles. This was sufficient to make the Monte Carlo uncertainty roughly one tenth of the experimental uncertainty. Generally the cross section library had to be updated. Although there was considerable help by starting with the input files given in the handbook, the ownership of the files was taken, as required by NUREG/CR-6698 [2] and as stated in section 2.3:

For specific critical experiments, the facility or site may choose to use input files generated elsewhere to expedite the validation process. The site has the responsibility for ensuring that input files and the options selected are appropriate for use. Regardless of the source of the input file, the site must have reviewed the description of each critical experiment and determined that

the representation of the experiment, including simplifying assumptions and options, are consistent with the intended use. In other words, the site must assume ownership of the input file.

Table A.2 shows the results of the analysis of the 131 fresh fuel critical experiments, along with parameters that are used to check for trends in the results. The spectral index, the Energy of the Average Lethargy of the neutrons causing Fission (EALF), is a calculated value extracted from the MCNP output.

Table A.2: Fresh Fuel Critical Experiment Results

Benchmark ID	Case No.	Enrichment (wt% U-235)	Fuel Pin Pitch (cm)	EALF (eV)	Experiment Uncertainty	k _{eff} (norm)	Monte Carlo Sigma
LCT-1	1	2.35	2.032	0.0987	0.0031	1.0000	0.00013
	2	2.35	2.032	0.0981	0.0031	0.9992	0.00012
	3	2.35	2.032	0.0971	0.0031	0.9986	0.00011
	4	2.35	2.032	0.0978	0.0031	0.9994	0.00012
	5	2.35	2.032	0.0964	0.0031	0.9973	0.00012
	6	2.35	2.032	0.0974	0.0031	0.9991	0.00012
	7	2.35	2.032	0.0956	0.0031	0.9986	0.00012
	8	2.35	2.032	0.0967	0.0031	0.9976	0.00012
LCT-2	1	4.31	2.54	0.1159	0.0020	0.9990	0.00025
	2	4.31	2.54	0.1158	0.0020	1.0001	0.00024
	3	4.31	2.54	0.1153	0.0020	0.9997	0.00025
	4	4.31	2.54	0.1146	0.0020	0.9994	0.00024
	5	4.31	2.54	0.1130	0.0020	0.9976	0.00025
LCT-6	1	2.596	1.849	0.2412	0.0020	1.0002	0.00036
	2	2.596	1.849	0.2484	0.0020	1.0003	0.00036
	3	2.596	1.849	0.2548	0.0020	1.0007	0.00037
	4	2.596	1.956	0.1861	0.0020	0.9993	0.00036
	5	2.596	1.956	0.1917	0.0020	0.9998	0.00034
	6	2.596	1.956	0.1971	0.0020	0.9999	0.00036
	7	2.596	1.956	0.2019	0.0020	0.9996	0.00037
	8	2.596	1.956	0.2066	0.0020	1.0008	0.00035
	9	2.596	2.150	0.1391	0.0020	1.0004	0.00034
	10	2.596	2.150	0.1427	0.0020	0.9998	0.00035
	11	2.596	2.150	0.1461	0.0020	0.9998	0.00037
	12	2.596	2.150	0.1498	0.0020	0.9996	0.00038
	14	2.596	2.293	0.1174	0.0020	1.0001	0.00035
	15	2.596	2.293	0.1205	0.0020	0.9989	0.00038
	16	2.596	2.293	0.1229	0.0020	0.9994	0.00033
LCT-8	1	2.459	1.636	0.2832	0.0012	1.0004	0.00035
	2	2.459	1.636	0.2494	0.0012	0.9997	0.00035
	3	2.459	1.636	0.2486	0.0012	1.0011	0.00033
	16	2.459	1.636	0.2312	0.0012	1.0001	0.00033
	17	2.459	1.636	0.2013	0.0012	0.9989	0.00035
LCT-9	1	4.31	2.54	0.1153	0.0021	0.9990	0.00027
	2	4.31	2.54	0.1148	0.0021	0.9989	0.00028
	3	4.31	2.54	0.1152	0.0021	0.9981	0.00028
	4	4.31	2.54	0.1146	0.0021	0.9991	0.00028
	5	4.31	2.54	0.1163	0.0021	0.9996	0.00027
	6	4.31	2.54	0.1153	0.0021	0.9985	0.00027
	7	4.31	2.54	0.1164	0.0021	0.9995	0.00028
	8	4.31	2.54	0.1156	0.0021	0.9986	0.00028
	9	4.31	2.54	0.1164	0.0021	0.9991	0.00027

Benchmark ID	Case No.	Enrichment (wt% U-235)	Fuel Pin Pitch (cm)	EALF (eV)	Experiment Uncertainty	k _{eff} (norm)	Monte Carlo Sigma
	24	4.31	2.54	0.1149	0.0021	0.9987	0.00029
	25	4.31	2.54	0.1144	0.0021	0.9990	0.00028
	26	4.31	2.54	0.1148	0.0021	0.9993	0.00029
	27	4.31	2.54	0.1144	0.0021	0.9990	0.00029
LCT-10	5	4.31	2.54	0.3587	0.0021	0.9995	0.00026
	6	4.31	2.54	0.2658	0.0021	0.9997	0.00024
	7	4.31	2.54	0.2121	0.0021	1.0016	0.00029
	8	4.31	2.54	0.1870	0.0021	0.9981	0.00027
	9	4.31	2.54	0.1249	0.0021	1.0008	0.00027
	10	4.31	2.54	0.1211	0.0021	1.0011	0.00028
	11	4.31	2.54	0.1183	0.0021	1.0010	0.00029
	12	4.31	2.54	0.1152	0.0021	0.9991	0.00028
	13	4.31	2.54	0.1128	0.0021	0.9975	0.00027
	14	4.31	1.892	0.3133	0.0028	1.0027	0.00029
	15	4.31	1.892	0.3009	0.0028	1.0032	0.00030
	16	4.31	1.892	0.2909	0.0028	1.0034	0.00029
	17	4.31	1.892	0.2847	0.0028	1.0024	0.00028
	18	4.31	1.892	0.2794	0.0028	1.0032	0.00029
	19	4.31	1.892	0.2732	0.0028	1.0022	0.00029
	24	4.31	1.892	0.6054	0.0028	0.9999	0.00027
	25	4.31	1.892	0.5592	0.0028	1.0017	0.00028
	26	4.31	1.892	0.5186	0.0028	1.0023	0.00027
	27	4.31	1.892	0.4830	0.0028	1.0028	0.00028
	28	4.31	1.892	0.4547	0.0028	1.0028	0.00030
	29	4.31	1.892	0.4293	0.0028	1.0021	0.00027
	30	4.31	1.892	0.3729	0.0028	1.0005	0.00028
LCT-13	1	4.31	1.892	0.2896	0.0018	1.0016	0.00029
	2	4.31	1.892	0.2967	0.0018	1.0019	0.00031
	3	4.31	1.892	0.3006	0.0018	1.0012	0.00031
	4	4.31	1.892	0.3005	0.0018	1.0013	0.00030
LCT-16	1	2.35	2.032	0.0981	0.0031	0.9985	0.00024
	2	2.35	2.032	0.0976	0.0031	0.9973	0.00024
	3	2.35	2.032	0.0975	0.0031	0.9985	0.00024
	4	2.35	2.032	0.0977	0.0031	0.9973	0.00024
	5	2.35	2.032	0.0975	0.0031	0.9981	0.00025
	8	2.35	2.032	0.0992	0.0031	0.9987	0.00023
	10	2.35	2.032	0.0992	0.0031	0.9978	0.00026
	12	2.35	2.032	0.0999	0.0031	0.9981	0.00024
	14	2.35	2.032	0.0999	0.0031	0.9993	0.00026
	28	2.35	2.032	0.0974	0.0031	0.9982	0.00024
	29	2.35	2.032	0.0972	0.0031	0.9975	0.00024
	30	2.35	2.032	0.0972	0.0031	0.9986	0.00025
	31	2.35	2.032	0.0971	0.0031	0.9992	0.00024
	32	2.35	2.032	0.0971	0.0031	0.9982	0.00025
LCT-42	1	2.35	1.684	0.1733	0.0016	0.9991	0.00025
	2	2.35	1.684	0.1795	0.0016	0.9984	0.00024
	3	2.35	1.684	0.1862	0.0016	0.9984	0.00025
	4	2.35	1.684	0.1845	0.0017	0.9999	0.00024
LCT-51	1 C10	2.459	1.636	0.1495	0.0020	0.9969	0.00023
	2 c11a	2.459	1.636	0.1997	0.0024	0.9982	0.00024
	3 c11b	2.459	1.636	0.1992	0.0024	0.9986	0.00024

Benchmark ID	Case No.	Enrichment (wt% U-235)	Fuel Pin Pitch (cm)	EALF (eV)	Experiment Uncertainty	k _{eff} (norm)	Monte Carlo Sigma
	4 c11c	2.459	1.636	0.2005	0.0024	0.9985	0.00024
	5 c11d	2.459	1.636	0.2015	0.0024	0.9985	0.00024
	6 c11e	2.459	1.636	0.2025	0.0024	0.9986	0.00024
	7 c11f	2.459	1.636	0.2031	0.0024	0.9981	0.00025
	8 c11g	2.459	1.636	0.2035	0.0024	0.9990	0.00025
	9 c12	2.459	1.636	0.1694	0.0019	0.9973	0.00023
LCT-62	1	2.6	1.9558	0.1887	0.0016	1.0034	0.00025
	2	2.6	1.9558	0.1911	0.0016	1.0050	0.00025
	3	2.6	1.9558	0.1928	0.0016	1.0041	0.00027
	4	2.6	1.9558	0.1915	0.0016	1.0045	0.00025
	5	2.6	1.9558	0.1904	0.0016	1.0037	0.00026
	6	2.6	1.9558	0.1942	0.0016	1.0037	0.00025
	7	2.6	1.9558	0.1950	0.0016	1.0041	0.00026
	8	2.6	1.9558	0.1926	0.0016	1.0049	0.00024
	9	2.6	1.9558	0.1934	0.0016	1.0023	0.00026
	10	2.6	1.9558	0.1910	0.0016	1.0047	0.00026
	11	2.6	1.9558	0.1919	0.0016	1.0032	0.00027
	12	2.6	1.9558	0.1947	0.0016	1.0032	0.00026
	13	2.6	1.9558	0.1950	0.0016	1.0039	0.00026
	14	2.6	1.9558	0.1933	0.0016	1.0040	0.00025
	15	2.6	1.9558	0.1922	0.0016	1.0041	0.00025
LCT-65	1	2.6	1.9558	0.1937	0.0014	1.0028	0.00024
	2	2.6	1.9558	0.1985	0.0014	1.0031	0.00025
	3	2.6	1.9558	0.2010	0.0015	1.0029	0.00026
	4	2.6	1.9558	0.2011	0.0015	1.0029	0.00027
	5	2.6	1.9558	0.1919	0.0014	1.0037	0.00025
	6	2.6	1.9558	0.1950	0.0014	1.0038	0.00025
	7	2.6	1.9558	0.1944	0.0014	1.0038	0.00026
	8	2.6	1.9558	0.1965	0.0016	1.0036	0.00025
	9	2.6	1.9558	0.1954	0.0015	1.0027	0.00025
	10	2.6	1.9558	0.1981	0.0016	1.0023	0.00025
	11	2.6	1.9558	0.1972	0.0016	1.0020	0.00025
	12	2.6	1.9558	0.1997	0.0017	1.0031	0.00026
	13	2.6	1.9558	0.1980	0.0016	1.0020	0.00025
	14	2.6	1.9558	0.1983	0.0016	1.0032	0.00026
	15	2.6	1.9558	0.1973	0.0016	1.0034	0.00026
	16	2.6	1.9558	0.2000	0.0017	1.0027	0.00027
	17	2.6	1.9558	0.1979	0.0016	1.0021	0.00025

A.1.5 Critical Benchmark Results Statistical Analysis

The statistical treatment used follows the guidance provided in NUREG/CR-6698 [2]. The first step of the statistical analysis is to test for normality. The Anderson-Darling normality test [4] was used, which concludes that this set of experiments fails the normality test. Figure A.1 is a histogram of the calculated k_{eff} of the experiments. Since the histogram shows that the data is not close to a normal distribution a non-parametric approach is used to determine the bias and uncertainty. However, to assure that the non-parametric approach is conservative the statistical approach for normal data from NUREG/CR-6698 is also used to determine a bias and uncertainty and the more limiting values are used.

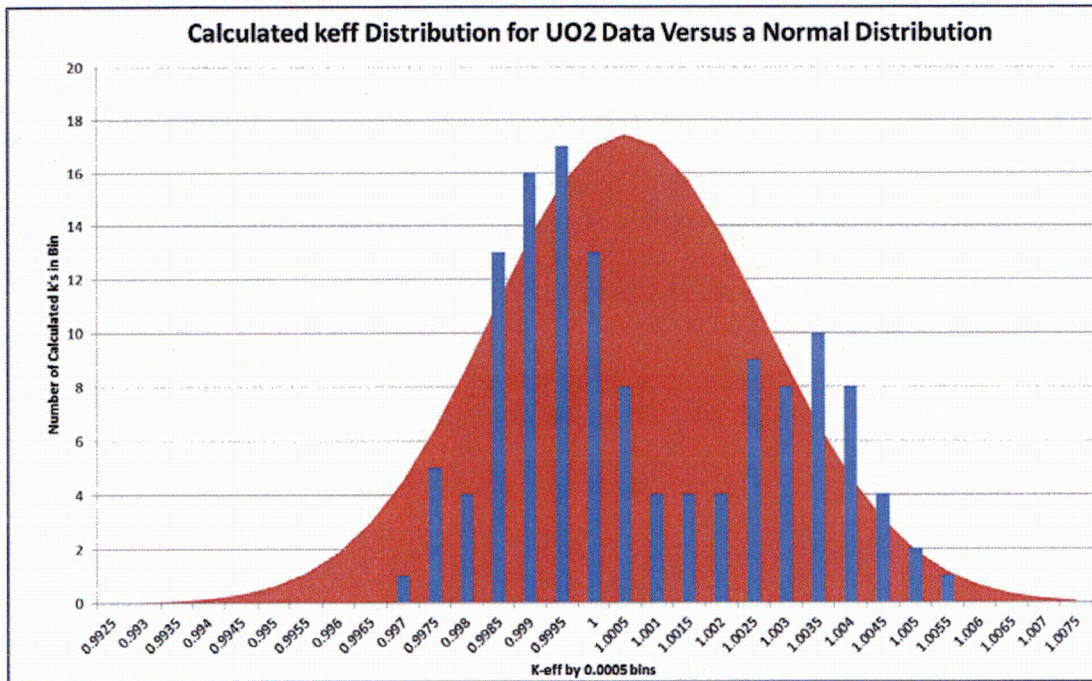


Figure A.1: Fresh Fuel Critical Experiments Histogram

Before presenting the results of the analysis, the equations used for the normal and non-parametric analysis are presented. Most of the equations come directly from NUREG/CR-6698, so to aid in comparing this document with NUREG/CR-6698, equation numbers from NUREG/CR-6698 are given in parentheses.

The first set of equations is used to calculate the bias and uncertainty without trends.

First, the normalized keff for each experiment is calculated using the following equation (9):

$$k_{\text{norm}} = k_{\text{calc}} / k_{\text{exp}}$$

Similarly, the combined error for each experiment is calculated (3):

$$\sigma_t = \sqrt{\sigma_{\text{calc}}^2 + \sigma_{\text{exp}}^2}$$

The weighted mean keff (6):

$$\bar{k}_{\text{eff}} = \frac{\sum \frac{1}{\sigma_i^2} k_{\text{eff},i}}{\sum \frac{1}{\sigma_i^2}}$$

The bias is calculated as follows (8):

$$\text{Bias} = \bar{k}_{\text{eff}} - 1; \text{ the bias is set to zero if calculated to be greater than zero.}$$

The variance about the mean (4):

$$s^2 = \frac{\frac{1}{n-1} \sum \left\{ \frac{1}{\sigma_i^2} [k_{\text{eff},i} - \bar{k}_{\text{eff}}]^2 \right\}}{\frac{1}{n} \sum \frac{1}{\sigma_i^2}}$$

The average total uncertainty (5):

$$\bar{\sigma}^2 = \frac{n}{\sum \frac{1}{\sigma_i^2}}$$

The square root of the pooled variance (7):

$$S_p = \sqrt{s^2 + \bar{\sigma}^2}$$

The uncertainty is calculated by multiplying the square root of the pooled variance by the one-sided lower tolerance factor. Table 2.1 of NUREG/CR-6698 provides one-sided lower tolerance factors up to n=50; for simplicity, that value will be used in the calculations here (2.065).

The second set of equations is used to calculate the bias and uncertainty with trends. For these equations parameter y is for the dependent variable (k_{eff}), and parameter x is for the independent variables (e.g., enrichment, EALF).

First, the linear equation for the fit (10):

$$Y(x) = a + bx$$

The coefficients are calculated using the next three equations (11, 12, 13):

$$a = \frac{1}{\Delta} \left[\sum \frac{x_i^2}{\sigma_i^2} \sum \frac{y_i}{\sigma_i^2} - \sum \frac{x_i}{\sigma_i^2} \sum \frac{x_i y_i}{\sigma_i^2} \right]$$

$$b = \frac{1}{\Delta} \left[\sum \frac{1}{\sigma_i^2} \sum \frac{x_i y_i}{\sigma_i^2} - \sum \frac{x_i}{\sigma_i^2} \sum \frac{y_i}{\sigma_i^2} \right]$$

$$\Delta = \sum \frac{1}{\sigma_i^2} \sum \frac{x_i^2}{\sigma_i^2} - \left[\sum \frac{x_i}{\sigma_i^2} \right]^2$$

The weighted mean for the independent parameter (15):

$$\bar{x} = \frac{\sum \frac{1}{\sigma_i^2} x_i}{\sum \frac{1}{\sigma_i^2}}$$

The bias is calculated as follows (23):

$$Bias = k_{fit}(x) - 1; \text{ the bias is set to zero if calculated to be greater than zero.}$$

Finally, the uncertainty is computed from (23):

$$S_{Pfit} \left\{ \sqrt{2F_a^{(2,n-2)} \left[\frac{1}{n} + \frac{(x - \bar{x})^2}{\sum (x_i - \bar{x})^2} \right]} + Z_{2p-1} \sqrt{\frac{(n-2)}{\chi_{1-\gamma, n-2}^2}} \right\}$$

where p = desired confidence (0.95) and the remaining parameters are computed as follows (26, 25, 30, 28):

$$\sum (x_i - \bar{x})^2 = \frac{\sum \frac{1}{\sigma_i^2} (x_i - \bar{x})^2}{\frac{1}{n} \sum \frac{1}{\sigma_i^2}}$$

$$\gamma = \frac{1-p}{2}$$

$$s_{fit}^2 = \frac{\frac{1}{n-2} \sum \left\{ \frac{1}{\sigma_i^2} [k_{eff,i} - k_{fit}(x_i)]^2 \right\}}{\frac{1}{n} \sum \frac{1}{\sigma_i^2}}$$

$$S_{Pfit} = \sqrt{s_{fit}^2 + \bar{\sigma}^2}$$

For the non-parametric analysis the following equations are used to determine its bias and uncertainty.

The percent confidence that 95% of the population is above the lowest observed value (32):

$$\beta = 1 - 0.95^n$$

The bias is calculated as follows:

$$Bias = Smallest k_{eff} - 1$$

The uncertainty is noted in (33) to be the uncertainty for the smallest k_{eff} . If the sample size is much smaller than used here, there's an additional term to be included with the bias and uncertainty, "NPM", or non-parametric margin. For the sample size used here, NPM is zero.

The non-trended weighted mean k_{eff} of the 131 critical experiments is greater than 1.0, therefore the bias is conservatively taken as zero. The non-trended uncertainty is 0.0060.

Using the non-parametric analysis of the data, the lowest calculated k is used to establish the bias. The lowest calculated k is 0.9969. Therefore the non-parametric derived bias is -0.0031. The uncertainty in the lowest point is 0.0020. There is a 99.9% confidence that the lowest k is exceeded. This confidence level exceeds the required 95% confidence.

The next step in the analysis is to look for trends in the data. The uncertainty given above is a function of the trending parameter. For this analysis, the uncertainty is calculated at the maximum and minimum value of the application range of the trending parameter and the maximum of these two is the uncertainty used.

Neutron spectrum

Trends in the calculated k_{eff} of the benchmarks were sought as a function of the neutron spectrum. Since a large number of things can affect the spectrum, a single index calculated by MCNP6 is used. This index is the Energy of the Average Lethargy causing Fission (EALF). Figure A.2 shows the distribution of k_{eff} around the mean value, which is shown as the red line. The predicted mean k_{eff} as a function of EALF is:

$$k(EALF) = 0.9992 + 0.00946 * EALF$$

The units for EALF are eV. The largest bias in the application range (0.1 to 0.4 eV) is 0.0. The maximum uncertainty is 0.0072.

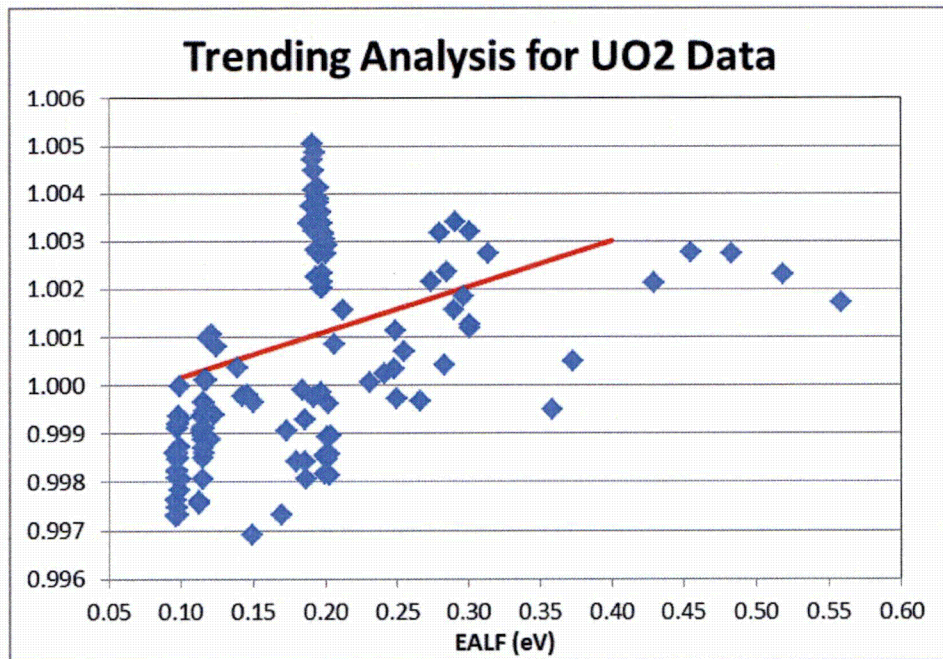


Figure A.2: Fresh Fuel Experiments as a Function of EALF

Enrichment

The fuel to be stored in the racks ranges in enrichment from 1.1 wt% ^{235}U to 5 wt% ^{235}U . The trend in the mean k_{eff} as a function of enrichment is:

$$k(\text{Enrichment}) = 1.0026 - (5.23\text{E-}04) \cdot \text{Enrichment}$$

where Enrichment is wt% ^{235}U .

The bias is zero but the uncertainty in the range of 1 to 5 wt% ^{235}U is 0.0071. Figure A.3 graphically presents the results.

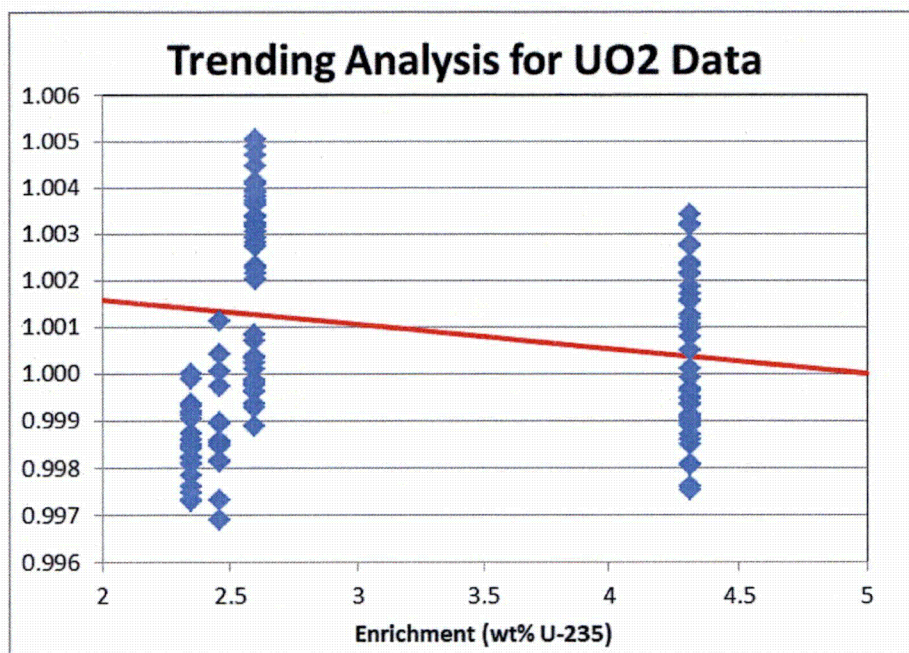


Figure A.3: Fresh Fuel Experiments as a Function of Enrichment

A.1.6 Bias and Uncertainty

To make the incorporation of the bias and bias uncertainty in the criticality analysis conservative, the most limiting bias and bias uncertainty from the trends in the range of interest, the set as a whole, and the non-parametric analysis is used. The most limiting bias is 0.0031 and the most limiting uncertainty is 0.0071.

A.1.7 Subcritical Margin

The NRC has established subcritical margins for rack analysis. A subcritical margin of 5% in k is required. In the analysis of 131 critical experiments, the lowest calculated k was 0.9969. This supports the position that the subcritical margin is sufficient.

A.1.8 Area of Applicability (Benchmark Applicability)

The critical benchmarks selected cover all commercial light water reactor fuel storage racks or casks. To summarize the range of the benchmark applicability (or area of applicability), Table A.3 is provided below.

Table A.3: Area of Applicability

Parameter	Range	Comments
Fissionable Material/Physical Form	UO ₂	The fuel material is the same as in the benchmark experiments
Enrichment (wt% U-235)	2.35 to 4.31	Extrapolation above 4.31% and below 2.35% is needed. Table 2.3 of NUREG/CR-6698 states that an extrapolation of 1.5 wt% is allowable.
Spectrum - EALF (eV)	0.096 to 0.6	Expected range in applications: 0.1 to 0.4 eV
Lattice Characteristics Type Pin Pitch (cm)	Square 1.64 to 2.54	The range of pin pitch in expected range of [[]]. Using continuous energy Monte Carlo reduces the dependence on pitch to the resulting dependence on spectrum, which is covered. Thus the extrapolation on pin pitch has no effect.
Absorbers Boron Areal Density (gm B-10/cm ²)	0 to 0.067	Credit is taken for 0.015 gm B-10/cm ² which is within the range.
Reflector Experiments included water and steel	Reflectors adequately covered	The analysis is done with infinite models so the reflector is not important.
Temperature	Room Temperature	The criticality calculations are performed with the fuel at room temperatures.
Moderating material	Water	The moderator in all benchmark experiments is water.

A.2 HTC Critical Experiments

Burned fuel contains a low concentration of plutonium (about less than 1 wt%), as well as the uranium and thus is actually Mixed Oxide (MOX) fuel. Most classical MOX experiments have plutonium concentrations at least twice as high as that contained in burned fuel. A series of experiments were performed in France which model a uranium and plutonium concentration that approximately matches 4.5 wt % U-235 fuel burned to 37.5 GWd/MTU [5]. This fuel has 1.1 wt% plutonium and 1.57 wt% U-235. These critical experiments, referred to as “HTC”, were analyzed as an independent set and included in the code validation. Since BWRs use peak reactivity in the criticality safety analyses, the plutonium content never exceeds 1.1 wt% plutonium. All of the MOX experiments in the International Handbook [3] have much higher plutonium content and therefore are inappropriate for the validation analysis for BWRs.

All the HTC critical experiments used the same fuel pins. The criticality of these experiments was controlled by adjusting the critical water height. The experiments were performed in four phases.

Phase 1 [6] consists of 17 cases where the pin pitch was varied from 1.3 cm to 2.3 cm and different quantities of pins were used to change the critical height. An 18th case was done where the array was moved to the edge of the tank, so the boundary was the steel tank followed by void. This condition is not typical of a spent fuel pool, so this case was not analyzed. The average calculated k_{eff} of the Phase 1 cases was 1.0000.

Phase 2 [7] consisted of 20 cases where gadolinium of various concentrations was dissolved in the water (Phase 2a) and 21 cases where boron was dissolved in the water (Phase 2b). These experiments also varied the pitch (1.3 to 1.9 cm) and the number of pins. Since there is no soluble boron in a BWR Phase 2b cases were not included in the analysis. The average k_{eff} of the gadolinium cases was 0.9997.

Phase 3 [8] consists of 26 experiments where the pins were arranged as 4 “assemblies.” Each assembly used a 1.6 cm pin pitch. The assembly separation was varied, as well as the number of pins in each assembly. Eleven cases boxed the assemblies with an absorber (borated steel, Boral, or cadmium). All the boxed assembly cases were eliminated except for the single Boral case since the other absorbers are not part of the DAEC pool. Thus 16 Phase 3 cases are included. The average k_{eff} of these 16 cases was 1.0002.

Finally, Phase 4 consisted of redoing the same type of experiments as Phase 3, except with reflector screens. Since this analysis uses infinite models the reflector is not important so no Phase 4 cases were analyzed.

References [6] through [8] provided all the details for the analysis of the HTC critical experiments. The references gave a simple model and a detailed model. The model created for this work followed the detailed model.

Tables A.4 through A.6 present the results of the analysis, following the same process for the fresh fuel experiments in Section A.1.

Table A.4: HTC Phase 1 Results

Case No.	k_{eff}	Monte Carlo Sigma	EALF (eV)	Pitch (cm)
1	0.9997	0.00009	0.0713	2.3
2	0.9997	0.00010	0.0683	2.3
3	0.9995	0.00009	0.0681	2.3
4	1.0003	0.00011	0.0871	1.9
5	1.0005	0.00011	0.0850	1.9
6	0.9999	0.00011	0.0842	1.9
7	1.0004	0.00012	0.1050	1.7
8	1.0003	0.00012	0.1034	1.7
9	1.0002	0.00012	0.1024	1.7
10	1.0007	0.00013	0.1446	1.5
11	1.0000	0.00013	0.1396	1.5
12	0.9997	0.00013	0.1378	1.5
13	1.0003	0.00013	0.2641	1.3
14	0.9998	0.00013	0.2411	1.3
15	0.9995	0.00013	0.2374	1.3
16	1.0000	0.00013	0.1043	1.7
17	0.9999	0.00012	0.1022	1.7

Table A.5: HTC Phase 2a, Gadolinium Solutions, Results

Case No.	k_{eff}	Monte Carlo Sigma	EALF (eV)	Pitch (cm)	Gadolinium Concentration (g/l)
1	0.9998	0.00014	0.2607	1.3	0.0520
2	0.9994	0.00013	0.2570	1.3	0.0520
3	0.9997	0.00013	0.2786	1.3	0.1005
4	0.9994	0.00013	0.2753	1.3	0.1005
5	0.9992	0.00013	0.2716	1.3	0.1005
6	0.9989	0.00013	0.2937	1.3	0.1505
7	0.9984	0.00014	0.2870	1.3	0.1505
8	0.9982	0.00013	0.3042	1.3	0.1997
9	0.9986	0.00013	0.3014	1.3	0.1997
10	0.9986	0.00012	0.1747	1.5	0.1997
11	0.9994	0.00013	0.1671	1.5	0.1495
12	0.9993	0.00012	0.1655	1.5	0.1495
13	1.0001	0.00012	0.1584	1.5	0.1000
14	0.9999	0.00013	0.1565	1.5	0.1000
15	1.0014	0.00012	0.1514	1.5	0.0492
16	1.0008	0.00013	0.1484	1.5	0.0492
17	1.0014	0.00012	0.1094	1.7	0.0492
18	1.0015	0.00012	0.0902	1.9	0.0492
19	0.9980	0.00012	0.1168	1.7	0.1010
20	1.0013	0.00012	0.1096	1.7	0.0492

Table A.6: HTC Phase 3 Results – Water Reflected Assemblies
(1.6 cm pin pitch)

Case No.	k_{eff}	Monte Carlo Sigma	EALF (eV)	Absorber Box Material	Assembly Separation (cm)
6	1.0005	0.00012	0.1336	Boral	0
12	1.0001	0.00013	0.1159	none	18
13	1.0001	0.00012	0.1148	none	14.5
14	1.0006	0.00012	0.1149	none	11
15	1.0001	0.00012	0.1141	none	10
16	1.0003	0.00013	0.1134	none	9
17	1.0000	0.00012	0.1115	none	8
18	1.0004	0.00012	0.1096	none	6
19	1.0009	0.00011	0.1071	none	4
20	1.0008	0.00012	0.1049	none	4
21	0.9999	0.00012	0.1077	none	2
22	1.0008	0.00012	0.1102	none	1
23	0.9998	0.00013	0.1182	none	0
24	0.9996	0.00012	0.1552	none	0
25	1.0004	0.00012	0.1305	none	4
26	0.9998	0.00012	0.1187	none	10

The first statistical test is to check for normality. The Anderson-Darling normality test was performed and the HTC set of experiments passed the normality test. Figure A.4 provides a histogram of the calculated k_{eff} for the HTC experiments.

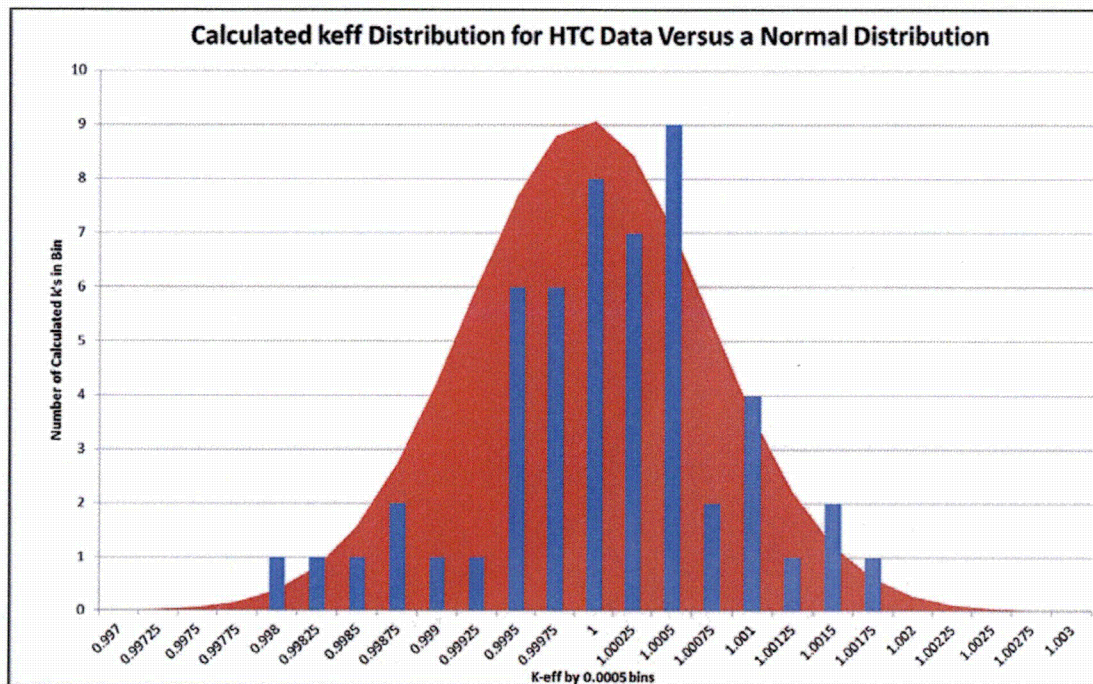


Figure A.4: HTC Critical Experiments Histogram

Since the HTC set passed the normality test the statistical analysis of the set as a whole and with trends is performed using the NUREG/CR-6698 approach previously described in Section A.1. The set as a whole has mean uncertainty weighted k_{eff} of 1.0000 and the uncertainty is 0.0053. The bias is zero.

The pin pitch changes are made to adjust the spectrum. The trend analysis (performed consistent with NUREG/CR-6698) on EALF yielded the following function:

$$k(\text{EALF}) = 1.0004 - 0.00268 * \text{EALF}$$

The units for EALF are eV. In the range of the application (0.1 to 0.3 eV) the maximum bias is -0.0004. The maximum uncertainty is 0.0079. Figure A.5 shows the results of the HTC analysis.

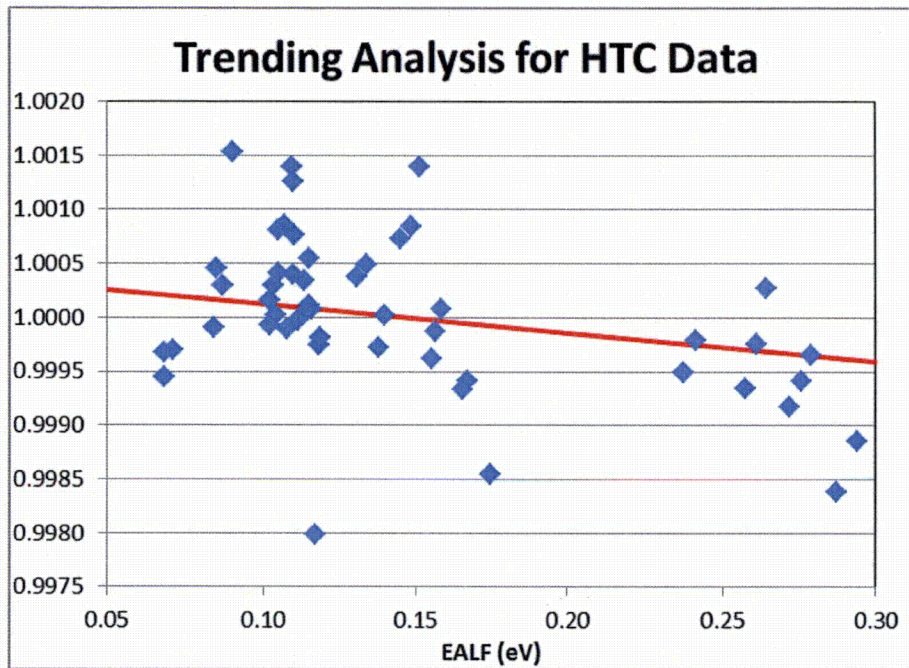


Figure A.5: HTC Experiments as a Function of EALF

A.3 Summary

In order to be conservative, the largest bias and uncertainty from either the fresh fuel or HTC critical experiment analysis is used. Further, the largest bias and uncertainty from any trend or set as a whole is used, including non-normal distribution. Table A.7 shows all the biases and uncertainties from all the analyses. For the criticality analysis of the DAEC PaR racks using MCNP6 version 1.0 and the ENDF/B-VII.1 cross sections, the conservative bias and uncertainty are 0.0031 and 0.0079, respectively.

Table A.7: Biases and Uncertainties

Data Set	N	Trend	Range	Bias	Uncertainty
UO ₂	131	---	---	0.0000	0.0060
UO ₂	131	Enrichment	1 – 5	0.0000	0.0071
UO ₂	131	EALF	0.1 – 0.4	0.0000	0.0072
UO ₂ non-normal	131	---	---	-0.0031	0.0020
HTC	53	---	---	0.0000	0.0053
HTC	53	EALF	0.1 – 0.3	-0.0004	0.0079
HTC non-normal	53	---	---	-0.0020	0.0050

A.4 References

- [1] J. T. Goorley, et al., *Initial MCNP6 Release Overview – MCNP6 version 1.0*, LA-UR-13-22934, Los Alamos National Laboratory (2013).
- [2] J.C. Dean and R.W. Tayloe, Jr., “Guide for Validation of Nuclear Criticality Safety Calculational Methodology,” NUREG/CR-6698, Nuclear Regulatory Commission, January 2001.
- [3] International Handbook of Evaluated Criticality Safety Benchmark Experiments, NEA/NSC/DOC(95)3, Volume IV, Nuclear Energy Agency, OECD, September 2014.
- [4] SPC for Excel Software, “Anderson-Darling Test for Normality,” June 2011 (<https://www.spcforexcel.com/knowledge/basic-statistics/anderson-darling-test-for-normality>)
- [5] D. E. Mueller, K. R. Elam, and P. B. Fox, “Evaluation of the French Haut Taux de Combustion (HTC) Critical Experiment Data,” NUREG/CR-6979 (ORNL/TM-2007/083), Oak Ridge National Laboratory, September 2008.
- [6] F. Fernex, “Programme HTC – Phase 1: Réseaux de crayons dans l’eau pure (Water-moderated and reflected simple arrays) Réévaluation des expériences,” DSU/SEC/T/2005-33/D.R., Institut de Radioprotection et de Sécurité Nucléaire, 2008.
- [7] F. Fernex, Programme HTC – Phase 2: Réseaux simples en eau empoisonnée (bore et gadolinium) (Reflected simple arrays moderated by poisoned water with gadolinium or boron) Réévaluation des expériences, DSU/SEC/T/2005-38/D.R., Institut de Radioprotection et de Sécurité Nucléaire, 2008.
- [8] F. Fernex, Programme HTC – Phase 3: Configurations “stockage en piscine” (Pool storage) Réévaluation des expériences, DSU/SEC/T/2005-37/D.R., Institut de Radioprotection et de Sécurité Nucléaire, 2008.

Appendix B: Results

Output File Name	Max K-inf (20 degC)	Bundle	Lattice
C25_251012.out.txt	1.18515	GNF2-P10DG2B394-13GZ-100T2-150-T6-25101	[[
C25_251013.out.txt	1.19285	GNF2-P10DG2B394-13GZ-100T2-150-T6-25101	
C25_251014.out.txt	1.19126	GNF2-P10DG2B394-13GZ-100T2-150-T6-25101	
C25_251015.out.txt	1.21032	GNF2-P10DG2B394-13GZ-100T2-150-T6-25101	
C25_251016.out.txt	1.20416	GNF2-P10DG2B394-13GZ-100T2-150-T6-25101	
C25_251022.out.txt	1.19473	GNF2-P10DG2B399-12GZ-100T2-150-T6-25102	
C25_251023.out.txt	1.19820	GNF2-P10DG2B399-12GZ-100T2-150-T6-25102	
C25_251024.out.txt	1.19607	GNF2-P10DG2B399-12GZ-100T2-150-T6-25102	
C25_251025.out.txt	1.21621	GNF2-P10DG2B399-12GZ-100T2-150-T6-25102	
C25_251026.out.txt	1.20950	GNF2-P10DG2B399-12GZ-100T2-150-T6-25102	
C25_251032.out.txt	1.21356	GNF2-P10DG2B413-14GZ-100T2-150-T6-25103	
C25_251033.out.txt	1.21829	GNF2-P10DG2B413-14GZ-100T2-150-T6-25103	
C25_251034.out.txt	1.21644	GNF2-P10DG2B413-14GZ-100T2-150-T6-25103	
C25_251035.out.txt	1.23125	GNF2-P10DG2B413-14GZ-100T2-150-T6-25103	
C25_251036.out.txt	1.22421	GNF2-P10DG2B413-14GZ-100T2-150-T6-25103	
C25_251042.out.txt	1.24048	GNF2-P10DG2B423-15GZ-100T2-150-T6-25104	
C25_251043.out.txt	1.24747	GNF2-P10DG2B423-15GZ-100T2-150-T6-25104	
C25_251044.out.txt	1.24463	GNF2-P10DG2B423-15GZ-100T2-150-T6-25104	
C25_251045.out.txt	1.25368	GNF2-P10DG2B423-15GZ-100T2-150-T6-25104	
C25_251046.out.txt	1.24704	GNF2-P10DG2B423-15GZ-100T2-150-T6-25104	
C25_251052.out.txt	1.25430	GNF2-P10DG2B436-12GZ-100T2-150-T6-25105	
C25_251053.out.txt	1.25528	GNF2-P10DG2B436-12GZ-100T2-150-T6-25105	
C25_251054.out.txt	1.25145	GNF2-P10DG2B436-12GZ-100T2-150-T6-25105	
C25_251055.out.txt	1.26516	GNF2-P10DG2B436-12GZ-100T2-150-T6-25105	
C25_251056.out.txt	1.25914	GNF2-P10DG2B436-12GZ-100T2-150-T6-25105	
C25_251062.out.txt	1.25405	GNF2-P10DG2B436-14GZ-100T2-150-T6-25106]]

Non-Proprietary Information

Output File Name	Max K-inf (20 degC)	Bundle	Lattice
C24_241012.out.txt	1.18927	GNF2-P10DG2B401-13GZ-100T2-150-T6-24101	[[
C24_241013.out.txt	1.19719	GNF2-P10DG2B401-13GZ-100T2-150-T6-24101	
C24_241014.out.txt	1.19491	GNF2-P10DG2B401-13GZ-100T2-150-T6-24101	
C24_241015.out.txt	1.21558	GNF2-P10DG2B401-13GZ-100T2-150-T6-24101	
C24_241016.out.txt	1.20887	GNF2-P10DG2B401-13GZ-100T2-150-T6-24101	
C24_241022.out.txt	1.19912	GNF2-P10DG2B408-12GZ-100T2-150-T6-24102	
C24_241023.out.txt	1.20247	GNF2-P10DG2B408-12GZ-100T2-150-T6-24102	
C24_241024.out.txt	1.20027	GNF2-P10DG2B408-12GZ-100T2-150-T6-24102	
C24_241025.out.txt	1.22136	GNF2-P10DG2B408-12GZ-100T2-150-T6-24102	
C24_241026.out.txt	1.21450	GNF2-P10DG2B408-12GZ-100T2-150-T6-24102	
C24_241032.out.txt	1.21197	GNF2-P10DG2B412-16GZ-100T2-150-T6-24103	
C24_241033.out.txt	1.21796	GNF2-P10DG2B412-16GZ-100T2-150-T6-24103	
C24_241034.out.txt	1.21630	GNF2-P10DG2B412-16GZ-100T2-150-T6-24103	
C24_241035.out.txt	1.23041	GNF2-P10DG2B412-16GZ-100T2-150-T6-24103	
C24_241036.out.txt	1.22345	GNF2-P10DG2B412-16GZ-100T2-150-T6-24103	
C24_241042.out.txt	1.22032	GNF2-P10DG2B424-15GZ-100T2-150-T6-24104	
C24_241043.out.txt	1.22774	GNF2-P10DG2B424-15GZ-100T2-150-T6-24104	
C24_241044.out.txt	1.22620	GNF2-P10DG2B424-15GZ-100T2-150-T6-24104	
C24_241045.out.txt	1.24687	GNF2-P10DG2B424-15GZ-100T2-150-T6-24104	
C24_241046.out.txt	1.24010	GNF2-P10DG2B424-15GZ-100T2-150-T6-24104	
C24_241011.out.txt	0.96069	GNF2-P10DG2B439-13GZ-100T2-150-T6-24105	
C24_241052.out.txt	1.25590	GNF2-P10DG2B439-13GZ-100T2-150-T6-24105	
C24_241053.out.txt	1.25717	GNF2-P10DG2B439-13GZ-100T2-150-T6-24105	
C24_241054.out.txt	1.25337	GNF2-P10DG2B439-13GZ-100T2-150-T6-24105	
C24_241055.out.txt	1.26736	GNF2-P10DG2B439-13GZ-100T2-150-T6-24105	
C24_241056.out.txt	1.26145	GNF2-P10DG2B439-13GZ-100T2-150-T6-24105	
C24_241017.out.txt	0.88774	GNF2-P10DG2B439-13GZ-100T2-150-T6-24105]]

Output File Name	Max K-inf (20 degC)	Bundle	Lattice
C23_9326.out.txt	1.22259	GE14-P10DNAB421-14G7.0-100T-150-T6-3301	[[
C23_9327.out.txt	1.22259	GE14-P10DNAB421-14G7.0-100T-150-T6-3301	
C23_9328.out.txt	1.22182	GE14-P10DNAB421-14G7.0-100T-150-T6-3301	
C23_9329.out.txt	1.22668	GE14-P10DNAB421-14G7.0-100T-150-T6-3301	
C23_9331.out.txt	1.19485	GE14-P10DNAB410-16GZ-100T-150-T6-3303	
C23_9332.out.txt	1.21908	GE14-P10DNAB410-16GZ-100T-150-T6-3303	
C23_9333.out.txt	1.21686	GE14-P10DNAB410-16GZ-100T-150-T6-3303	
C23_9334.out.txt	1.22026	GE14-P10DNAB410-16GZ-100T-150-T6-3303	
C23_9336.out.txt	1.20004	GE14-P10DNAB411-14G8.0-100T-150-T6-3304	
C23_9337.out.txt	1.20004	GE14-P10DNAB411-14G8.0-100T-150-T6-3304	
C23_9338.out.txt	1.19665	GE14-P10DNAB411-14G8.0-100T-150-T6-3304	
C23_9339.out.txt	1.20097	GE14-P10DNAB411-14G8.0-100T-150-T6-3304	
C23_9346.out.txt	1.18641	GE14-P10DNAB397-15GZ-100T-150-T6-3307	
C23_9347.out.txt	1.20628	GE14-P10DNAB397-15GZ-100T-150-T6-3307	
C23_9348.out.txt	1.20412	GE14-P10DNAB397-15GZ-100T-150-T6-3307	
C23_9349.out.txt	1.20696	GE14-P10DNAB397-15GZ-100T-150-T6-3307]]

Non-Proprietary Information

Output File Name	Max K-inf (20 degC)	Bundle	Lattice
C22_8564.out.txt	1.19956	GE14-P10DNAB405-14GZ-100T-150-T6-3118	[[
C22_8565.out.txt	1.21720	GE14-P10DNAB405-14GZ-100T-150-T6-3118	
C22_8566.out.txt	1.21378	GE14-P10DNAB405-14GZ-100T-150-T6-3118	
C22_8567.out.txt	1.21772	GE14-P10DNAB405-14GZ-100T-150-T6-3118	
C22_8569.out.txt	1.19870	GE14-P10DNAB407-16GZ-100T-150-T6-3119	
C22_8570.out.txt	1.21735	GE14-P10DNAB407-16GZ-100T-150-T6-3119	
C22_8571.out.txt	1.21239	GE14-P10DNAB407-16GZ-100T-150-T6-3119	
C22_8572.out.txt	1.21547	GE14-P10DNAB407-16GZ-100T-150-T6-3119	
C22_8574.out.txt	1.19995	GE14-P10DNAB409-16GZ-100T-150-T6-3120	
C22_8575.out.txt	1.21869	GE14-P10DNAB409-16GZ-100T-150-T6-3120	
C22_8576.out.txt	1.21481	GE14-P10DNAB409-16GZ-100T-150-T6-3120	
C22_8577.out.txt	1.21701	GE14-P10DNAB409-16GZ-100T-150-T6-3120	
C22_8579.out.txt	1.20194	GE14-P10DNAB413-15GZ-100T-150-T6-3121	
C22_8580.out.txt	1.22118	GE14-P10DNAB413-15GZ-100T-150-T6-3121	
C22_8581.out.txt	1.21837	GE14-P10DNAB413-15GZ-100T-150-T6-3121	
C22_8582.out.txt	1.22080	GE14-P10DNAB413-15GZ-100T-150-T6-3121	
C22_8584.out.txt	1.22164	GE14-P10DNAB421-8G7.0/7G6.0-100T-150-T6-3122	
C22_8585.out.txt	1.22164	GE14-P10DNAB421-8G7.0/7G6.0-100T-150-T6-3122	
C22_8586.out.txt	1.22147	GE14-P10DNAB421-8G7.0/7G6.0-100T-150-T6-3122	
C22_8587.out.txt	1.22558	GE14-P10DNAB421-8G7.0/7G6.0-100T-150-T6-3122]]

Non-Proprietary Information

Output File Name	Max K-inf (20 degC)	Bundle	Lattice
C21_7300.out.txt	1.19600	GE14-P10DNAB410-16GZ-100T-150-T6-2919	[[
C21_7301.out.txt	1.21392	GE14-P10DNAB410-16GZ-100T-150-T6-2919	
C21_7302.out.txt	1.21323	GE14-P10DNAB410-16GZ-100T-150-T6-2919	
C21_7303.out.txt	1.21733	GE14-P10DNAB410-16GZ-100T-150-T6-2919	
C21_7306.out.txt	1.19644	GE14-P10DNAB407-18GZ-100T-150-T6-2920	
C21_7307.out.txt	1.21264	GE14-P10DNAB407-18GZ-100T-150-T6-2920	
C21_7308.out.txt	1.21273	GE14-P10DNAB407-18GZ-100T-150-T6-2920	
C21_7309.out.txt	1.21669	GE14-P10DNAB407-18GZ-100T-150-T6-2920	

Output File Name	Max K-inf (20 degC)	Bundle	Lattice
C20_6768.out.txt	1.21298	GE14-P10DNAB420-16GZ-100T-150-T6-2814	[[
C20_6769.out.txt	1.22553	GE14-P10DNAB420-16GZ-100T-150-T6-2814	
C20_6770.out.txt	1.22557	GE14-P10DNAB420-16GZ-100T-150-T6-2814	
C20_6771.out.txt	1.23033	GE14-P10DNAB420-16GZ-100T-150-T6-2814	
C20_6773.out.txt	1.25688	GE14-P10DNAB438-14G6.0-100T-150-T6-2815	
C20_6774.out.txt	1.26265	GE14-P10DNAB438-14G6.0-100T-150-T6-2815	
C20_6775.out.txt	1.26748	GE14-P10DNAB438-14G6.0-100T-150-T6-2815	
C20_6777.out.txt	1.20815	GE14-P10DNAB420-16GZ-100T-150-T6-2816	
C20_6778.out.txt	1.22232	GE14-P10DNAB420-16GZ-100T-150-T6-2816	
C20_6779.out.txt	1.22319	GE14-P10DNAB420-16GZ-100T-150-T6-2816	
C20_6780.out.txt	1.22754	GE14-P10DNAB420-16GZ-100T-150-T6-2816	

Output File Name	Max K-inf (20 degC)	Bundle	Lattice
C19_5444.out.txt	1.25787	GE14-P10DNAB438-12G6.0-100T-150-T6-2541	[[
C19_5445.out.txt	1.26166	GE14-P10DNAB438-12G6.0-100T-150-T6-2541	
C19_5446.out.txt	1.26728	GE14-P10DNAB438-12G6.0-100T-150-T6-2541	
C19_5551.out.txt	1.25039	GE14-P10DNAB440-14G6.0-100T-150-T6-2561	
C19_5552.out.txt	1.25510	GE14-P10DNAB440-14G6.0-100T-150-T6-2561	
C19_5553.out.txt	1.26065	GE14-P10DNAB440-14G6.0-100T-150-T6-2561	

Output File Name	Max K-inf (20 degC)	Bundle	Lattice
C18_4799.out.txt	1.21083	GE14-P10DNAB398-15GZ-100T-150-T6-3896	[[
C18_4800.out.txt	1.22074	GE14-P10DNAB398-15GZ-100T-150-T6-3896	
C18_4801.out.txt	1.23205	GE14-P10DNAB398-15GZ-100T-150-T6-3896	
C18_4802.out.txt	1.23554	GE14-P10DNAB398-15GZ-100T-150-T6-3896	
C18_4804.out.txt	1.20400	GE14-P10DNAB402-17GZ-100T-150-T6-3897	
C18_4805.out.txt	1.22891	GE14-P10DNAB402-17GZ-100T-150-T6-3897	
C18_4806.out.txt	1.22909	GE14-P10DNAB402-17GZ-100T-150-T6-3897	
C18_4807.out.txt	1.23311	GE14-P10DNAB402-17GZ-100T-150-T6-3897	
C18_4809.out.txt	1.22415	GE14-P10DNAB407-16GZ-100T-150-T6-3898	
C18_4810.out.txt	1.23285	GE14-P10DNAB407-16GZ-100T-150-T6-3898	
C18_4811.out.txt	1.22949	GE14-P10DNAB407-16GZ-100T-150-T6-3898	
C18_4812.out.txt	1.23311	GE14-P10DNAB407-16GZ-100T-150-T6-3898]]

Output File Name	Max K-inf (20 degC)	Bundle	Lattice
C17_4263_td.out.txt	1.21772	GE12-P10DSB371-12GZ-100T-150-T6-3778	[[
C17_4264_td.out.txt	1.22442	GE12-P10DSB371-12GZ-100T-150-T6-3778	
C17_4312_td.out.txt	1.22154	GE12-P10DSB371-12GZ-100T-150-T6-3778	
C17_4265_td.out.txt	1.22529	GE12-P10DSB371-12GZ-100T-150-T6-3778	
C17_4267_td.out.txt	1.21214	GE12-P10DSB370-14GZ-100T-150-T6-3779	
C17_4268_td.out.txt	1.21787	GE12-P10DSB370-14GZ-100T-150-T6-3779	
C17_4314_td.out.txt	1.21293	GE12-P10DSB370-14GZ-100T-150-T6-3779	
C17_4269_td.out.txt	1.21714	GE12-P10DSB370-14GZ-100T-150-T6-3779	
C17_4263.out.txt	1.21733	GE12-P10DSB371-12GZ-100T-150-T6-3778	
C17_4264.out.txt	1.22404	GE12-P10DSB371-12GZ-100T-150-T6-3778	
C17_4312.out.txt	1.22128	GE12-P10DSB371-12GZ-100T-150-T6-3778	
C17_4265.out.txt	1.22514	GE12-P10DSB371-12GZ-100T-150-T6-3778	
C17_4267.out.txt	1.21182	GE12-P10DSB370-14GZ-100T-150-T6-3779	
C17_4268.out.txt	1.21755	GE12-P10DSB370-14GZ-100T-150-T6-3779	
C17_4314.out.txt	1.21278	GE12-P10DSB370-14GZ-100T-150-T6-3779	
C17_4269.out.txt	1.21702	GE12-P10DSB370-14GZ-100T-150-T6-3779]]

Non-Proprietary Information

Output File Name	Max K-inf (20 degC)	Bundle	Lattice
C11_18422.out.txt	1.21169	GE10-P8HXB317-7GZ-70M-150-T-1842	[[
C11_18423.out.txt	1.22933	GE10-P8HXB317-7GZ-70M-150-T-1842	
C11_18424.out.txt	1.21611	GE10-P8HXB317-7GZ-70M-150-T-1842	
C11-12_18412.out.txt	1.20679	GE10-P8HXB321-11GZ-70M-150-T-1841	
C11-12_18413.out.txt	1.22958	GE10-P8HXB321-11GZ-70M-150-T-1841	
C11-12_18414.out.txt	1.21810	GE10-P8HXB321-11GZ-70M-150-T-1841	
C11-12_18415.out.txt	1.22235	GE10-P8HXB321-11GZ-70M-150-T-1841	
C12_19442.out.txt	1.19397	GE10-P8HXB316-8GZ-100M-150-T-1944	
C12_19443.out.txt	1.21981	GE10-P8HXB316-8GZ-100M-150-T-1944	
C12_19444.out.txt	1.20982	GE10-P8HXB316-8GZ-100M-150-T-1944	
C13-15_20222.out.txt	1.20652	GE10-P8DXB327-8GZ2-100M-150-T-2022	
C13-15_20223.out.txt	1.22232	GE10-P8DXB327-8GZ2-100M-150-T-2022	
C13-15_20224.out.txt	1.21640	GE10-P8DXB327-8GZ2-100M-150-T-2022	
C13-15_20232.out.txt	1.19001	GE10-P8DXB327-10GZ1-100M-150-T-2023	
C13-15_20233.out.txt	1.20812	GE10-P8DXB327-10GZ1-100M-150-T-2023	
C13-15_20234.out.txt	1.20637	GE10-P8DXB327-10GZ1-100M-150-T-2023	
C13-15_20235.out.txt	1.20368	GE10-P8DXB327-10GZ1-100M-150-T-2023	
C16_22742.out.txt	1.19479	GE10-P8DXB341-9GZ-100T-150-T-2274	
C16_22743.out.txt	1.22295	GE10-P8DXB341-9GZ-100T-150-T-2274	
C16_22752.out.txt	1.18779	GE10-P8DXB342-12GZ-100T-150-T-2275	
C16_22753.out.txt	1.20740	GE10-P8DXB342-12GZ-100T-150-T-2275	
C16_22754.out.txt	1.20775	GE10-P8DXB342-12GZ-100T-150-T-2275]]

Non-Proprietary Information

Output File Name	Max K-inf (20 degC)	Bundle	Lattice
C9_15932.out.txt	1.20555	GE8B-P8DQB299-9GZ-80M-4WR-150-T-1593	[[
C9_15933.out.txt	1.19884	GE8B-P8DQB299-9GZ-80M-4WR-150-T-1593	
C9-10_16052.out.txt	1.22909	GE8B-P8DQB303-8GZ-80M-4WR-150-T-1605	
C9-10_16053.out.txt	1.21044	GE8B-P8DQB303-8GZ-80M-4WR-150-T-1605	
C9-10_16054.out.txt	1.20689	GE8B-P8DQB303-8GZ-80M-4WR-150-T-1605	
C10_17262.out.txt	1.18026	GE8B-P8DQB324-11GZ-80M-4WR-150-T-1726	
C10_17263.out.txt	1.20146	GE8B-P8DQB324-11GZ-80M-4WR-150-T-1726	
C10_17264.out.txt	1.20045	GE8B-P8DQB324-11GZ-80M-4WR-150-T-1726]]

Output File Name	Max K-inf (20 degC)	Bundle	Lattice
C8_303121.out.txt	1.20087	8DRB301-6G4.0-80M-150-30312	[[
C8_ELTA10.out.txt	1.17214	LTA-P8DRB299-4G8.0/4G3.0-100M-150-T-ELTA	
C8_ELTA10F.out.txt	1.17227	LTA-P8DRB299-4G8.0/4G3.0-100M-150-T-ELTA	
C8_LTA3112.out.txt	1.19579	LTA-P8DVB311-10GZ-100M-146-T-LTA311	
C8_LTA3113a.out.txt	1.21263	LTA-P8DVB311-10GZ-100M-146-T-LTA311	
C8_LTA3113b.out.txt	1.20078	LTA-P8DVB311-10GZ-100M-146-T-LTA311	
C8_LTA3113c.out.txt	1.20786	LTA-P8DVB311-10GZ-100M-146-T-LTA311	
C8_LTA3113d.out.txt	1.20636	LTA-P8DVB311-10GZ-100M-146-T-LTA311	
C8_LTA3114.out.txt	1.18875	LTA-P8DVB311-10GZ-100M-146-T-LTA311	
C8_LTA3115.out.txt	1.18694	LTA-P8DVB311-10GZ-100M-146-T-LTA311]]

Output File Name	Max K-inf (20 degC)	Bundle	Lattice
C5-6_219161.out.txt	1.20955	8DPB289-7G3.0-80M-150-21916	[[
C5-6_219162.out.txt	0.96103	8DPB289-7G3.0-80M-150-21916	
C5-6_219163.out.txt	1.23570	8DPB289-7G3.0-80M-150-21916	
C7_252341.out.txt	1.19306	8DRB284-7G4.0-80M-150-25234	
C7-8_252311.out.txt	1.18997	8DRB299-7G4.0-80M-150-25231]]

Non-Proprietary Information

Output File Name	Max K-inf (20 degC)	Bundle	Lattice
C2-3_21092R1B1.out.txt	1.21679	274-5G2.0-80M-144-21092R1B1	[[
C2-4_21092R1B2.out.txt	1.19746	274-5G3.0-80M-144-21092R1B2	
C2-3_21092R1B1wr.out.txt	1.21676	274-5G2.0-80M-144-21092R1B1	
C2-4_21092R1B2wr.out.txt	1.19740	274-5G3.0-80M-144-21092R1B2]]

Output File Name	Max K-inf (20 degC)	Bundle	Lattice
C1_21092B1L1.out.txt	1.03942	110-NOG-80M-144-21092B1	[[
C1_21092B2L1.out.txt	1.18037	212-2G2.0-80M-144-21092B2	
C1_21092B3L1.out.txt	1.15958	212-1G2.0/3G3.0-80M-144-21092B3	
C1_21092B3L2.out.txt	1.16696	212-1G2.0/3G3.0-80M-144-21092B3	
C1_21092B3L3.out.txt	1.16797	212-1G2.0/3G3.0-80M-144-21092B3	
C1B_21092B4L1.out.txt	1.17850	230-3G2.5-80M-144-21092B4]]

File Name	SCCG	Case #	keff	Std dev
C17_4265_1.o	1.20695	238	0.8098	2.50E-04
C17_4265_2.o	1.20744	291	0.81208	2.50E-04
C17_4265_3.o	1.20803	344	0.81359	2.50E-04
C17_4265_4.o	1.21243	398	0.82054	2.50E-04
C17_4265_5.o	1.22514	757	0.81991	2.50E-04
C17_4265_6.o	1.22438	811	0.82279	2.50E-04
C17_4265_7.o	1.22207	865	0.82429	2.50E-04
C17_4269_1.o	1.2075	239	0.81357	2.50E-04
C17_4269_2.o	1.20575	292	0.81407	2.50E-04
C17_4269_3.o	1.2031	346	0.8147	2.40E-04
C17_4269_4.o	1.20231	401	0.81748	2.50E-04
C17_4269_5.o	1.21702	756	0.81672	2.50E-04
C17_4269_6.o	1.21513	810	0.81898	2.50E-04
C17_4269_7.o	1.21167	865	0.82281	2.60E-04
C18_4802_1.o	1.1922	241	0.79833	2.40E-04
C18_4802_2.o	1.19054	295	0.80025	2.40E-04
C18_4802_3.o	1.18847	349	0.80159	2.50E-04
C18_4802_4.o	1.19016	404	0.80752	2.40E-04
C18_4802_5.o	1.23554	758	0.83329	2.60E-04
C18_4802_6.o	1.23364	812	0.83416	2.50E-04
C18_4802_7.o	1.22985	867	0.83601	2.50E-04
C18_4807_1.o	1.18219	244	0.795	2.40E-04
C18_4807_2.o	1.18047	298	0.7968	2.50E-04
C18_4807_3.o	1.17834	352	0.79731	2.40E-04
C18_4807_4.o	1.1799	407	0.80139	2.40E-04
C18_4807_5.o	1.23311	759	0.83222	2.40E-04
C18_4807_6.o	1.22943	814	0.83337	2.60E-04
C18_4807_7.o	1.22238	870	0.83154	2.60E-04
C18_4812_1.o	1.19922	242	0.80597	2.50E-04
C18_4812_2.o	1.19702	296	0.80776	2.50E-04
C18_4812_3.o	1.19444	350	0.8076	2.40E-04
C18_4812_4.o	1.19538	405	0.8126	2.50E-04
C18_4812_5.o	1.23311	759	0.8283	2.50E-04
C18_4812_6.o	1.22876	813	0.82711	2.50E-04
C18_4812_7.o	1.22165	869	0.82633	2.50E-04
C19_5446_1.o	1.24185	243	0.84225	2.50E-04
C19_5446_2.o	1.23659	297	0.84028	2.60E-04
C19_5446_3.o	1.22969	351	0.83691	0.00025
C19_5446_4.o	1.22263	406	0.83398	0.00025
C19_5446_5.o	1.26728	760	0.85847	0.00025
C19_5446_6.o	1.26263	814	0.85832	0.00026
C19_5446_7.o	1.2551	869	0.85696	0.00025
C19_5553_1.o	1.22831	244	0.82916	0.00025

File Name	SCCG	Case #	keff	Std dev
C19_5553_2.o	1.2237	298	0.82867	0.00024
C19_5553_3.o	1.21783	353	0.82828	0.00025
C19_5553_4.o	1.21387	408	0.82905	0.00025
C19_5553_5.o	1.26065	761	0.85312	0.00026
C19_5553_6.o	1.2544	815	0.85094	0.00026
C19_5553_7.o	1.24497	870	0.84707	0.00025
C20_6771_1.o	1.21448	243	0.82011	0.00026
C20_6771_2.o	1.21094	296	0.81795	0.00025
C20_6771_3.o	1.20638	351	0.8182	0.00024
C20_6771_4.o	1.20387	406	0.82051	0.00024
C20_6771_5.o	1.23033	761	0.82688	0.00024
C20_6771_6.o	1.22778	815	0.82851	0.00025
C20_6771_7.o	1.22199	871	0.82973	0.00025
C20_6775_1.o	1.22088	245	0.82348	0.00025
C20_6775_2.o	1.21661	299	0.82381	0.00025
C20_6775_3.o	1.21096	354	0.82283	0.00025
C20_6775_4.o	1.20787	410	0.82638	0.00025
C20_6775_5.o	1.26748	761	0.86203	0.00025
C20_6775_6.o	1.26307	815	0.86139	0.00025
C20_6775_7.o	1.25555	871	0.86076	0.00026
C20_6780_1.o	1.2083	242	0.81011	0.00025
C20_6780_2.o	1.20541	296	0.81074	0.00025
C20_6780_3.o	1.20135	350	0.81048	0.00025
C20_6780_4.o	1.19913	406	0.81464	0.00024
C20_6780_5.o	1.22754	762	0.82566	0.00024
C20_6780_6.o	1.22509	817	0.82849	0.00024
C20_6780_7.o	1.21968	872	0.82823	0.00025
C21_7303_1.o	1.1901	245	0.80151	0.00023
C21_7303_2.o	1.18828	299	0.80319	0.00025
C21_7303_3.o	1.18583	354	0.80472	0.00025
C21_7303_4.o	1.18724	409	0.80981	0.00025
C21_7303_5.o	1.21733	762	0.81829	0.00025
C21_7303_6.o	1.21456	817	0.82056	0.00025
C21_7303_7.o	1.20931	872	0.82138	0.00026
C21_7309_1.o	1.18038	246	0.79198	0.00024
C21_7309_2.o	1.1784	300	0.79373	0.00025
C21_7309_3.o	1.17565	355	0.7955	0.00024
C21_7309_4.o	1.17642	410	0.79907	0.00025
C21_7309_5.o	1.21669	763	0.81927	0.00025
C21_7309_6.o	1.21328	817	0.81922	0.00025
C21_7309_7.o	1.20695	873	0.81883	0.00025
C22_8567_1.o	1.19456	243	0.80152	0.00025
C22_8567_2.o	1.19283	297	0.80373	0.00025

File Name	SCCG	Case #	keff	Std dev
C22_8567_3.o	1.19031	351	0.80403	0.00024
C22_8567_4.o	1.19113	407	0.81102	0.00024
C22_8567_5.o	1.21772	761	0.81652	0.00024
C22_8567_6.o	1.21623	815	0.81922	0.00025
C22_8567_7.o	1.21238	870	0.82204	0.00026
C22_8572_1.o	1.18637	245	0.7988	0.00025
C22_8572_2.o	1.18484	299	0.80003	0.00025
C22_8572_3.o	1.18271	354	0.80234	0.00025
C22_8572_4.o	1.18456	409	0.80711	0.00025
C22_8572_5.o	1.21547	761	0.81519	0.00025
C22_8572_6.o	1.21229	816	0.81622	0.00025
C22_8572_7.o	1.20588	872	0.81703	0.00025
C22_8577_1.o	1.18793	242	0.79194	0.00024
C22_8577_2.o	1.18656	296	0.79441	0.00025
C22_8577_3.o	1.18442	350	0.79571	0.00024
C22_8577_4.o	1.18524	405	0.80072	0.00024
C22_8577_5.o	1.21701	761	0.81539	0.00026
C22_8577_6.o	1.21523	816	0.81877	0.00026
C22_8577_7.o	1.21015	872	0.81993	0.00025
C22_8582_1.o	1.19803	243	0.80236	0.00024
C22_8582_2.o	1.19622	296	0.80339	0.00025
C22_8582_3.o	1.19371	351	0.80576	0.00025
C22_8582_4.o	1.19413	406	0.8109	0.00025
C22_8582_5.o	1.2208	761	0.81775	0.00025
C22_8582_6.o	1.2181	816	0.82042	0.00024
C22_8582_7.o	1.2119	872	0.82071	0.00025
C22_8587_1.o	1.19656	244	0.80139	0.00024
C22_8587_2.o	1.19368	298	0.80184	0.00025
C22_8587_3.o	1.1902	352	0.8016	0.00025
C22_8587_4.o	1.18991	408	0.8074	0.00024
C22_8587_5.o	1.22558	764	0.82876	0.00026
C22_8587_6.o	1.21848	818	0.82468	0.00025
C22_8587_7.o	1.20817	874	0.81971	0.00025
C23_9329_1.o	1.20762	245	0.81729	0.00025
C23_9329_2.o	1.20395	299	0.81688	0.00025
C23_9329_3.o	1.19899	354	0.81628	0.00024
C23_9329_4.o	1.19565	409	0.81646	0.00024
C23_9329_5.o	1.22668	763	0.82598	0.00025
C23_9329_6.o	1.22241	817	0.82552	0.00024
C23_9329_7.o	1.21447	873	0.82333	0.00025
C23_9334_1.o	1.18837	245	0.80162	0.00026
C23_9334_2.o	1.18588	299	0.80133	0.00023
C23_9334_3.o	1.18222	354	0.80208	0.00025

File Name	SCCG	Case #	keff	Std dev
C23_9334_4.o	1.18	409	0.80213	0.00025
C23_9334_5.o	1.22026	761	0.81704	0.00025
C23_9334_6.o	1.21719	816	0.81854	0.00025
C23_9334_7.o	1.21073	871	0.81536	0.00024
C23_9339_1.o	1.17854	247	0.79484	0.00024
C23_9339_2.o	1.17644	301	0.79606	0.00026
C23_9339_3.o	1.17343	356	0.79676	0.00024
C23_9339_4.o	1.17287	411	0.79895	0.00025
C23_9339_5.o	1.20097	765	0.80409	0.00025
C23_9339_6.o	1.19917	820	0.80649	0.00024
C23_9339_7.o	1.19399	876	0.80776	0.00024
C23_9349_1.o	1.1649	246	0.77997	0.00023
C23_9349_2.o	1.16464	300	0.78266	0.00024
C23_9349_3.o	1.16381	354	0.78354	0.00024
C23_9349_4.o	1.1669	410	0.79294	0.00025
C23_9349_5.o	1.20696	764	0.81365	0.00024
C23_9349_6.o	1.20577	819	0.8157	0.00025
C23_9349_7.o	1.20083	874	0.81305	0.00025
C24_241012_1.o	1.16081	250	0.77932	0.00025
C24_241012_2.o	1.15969	303	0.7782	0.00024
C24_241012_3.o	1.15929	355	0.77512	0.00025
C24_241012_4.o	1.16321	408	0.78068	0.00025
C24_241012_5.o	1.18927	768	0.79665	0.00025
C24_241012_6.o	1.18763	822	0.79751	0.00025
C24_241012_7.o	1.18363	878	0.79966	0.00025
C24_241014_1.o	1.16864	248	0.78835	0.00024
C24_241014_2.o	1.16699	302	0.78928	0.00026
C24_241014_3.o	1.16179	357	0.7872	0.00024
C24_241014_4.o	1.15797	411	0.78247	0.00024
C24_241014_5.o	1.19456	765	0.80194	0.00024
C24_241014_6.o	1.19491	820	0.80766	0.00025
C24_241014_7.o	1.18823	877	0.80794	0.00024
C24_241022_1.o	1.16486	250	0.78027	0.00025
C24_241022_2.o	1.1643	302	0.77767	0.00024
C24_241022_3.o	1.16437	355	0.77898	0.00025
C24_241022_4.o	1.16809	408	0.78357	0.00024
C24_241022_5.o	1.19912	767	0.80311	0.00025
C24_241022_6.o	1.19819	822	0.80779	0.00025
C24_241022_7.o	1.19469	877	0.80942	0.00026
C24_241024_1.o	1.17257	249	0.79144	0.00024
C24_241024_2.o	1.17103	303	0.79259	0.00025
C24_241024_3.o	1.16593	357	0.78901	0.00024
C24_241024_4.o	1.16229	412	0.78678	0.00025

File Name	SCCG	Case #	keff	Std dev
C24_241024_5.o	1.20027	767	0.80935	0.00025
C24_241024_6.o	1.19974	821	0.81121	0.00025
C24_241024_7.o	1.19525	876	0.80982	0.00025
C24_241032_1.o	1.15649	248	0.76815	0.00025
C24_241032_2.o	1.15538	302	0.77105	0.00024
C24_241032_3.o	1.15319	356	0.77212	0.00023
C24_241032_4.o	1.1537	410	0.77454	0.00024
C24_241032_5.o	1.21197	766	0.81445	0.00025
C24_241032_6.o	1.20763	821	0.81576	0.00025
C24_241032_7.o	1.20018	877	0.81367	0.00025
C24_241034_1.o	1.1531	252	0.77493	0.00024
C24_241034_2.o	1.15273	304	0.77189	0.00024
C24_241034_3.o	1.1504	356	0.76854	0.00023
C24_241034_4.o	1.14782	413	0.77288	0.00025
C24_241034_5.o	1.2163	766	0.82395	0.00025
C24_241034_6.o	1.21385	820	0.82442	0.00025
C24_241034_7.o	1.20675	876	0.82326	0.00025
C24_241042_1.o	1.17443	246	0.78023	0.00025
C24_241042_2.o	1.17128	300	0.78127	0.00025
C24_241042_3.o	1.16759	354	0.78147	0.00025
C24_241042_4.o	1.16669	408	0.78358	0.00024
C24_241042_5.o	1.22032	766	0.81955	0.00026
C24_241042_6.o	1.21389	821	0.81923	0.00025
C24_241042_7.o	1.20452	877	0.81619	0.00025
C24_241044_1.o	1.17287	244	0.77462	0.00024
C24_241044_2.o	1.17077	298	0.77696	0.00025
C24_241044_3.o	1.16538	353	0.77759	0.00024
C24_241044_4.o	1.15915	410	0.77897	0.00024
C24_241044_5.o	1.2262	765	0.83015	0.00025
C24_241044_6.o	1.22258	820	0.83142	0.00025
C24_241044_7.o	1.21296	876	0.82828	0.00025
C24_241052_1.o	1.21322	247	0.81708	0.00025
C24_241052_2.o	1.20724	302	0.81621	0.00025
C24_241052_3.o	1.20013	356	0.81279	0.00025
C24_241052_4.o	1.19407	409	0.80735	0.00025
C24_241052_5.o	1.2559	763	0.85014	0.00025
C24_241052_6.o	1.24948	818	0.8496	0.00025
C24_241052_7.o	1.2397	873	0.84574	0.00025
C24_241054_1.o	1.21633	245	0.81986	0.00025
C24_241054_2.o	1.2132	299	0.82067	0.00025
C24_241054_3.o	1.20557	355	0.81991	0.00026
C24_241054_4.o	1.19291	413	0.81509	0.00024
C24_241054_5.o	1.25337	762	0.84935	0.00025

File Name	SCCG	Case #	keff	Std dev
C24_241054_6.o	1.25004	816	0.85019	0.00026
C24_241054_7.o	1.24218	872	0.84937	0.00026
C25_251012_1.o	1.15583	249	0.77419	0.00024
C25_251012_2.o	1.15523	302	0.77319	0.00024
C25_251012_3.o	1.15543	354	0.77223	0.00024
C25_251012_4.o	1.16008	407	0.77771	0.00025
C25_251012_5.o	1.18515	767	0.79287	0.00024
C25_251012_6.o	1.18399	822	0.79593	0.00024
C25_251012_7.o	1.18058	877	0.79716	0.00025
C25_251014_1.o	1.163	247	0.7829	0.00024
C25_251014_2.o	1.16149	301	0.78403	0.00025
C25_251014_3.o	1.15693	356	0.78259	0.00025
C25_251014_4.o	1.15421	411	0.78083	0.00025
C25_251014_5.o	1.19013	765	0.79997	0.00024
C25_251014_6.o	1.19126	820	0.80598	0.00025
C25_251014_7.o	1.18517	876	0.80534	0.00025
C25_251022_1.o	1.16016	249	0.77545	0.00025
C25_251022_2.o	1.16004	301	0.77309	0.00025
C25_251022_3.o	1.16058	354	0.77559	0.00026
C25_251022_4.o	1.16494	407	0.7815	0.00026
C25_251022_5.o	1.19473	767	0.80072	0.00025
C25_251022_6.o	1.19415	822	0.80453	0.00025
C25_251022_7.o	1.19122	877	0.80731	0.00025
C25_251024_1.o	1.16683	248	0.78594	0.00024
C25_251024_2.o	1.16545	302	0.78682	0.00025
C25_251024_3.o	1.16086	356	0.78411	0.00024
C25_251024_4.o	1.15836	411	0.78269	0.00024
C25_251024_5.o	1.19607	766	0.80583	0.00025
C25_251024_6.o	1.1959	820	0.80737	0.00025
C25_251024_7.o	1.19173	876	0.80777	0.00025
C25_251032_1.o	1.15603	247	0.76542	0.00025
C25_251032_2.o	1.15539	301	0.76931	0.00024
C25_251032_3.o	1.15379	354	0.76971	0.00025
C25_251032_4.o	1.15526	404	0.76915	0.00024
C25_251032_5.o	1.21356	766	0.81626	0.00025
C25_251032_6.o	1.21112	821	0.81903	0.00025
C25_251032_7.o	1.2059	876	0.81905	0.00024
C25_251034_1.o	1.15187	252	0.77308	0.00023
C25_251034_2.o	1.15206	300	0.76239	0.00024
C25_251034_3.o	1.15027	356	0.7683	0.00023
C25_251034_4.o	1.1485	413	0.77319	0.00024
C25_251034_5.o	1.21644	766	0.82366	0.00025
C25_251034_6.o	1.21464	821	0.82682	0.00025

File Name	SCCG	Case #	keff	Std dev
C25_251034_7.o	1.2084	876	0.82526	0.00026
C25_251042_1.o	1.18923	247	0.79778	0.00024
C25_251042_2.o	1.18463	301	0.79697	0.00025
C25_251042_3.o	1.17943	355	0.79438	0.00024
C25_251042_4.o	1.17655	410	0.79505	0.00025
C25_251042_5.o	1.24048	764	0.84024	0.00025
C25_251042_6.o	1.23363	819	0.83777	0.00024
C25_251042_7.o	1.22318	875	0.83307	0.00026
C25_251044_1.o	1.19232	246	0.80222	0.00026
C25_251044_2.o	1.18864	300	0.80203	0.00025
C25_251044_3.o	1.18189	355	0.79968	0.00025
C25_251044_4.o	1.17398	412	0.7985	0.00024
C25_251044_5.o	1.24463	761	0.84282	0.00025
C25_251044_6.o	1.24207	816	0.84598	0.00025
C25_251044_7.o	1.23259	873	0.84402	0.00025
C25_251052_1.o	1.21082	247	0.81558	0.00024
C25_251052_2.o	1.20514	301	0.81329	0.00025
C25_251052_3.o	1.20176	313	0.79484	0.00026
C25_251052_4.o	1.20176	365	0.79484	0.00026
C25_251052_5.o	1.2543	763	0.84882	0.00025
C25_251052_6.o	1.24826	818	0.84837	0.00024
C25_251052_7.o	1.23903	873	0.84553	0.00026
C25_251054_1.o	1.21407	245	0.81864	0.00025
C25_251054_2.o	1.21112	299	0.81986	0.00025
C25_251054_3.o	1.20362	355	0.81866	0.00026
C25_251054_4.o	1.19138	412	0.81264	0.00025
C25_251054_5.o	1.25145	762	0.84746	0.00026
C25_251054_6.o	1.24833	816	0.84906	0.00026
C25_251054_7.o	1.24072	871	0.84682	0.00026
C25_251062_1.o	1.21118	247	0.81621	0.00025
C25_251062_2.o	1.2052	301	0.81415	0.00026
C25_251062_3.o	1.19821	355	0.80961	0.00025
C25_251062_4.o	1.19241	409	0.80605	0.00025
C25_251062_5.o	1.25405	763	0.84858	0.00027
C25_251062_6.o	1.24757	818	0.84893	0.00027
C25_251062_7.o	1.23784	873	0.84457	0.00025

File Name	Series	SCCG	Case #	keff	std dev
0B-NR-0	0V10G4B	1.284	83	0.86837	0.00016
0B-ROD-0	0V10G4B	1.298	288	0.87975	0.00017
0B-ROD-4	0V10G4B	1.288	341	0.87408	0.00016
0B-ROD-7	0V10G4B	1.276	395	0.86827	0.00016
0V-NR-0	0V10G4	1.288	83	0.87283	0.00017
0V-ROD-0	0V10G4	1.273	284	0.85304	0.00016
0V-ROD-4	0V10G4	1.266	334	0.84835	0.00016
0V-ROD-7	0V10G4	1.275	367	0.85747	0.00018
10G4C134	6V10G4C	1.286	134	0.8739	0.00016
10G4C188	6V10G4C	1.279	188	0.87109	0.00017
10G4C389	6V10G4C	1.322	389	0.90075	0.00016
10G4C443	6V10G4C	1.316	443	0.89965	0.00017
10G4C499	6V10G4C	1.303	499	0.89484	0.00017
10G4D388	6V10G4C2	1.300	388	0.88054	0.00016
10G4D441	6V10G4C2	1.296	441	0.88084	0.00016
10G6A291	6V10G6	1.243	291	0.83558	0.00016
10G6A346	6V10G6	1.234	346	0.83269	0.00016
10G6A399	6V10G6	1.220	399	0.81962	0.00016
10G6A88	6V10G6	1.252	88	0.84607	0.00017
10G6B291	6V10G6B	1.266	291	0.8557	0.00017
10G6B346	6V10G6B	1.261	346	0.85744	0.00016
10G6B403	6V10G6B	1.249	403	0.85386	0.00016
10G6B88	6V10G6B	1.247	88	0.84064	0.00016
10G6C105	6V10G6C	1.240	105	0.81598	0.00017
10G6C396	6V10G6C	1.286	396	0.87328	0.00016
10G6C451	6V10G6C	1.282	451	0.87539	0.00017
10G6C507	6V10G6C	1.270	507	0.87088	0.00016
12G4B135	6V12G4B	1.284	135	0.87353	0.00017
12G4B189	6V12G4B	1.276	189	0.86992	0.00016
12G4B390	6V12G4B	1.320	390	0.90059	0.00016
12G4B444	6V12G4B	1.313	444	0.89834	0.00016
12G4B500	6V12G4B	1.299	500	0.89217	0.00017
12G4D388	6V12G4B2	1.299	388	0.8806	0.00016
12G4D442	6V12G4B2	1.294	442	0.8804	0.00017
12G6B143	6V12G6B	1.236	143	0.83515	0.00015
12G6B198	6V12G6B	1.229	198	0.83456	0.00016
12G6B397	6V12G6B	1.284	397	0.87384	0.00017
12G6B451	6V12G6B	1.279	451	0.87312	0.00016
12G6B508	6V12G6B	1.265	508	0.86862	0.00016
20G2B125	6V20G2B	1.337	125	0.91291	0.00017

File Name	Series	SCCG	Case #	keff	std dev
20G2B179	6V20G2B	1.328	179	0.90767	0.00016
20G2B383	6V20G2B	1.340	383	0.91594	0.00017
20G2B437	6V20G2B	1.329	437	0.90972	0.00017
20G2B493	6V20G2B	1.312	493	0.90063	0.00017
20G2D383	6V20G2B2	1.321	383	0.89775	0.00017
20G3B130	6V20G3B	1.309	130	0.89299	0.00016
20G3B184	6V20G3B	1.299	184	0.88787	0.00016
20G3B387	6V20G3B	1.316	387	0.89742	0.00017
20G3B442	6V20G3B	1.304	442	0.89155	0.00017
20G3B498	6V20G3B	1.285	498	0.88073	0.00016
20G3D386	6V20G3B2	1.297	386	0.87929	0.00016
5G8B105	6V5G8B	1.344	105	0.90756	0.00018
6B-NR-0	6V10G4B	1.291	81	0.87762	0.00016
6B-ROD-0	6V10G4B	1.303	285	0.8853	0.00016
6B-ROD-4	6V10G4B	1.296	339	0.88397	0.00017
6B-ROD-7	6V10G4B	1.283	394	0.87774	0.00016
6G10B105	6V6G10B	1.321	105	0.88742	0.00017
6-NR-0	6V10G4	1.296	81	0.88181	0.00017
6-ROD-0	6V10G4	1.281	285	0.86651	0.00016
6-ROD-4	6V10G4	1.271	339	0.86168	0.00016
6-ROD-7	6V10G4	1.256	395	0.85378	0.00016
8G4B132	6V8G4B	1.293	132	0.87734	0.00016
8G4B186	6V8G4B	1.286	186	0.87455	0.00016
8G4B388	6V8G4B	1.326	388	0.90315	0.00016
8G4B442	6V8G4B	1.320	442	0.90222	0.00016
8G4B498	6V8G4B	1.308	498	0.89722	0.00017
8G4D386	6V8G4B2	1.304	386	0.88136	0.00016
8G4D444	6V8G4B2	1.294	444	0.88214	0.00015
8G6B105	6V8G6B	1.275	105	0.84365	0.00017
8G6B394	6V8G6B	1.292	394	0.87536	0.00016
8G6B449	6V8G6B	1.287	449	0.87747	0.00017
8G6B506	6V8G6B	1.275	506	0.8741	0.00016

File Name	keff	Std dev	EALF (eV)	Description
COR-AL4B.o	0.8637	0.00017	0.272	Extra Aluminum in corners of limiting base model
DROPPED.o	0.8584	0.00016	0.272	Dropped bundle in large model
H-40X20B.o	0.8591	0.00014	0.207	Holtec 20x20 model with reduced keff to match PaR keff
misplacedPaR_assy_ecc.o	0.8659	0.00011	0.270	PaR pool with misplaced bundle, 4 eccentric bundles
misplacedPaR_base.o	0.8655	0.00032	0.271	PaR pool with no misplaced bundle
P2H540B.o	0.8573	0.00015	0.262	PaR to Holtec Interface
PAR-1MP.o	0.8597	0.00015	0.272	One missing Boral panel in large model
PAR-A50.o	0.8624	0.00013	0.272	Adl Limiting base model, Single cell
PAR-Adl_Dens.o	0.8631	0.00016	0.276	Increased UO2 stack density by [[]]
PAR-AWAW.o	0.8518	0.00015	0.273	PaR to PaR module interface
PAR-BLS2.o	0.8643	0.00016	0.284	Boral blister
PAR-BoralThk.o	0.8628	0.00017	0.273	Increase Boral cladding thickness by .01 in
PAR-BU25.o	0.7985	0.00012	0.261	Fuel at 25 GWD/T
PAR-BWID.o	0.8635	0.00017	0.271	Decrease Boral panel width by .031 in
PAR-CHTH.o	0.8686	0.00016	0.292	Increase channel thickness by [[]]
PAR-CLAD.o	0.8659	0.00017	0.266	Decrease fuel cladding thickness by [[]]
PAR-FPMA.o	0.9141	0.00017	0.245	Fission product and minor actinide worth
PAR-IS04.o	0.6762	0.00016	0.196	Isolated bundle, 4 pins removed
PAR-IS08.o	0.6815	0.00017	0.177	Isolated bundle, 8 pins removed
PAR-IS10.o	0.6782	0.00016	0.169	Isolated bundle, 10 pins removed

Non-Proprietary Information

File Name	keff	Std dev	EALF (eV)	Description
PAR-IS14.o	0.6741	0.00017	0.155	Isolated bundle, 14 pins removed
PAR-IS18.o	0.6668	0.00017	0.143	Isolated bundle, 18 pins removed
PAR-ISOL.o	0.6739	0.00017	0.214	Isolated bundle, all pins present
PAR-N131.o	0.8645	0.00016	0.271	Xe-131 worth
PAR-NOCH.o	0.8600	0.00017	0.261	Dechanneled bundle
PAR-OVTM.o	0.8611	0.00016	0.280	Overttemperature (water density at 0.98 g/cc)
PAR-POD.o	0.8631	0.00015	0.274	Increase pellet outer diameter by [[]]
PAR-PPIT.o	0.8635	0.00017	0.271	Increase pin pitch by [[]]
PAR-RPIT.o	0.8659	0.00016	0.278	Decrease rack pitch by .05 in
PAR-WALL.o	0.8635	0.00016	0.273	Increase rack wall thickness by 0.007 in
PAR-WHTH.o	0.8628	0.00016	0.271	Decrease water hole thickness by [[]]
PAR-ZERO.o	0.9714	0.00017	0.251	Fresh bundle, no Gadolinium fuel
PAR-ZIRC.o	0.8632	0.00012	0.272	Zirconium cladding and channel material
PAR20X20.o	0.8571	0.00014	0.273	PaR 20x20 model for missing panel & PaR to PaR interface
PAR40X20.o	0.8592	0.00015	0.272	PaR 40x20 model for interface effect comparison
PaR_30x30_6V.o	0.8794	0.0001	0.301	Orientation & eccentricity large base model with Fuel 6V20G3B2
PaR_30x30_Adl.o	0.8625	0.0001	0.272	Orientation & eccentricity large base model with limiting fuel
PaR_EccIn1_6V.o	0.8753	0.00009	0.318	Eccentric-In of orientation #1 of 6V20G3B2
PaR_EccIn1_Adl.o	0.8568	0.00009	0.288	Eccentric-In of orientation #1 of limiting fuel
PaR_EccInDech1_6V.o	0.8655	0.0001	0.326	Eccentric-In & dechanneled of orientation #1 of 6V20G3B2

Non-Proprietary Information

File Name	keff	Std dev	EALF (eV)	Description
PaR_EccInDech1_Adl.o	0.8454	0.0001	0.297	Eccentric-In & dechanneled of orientation #1 of limiting fuel
PaR_orient1_6V.o	0.8797	0.00009	0.301	Orientation #1 of 6V20G3B2
PaR_orient1_Adl.o	0.8626	0.0001	0.272	Orientation #1 of limiting fuel
PaR_orient2_6V.o	0.8794	0.0001	0.301	Orientation #2 of 6V20G3B2
PaR_orient2_Adl.o	0.8623	0.0001	0.272	Orientation #2 of limiting fuel
PaR_orient3_6V.o	0.8795	0.0001	0.301	Orientation #3 of 6V20G3B2
PaR_orient3_Adl.o	0.8626	0.0001	0.272	Orientation #3 of limiting fuel
A50NOLFP.inp (CASMO FILE)	-	-	-	Depletion with no lumped fission products
CAS-Adl_Dens.inp (CASMO FILE)	-	-	-	Increased UO2 Density by [[]]